



Centro de Investigación y de Estudios Avanzados del
Instituto Politécnico Nacional
Unidad Querétaro

Disolventes eutécticos como precursores y medios de reacción para síntesis novedosas y sustentables de polímeros

Tesis que presenta
Regina Janet Sánchez Leija

para obtener el Grado de
Doctora en Ciencias
en la Especialidad de Materiales

Director de la Tesis: Dr. J. Gabriel Luna Bárcenas
Coordinador de la Tesis: Dr. Josué David Mota Morales

Santiago de Querétaro, Qro.

Marzo de 2017



Centro de Investigación y de Estudios Avanzados del
Instituto Politécnico Nacional
Unidad Querétaro

Deep eutectic solvents as precursors and reaction media for novel and sustainable polymer synthesis

A dissertation submitted by
Regina Janet Sánchez Leija

for the degree of
Doctor of Philosophy

Adviser: Ph.D. J. Gabriel Luna Bárcenas
Co-adviser: Ph.D. Josué David Mota Morales

Santiago de Querétaro, Qro.

March, 2017

Acknowledgments

I would like to thank the National Council of Science and Technology of Mexico (CONACYT) for financial support through Ph.D scholarships No. 290747 and 290936 (CVU 231800).

This dissertation could not have been completed without the great support that I have received from so many people over these years. I wish to offer my sincere acknowledgements to the following people:

First I want to thank to my adviser Dr. Gabriel Luna Bárcenas for giving me the opportunity to work in this research project and being part of the polymers and biopolymers group at Cinvestav-Qro., with all the research facilities needed to develop this work.

To my co-adviser Dr. Josué David Mota Morales for his assistance and valuable suggestions and comments.

My deepest gratitude to Dr. Francisco del Monte, Dr. Ma. Concepción Gutiérrez and Dr. Marisa Ferrer from the bionspired materials group at ICMM in Madrid, Spain, with whom I had the pleasure to work during the last year of my Ph.D. I am enormously grateful with them for giving me the opportunity to work in their research group where I always felt welcomed. Thank you so much for the guidance and definitely valuable scientific discussions, which greatly contribute to the work regarding conductive polymers in this thesis.

To Prof. Dr. Arturo Mendoza Galván, for allowing me to carry out some experimental work at his laboratory.

To research assistant M.C. Reina Araceli Mauricio, not only for her assistance in all the issues regarding the materials, equipment and facilities of laboratory 12 at Cinvestav and for her suggestions during the setup of some experiments, but also for her great support as a friend.

I big thank you goes for my friend and husband Pablo Zubieta, to whom I admire, not only as a person but also as a scientist and colleague. For his great support, love, patience and valuable scientific discussions that definitely helped me to have a greater comprehension of some chemical and physical concepts needed to develop this project.

Contents

1	Introduction	1
1.1	Deep eutectic solvents	3
1.2	Physicochemical properties of DESs	6
1.2.1	Melting point	7
1.2.2	Viscosity and ionic conductivity	7
1.2.3	Polarity	9
1.3	Assessing the greenness of DESs	10
1.4	DESs applications	12
1.4.1	Electrochemistry	12
1.4.2	Dissolution and purification processes	13
1.4.3	Catalytic processes	15
1.4.4	Materials synthesis	16
1.4.4.1	Polymer synthesis	17
1.5	Overview and aim of the thesis	19
2	Controlled release of lidocaine hydrochloride from polymerized deep eutectic solvents	27
2.1	Background	28
2.2	Materials and experimental methods	29
2.2.1	Deep eutectic solvent synthesis	30
2.2.2	Polymerization of DESs	30
2.2.3	Release experiments	30
2.2.4	DESs characterization	31
2.2.5	Polymer-drug characterization	31
2.3	Results and discussion	32
2.3.1	Drug-based DESs	32
2.3.2	Polymerization of DESs	33
2.3.3	Kinetics of LidHCl release	36
2.4	Conclusions	41

3 Enzyme-mediated free-radical polymerization of acrylamide in deep eutectic solvents	47
3.1 Background	48
3.2 Materials and experimental methods	49
3.2.1 Materials	49
3.2.2 Deep eutectic solvent synthesis	50
3.2.3 Enzymatic activity assays	50
3.2.4 Thermal stability tests	50
3.2.5 HRP-mediated free-radical polymerization	51
3.2.6 DESs characterization	52
3.2.7 Enzyme characterization	52
3.2.8 Polymer characterization	53
3.3 Results and discussion	53
3.3.1 Catalytic activity and enzyme conformation	53
3.3.2 Thermal stability	56
3.3.3 HRP-mediated free-radical polymerization	57
3.4 Conclusions	61
4 Synthesis of conductive polyaniline monoliths from deep eutectic solvents	67
4.1 Background	68
4.2 Materials and experimental methods	70
4.2.1 Deep eutectic solvents synthesis	71
4.2.2 Polymerization of aniline hydrochloride-based DESs	71
4.2.3 Crosslinking of polyaniline monoliths	72
4.2.4 DESs characterization	72
4.2.5 Polymer characterization	73
4.3 Results and discussion	74
4.3.1 AHCl-based DESs characterization	74
4.3.2 PANI monoliths characterization	75
4.4 Conclusions	87
5 Concluding remarks and future perspectives	95
Appendices	99

A Appendix A: Supplementary information of Chapter 2	101
B Appendix B: Supplementary information of Chapter 3	110

List of Abbreviations

AA	acrylic acid
AA–LidHCl	acrylic acid/lidocaine hydrochloride DES
AAm	acrylamide
AHCl	aniline hydrochloride
AHCl–Egly	aniline hydrochloride/ethylene glycol DES
AHCl–Gly	aniline hydrochloride/glycerol DES
AHCl–GlyAc	aniline hydrochloride/glycolic acid DES
AHCl–LAc	aniline hydrochloride/L-lactic acid DES
API	active pharmaceutical ingredient
APS	ammonium persulfate
ATR	attenuated total reflectance
[BMIM] ⁺	1–butyl–3–methylimidazolium
CALB	candida antarctica lipase B
CCl–Gly	choline chloride/glycerol DES
CCl–U	choline chloride/urea DES
CPs	conductive polymers
DESSs	deep eutectic solvents
DMF	dimethylformamide
DMSO	dimethylsulfoxide
DSC	differential scanning calorimetry
EGDMA	ethylene glycol dimethacrylate
[EMIM] ⁺	1–ethyl–3–methylimidazolium
FTIR	Fourier transform infrared spectroscopy
GA	glutaraldehyde
HBD	hydrogen bond donor
HIPEs	high internal phase emulsions
HMF	5–hydroxymethylfurfural
H NMR	proton nuclear magnetic resonance
HRP	horseradish peroxidase
iCALB	immobilized candida antarctica lipase B

ILs	ionic liquids
LidHCl	lidocaine hydrochloride
MAA	methacrylic acid
MAA–LidHCl	methacrylic acid/lidocaine hydrochloride DES
MDSC	modulated differential scanning calorimetry
MOFs	metal organic frameworks
NADES	natural deep eutectic solvents
NMP	<i>N</i> –methylpyrrolidone
PA	phytic acid
PAA	poly(acrylic acid)
PAAm	poly(acrylamide)
PANI	polyaniline
PANI–EB	polyaniline emeraldine base
PANI–ES	polyaniline emeraldine salt
PANI–P	polyaniline obtained from AHCl-based DES with PPDA
PANI–S	polyaniline obtained from AHCl-based DES
PBS	phosphate buffer solution
PDI	polydispersity index
PETA	pentaerythritol triacrylate
PGA–HCl	crosslinked PANI–P with GA and redoped with HCl
PGA–PA	crosslinked PANI–P with GA and redoped with PA
PPA–HCl	crosslinked PANI–P with PA and redoped with HCl
PMAA	poly(methacrylic acid)
POC	poly(octanediol–co–citrate)
PPDA	<i>p</i> –phenylenediamine
QAS	quaternary ammonium salt
RT	room temperature
SDA	structure-directing agent
SEC	size exclusion chromatography
SEM	scanning electron microscopy
SEC	size exclusion chromatography
TGA	thermogravimetric analysis
UV-Vis	ultraviolet-visible spectroscopy
XPS	x-ray photoelectron spectroscopy

List of Symbols

a_w	water activity
c	speed of light
E_T^N	Reichardt's normalized polarity scale
h	Plank constant
k	proportionality constant
k_1	correction factor based on the ratio of sample thickness to probe spacing (thick sample)
k_2	correction factor based on the ratio of sample thickness to probe spacing (thin sample)
λ_{\max}	wavelength of the maximum absorption
M_n	number average molecular weight
M_w	weight average molecular weight
M_t	amount of release at time t
M_∞	amount of release at equilibrium
N_A	Avogadro number
n	diffusional exponent
R	electrical resistance
s	distance between probes
σ	electrical conductivity
$t_{1/2}$	half-life time
T_f	freezing point temperature
T_g	glass transition temperature
T_m	melting point temperature
w	thickness of the sample

List of Figures

1.1 Examples of ILs and DESs.	2
1.2 Freezing point of choline chloride/urea mixtures as a function of composition.	4
1.3 Typical structures of the halide salts and hydrogen bond donors used for DES syntheses.	6
2.1 Structures of polymerizable LidHCl-based DESs and crosslinkers. .	32
2.2 FTIR Analysis of the carbonyl region in AA, MAA, and AA-LidHCl and MAA-LidHCl DESs.	34
2.3 ATR-FTIR spectra of polymerizable LidHCl-based DESs and their components.	35
2.4 Photograph of the polymer-drug monoliths.	36
2.5 ATR-FTIR spectra of polymerizable DESs, the polymer complexes resulting after polymerization of DESs, and the pure polymers. . .	36
2.6 Kinetics of the release of LidHCl from PAA and PMAA crosslinked with EGDMA in phosphate buffer at different pH and ionic strength under sink conditions at 24 °C.	37
2.7 Swelling behavior of PAA crosslinked with EGDMA in phosphate buffer at different pH values.	39
2.8 Effect of pH and ionic strength on the release of LidHCl from PAA and PMAA hydrogels crosslinked with EGDMA in phosphate buffer under sink conditions at 24 °C.	40
2.9 Effect of crosslinkers on the release of LidHCl from PAA and PMAA in phosphate buffer under sink conditions at 24 °C.	41
2.10 Release of LidHCl from PAA, PMAA and PAA- <i>co</i> -PMAA, crosslinked with PETA in phosphate buffer under sink conditions at 24 °C. . .	42
3.1 Reaction scheme of HRP-mediated free-radical polymerization of AAm in water.	51

3.2	Relative specific activity of HRP in DESs-aqueous mixtures at RT and different DES concentration.	54
3.3	Tryptophan fluorescence emission spectra, and UV-Vis spectra of the Soret region of HRP in PBS and DESs-aqueous mixtures at RT. . .	55
3.4	Thermal stability of HRP in PBS and DES aqueous mixtures at 50 °C.	56
3.5	PAAm solutions in H_2O and DESs-aqueous mixtures, PAAm precipitated with methanol and PAAm synthesized in DESs-aqueous mixtures and H_2O at RT.	58
3.6	FTIR spectra of PAAm synthesized in H_2O and DESs aqueous mixtures.	59
3.7	Thermodynamic activity of water (a_w) as a function of water content in DESs-aqueous mixtures.	60
4.1	AHCl-based DESs and DSC scans of the eutectic mixtures.	76
4.2	Synthesis procedure to obtain conductive PANI-S monoliths.	76
4.3	Polyaniline forms.	78
4.4	Deconvoluted N1s core-level spectra of PANI-S and PANI-P samples from AHCl-Egly DES.	79
4.5	SEM micrographs of PANI-S monoliths.	81
4.6	SEM micrographs of PANI-P monoliths.	81
4.7	Chemical structures of glutaraldehyde and phytic acid crosslinkers.	82
4.8	FTIR spectra of PANI-P and crosslinked PANI samples.	83
4.9	Absorption spectra of PANI-P and crosslinked PANI samples in NMP.	84
4.10	Absorption spectra of PANI-P and crosslinked PANI samples in 1M HCl.	85
A.1	Experimental setup for the frontal polymerization of LidHCl-based DESs.	101
A.2	Calibration curve for LidHCl quantification by UV-Vis spectroscopy.	102
A.3	Scheme representating frontal polymerization of acrylic acid / choline chloride DES.	102
A.4	DSC scans of AA-LidHCl and MAA-LidHCl DESs.	103
A.5	1H NMR spectrum of AA-LidHCl DES in $CDCl_3$	104
A.6	1H NMR spectrum of MAA-LidHCl DES in $CDCl_3$	105

A.7	Thermogravimetric analysis of the polyacrylates–LidHCl and LidHCl monohydrate.	106
A.8	^1H NMR spectra of pure LidHCl monohydrate, LidHCl from PAA–LidHCl, PMAA–LidHCl and P(AA–co–MAA)–LidHCl with PETA as crosslinker	107
A.9	Cumulative release of LidHCl <i>vs</i> the square root of time and linear fitting to Fickian model.	108
A.10	Diameter of PAA–LidHCl with EDGMA as crosslinker <i>vs</i> the square root of time and linear fitting to Fickian model.	109
B.1	Raw tryptophan fluorescence emission spectra of HRP in PBS and DESs-aqueous mixtures.	110
B.2	Specific activity of HRP in DESs-aqueous mixtures at RT and different DES concentrations.	110
B.3	^1H -NMR spectra of PAAm samples synthesized in H_2O and DESs-aqueous mixtures.	111
B.4	ATR–FTIR spectra of CCl–U and CCl–Gly DESs in pure state and DESs-aqueous mixtures.	112
B.5	ATR–FTIR spectra of CCl–U and CCl–Gly in its pure state and PAAm solutions in DESs-aqueous mixtures synthesized at different temperatures.	113
B.6	^1H -NMR spectra of CCl, CCl–Gly, CCl–U and PAAm synthesized in CCl–U aqueous mixture at RT.	114

List of Tables

1.1	General classification of DESs.	5
1.2	Freezing point temperatures of some DESs and melting point temperatures of their individual components.	8
1.3	Viscosities and ionic conductivities of some DESs at specific temperatures.	8
1.4	E_T^N values of some common molecular solvents, ILs and DESs. . . .	10
2.1	Viscosity and melting point (T_m) of polymerizable the LidHCl-based DESs and their components.	33
2.2	Experimental setup and polymerization results.	35
3.1	Freezing temperature and viscosity of the used DESs and DESs-aqueous mixtures.	54
3.2	Half-life time values ($t_{1/2}$) for HRP obtained in PBS and DESs-aqueous mixtures (80% v/v DES) at 50 °C.	57
3.3	Yield and M_n of PAAm samples obtained by HRP-mediated initiation in H_2O and DESs-aqueous mixtures (80% v/v DES).	57
4.1	Experimental procedures to obtain crosslinked PANI–P monoliths from AHCl–Egly DES.	72
4.2	Meltig point of polymerizable AHCl-based DESs and their individual components.	75
4.3	Electrical conductivity of PANI–S and PANI–P monoliths.	77
4.4	Binding energies of N1s core-level of PANI–S and PANI–P samples from AHCl–Egly DES.	80
4.5	Electrical conductivity of crosslinked PANI–P monoliths from AHCl–Egly DES.	82
A.1	1H NMR signal assignment of AA–LidHCl DES.	104
A.2	1H NMR signal assignment of MAA–LidHCl DES.	105

Resumen

Los disolventes eutécticos (DESs por sus siglas en inglés), una nueva clase de líquidos iónicos formados por sales cuaternarias de amonio y donadores de enlace de hidrógeno, han resultado atractivos como medios de reacción sustentables para la síntesis de materiales. Su baja presión de vapor y fácil síntesis a partir de compuestos biodegradables o de baja toxicidad, han hecho de los DESs una alternativa “verde” para reemplazar a los disolventes orgánicos y líquidos iónicos convencionales.

En este trabajo se demuestra su versatilidad y potencial como disolventes multifuncionales para la síntesis de polímeros. Los casos de estudio incluyeron la síntesis todo en uno de complejos poli(acrilato)-fármaco y redes interconectadas tridimensionalmente de polianilina conductora en ausencia de agua o cualquier otro disolvente, así como la síntesis biocatalítica de poliacrilamida en DESs.

El ambiente químico provisto por los DESs ofreció ventajas adicionales sobre los métodos de síntesis clásicos. Por ejemplo, la exotermicidad de la reacción de polimerización de DESs de acrilatos e hidrocloruro de lidocaina fue controlada gracias a la alta viscosidad de estos disolventes, permitiendo llevar a cabo la reacción a temperaturas relativamente bajas y evitando así la degradación del fármaco. En cuanto a la síntesis biocatalítica de poliacrilamida, se obtuvieron altas conversiones y pesos moleculares debido a la mejorada estabilidad térmica de la enzima en los DESs en comparación con el medio acuoso. Adicionalmente, la incorporación de altas concentraciones de hidrocloruro de anilina a través de la formación de DESs, permitió la síntesis en un sólo paso de monolitos porosos de polianilina conductora con los valores de conductividad eléctrica más altos reportados hasta ahora para arquitecturas tridimensionales de polianilina pura.

Dada la amplia variedad disponible de sales cuaternarias de amonio y donadores de enlace de hidrógeno, fue posible preparar DESs con propiedades específicas para la síntesis todo en uno de polímeros, los cuales jugaron simultáneamente el papel de monómero, disolvente y compuesto con funcionalidad específica. Definitivamente, la multifuncionalidad de los DESs representa una característica atractiva, ya que se evita el uso en gran cantidad de compuestos químicos tóxicos y la generación de productos de desecho, haciendo de estas novedosas rutas de síntesis, alternativas amigables con el medio ambiente para síntesis de polímeros.

Abstract

Deep eutectic solvents (DESs), a novel class of ionic liquids formed by quaternary ammonium salts and hydrogen bond donors, have resulted attractive as sustainable reaction media for materials synthesis. Their low vapor pressure and easy synthesis from biodegradable or low toxic compounds, have made DESs a “green” alternative to replace conventional organic solvents and ionic liquids.

In this work, their versatility and potential as multifunctional solvents for polymer synthesis is demonstrated. The case studies included the all-in-one synthesis of poly(acrylate)-drug complexes and 3D-interconnected conductive polyaniline networks from polymerizable DESs in the absence of water or any further solvent, as well as the biocatalytic synthesis of polyacrylamide in DESs.

The chemical environment provided by DESs offered additional advantages over the classic synthetic methods. For instance, the exothermicity of the polymerization reaction of acrylate/lidocaine hydrochloride DESs was controlled given the high viscosity of these solvents, allowing to carry out the reaction at relatively low temperatures, and thus avoiding degradation of the drug. Regarding to the biocatalytic synthesis of polyacrylamide, high conversions and molecular weights were obtained owing to the enhanced thermal stability of the enzyme in DESs in comparison with the aqueous media. Additionally, the incorporation of high aniline hydrochloride concentrations through DESs formation, allowed the one-step synthesis of conductive porous polyaniline monoliths with the highest electrical conductivity values for pristine polyaniline 3D-interconnected architectures reported to date.

Given the wide variety of quaternary ammonium salts and hydrogen bond donors available, it was possible to prepare DESs with tailored properties for the all-in-one synthesis of polymers, which simultaneously played the role of monomer, solvent and compound with specific functionality. Definitively, the multifunctionality of DESs represents an attractive feature as greater use of toxic chemical compounds and generation of waste products are avoided, making these novel synthetic routes eco-friendly alternatives for polymer synthesis.

A scientist in his laboratory is not a mere technician: he is also a child confronting natural phenomena that impress him as though they were fairy tales.

— Marie Curie

1

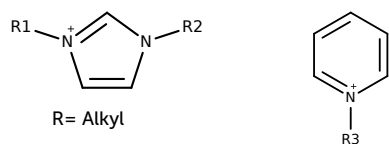
Introduction

Nowadays there are many efforts in searching for sustainable routes in chemical processes and materials synthesis. Special attention has been paid to the replacement of harmful precursors, solvents and catalysts in favor of eco-friendlier alternatives. In this context, ionic liquids (ILs) have resulted an attractive option to substitute traditional industrial solvents and thus to prevent emission of volatile organic compounds to the atmosphere owing to their “non-volatility”, *i.e.*, negligible vapor pressure.

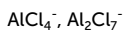
ILs are defined as salts comprised entirely of ions with a melting point below 100 °C,^[1,2] being many of them liquids at room temperature. They consist of bulky asymmetric organic cations and organic or inorganic anions.^[3] Besides their negligible vapor pressure, ILs are thermally stable, exhibit good solvating properties for a wide variety of compounds and are easy to handle.^[1,2] Another important feature of ILs is the possibility to synthesize them with tailored properties (*e.g.* melting point, viscosity and polarity) by carefully selecting the cations and anions. This unique combination of properties, makes ILs suitable for use as media for organic synthesis,^[4] materials preparation^[5,6] and even for biotransformations catalyzed by either enzymes or whole microorganism.^[7] Furthermore, given the large number of cations and anions available, at least 10^6 binary ILs and 10^{18} ternary ILs are possible, in contrast with the around 600 molecular solvents used today.^[8]

First generation of ILs

Typical cations:

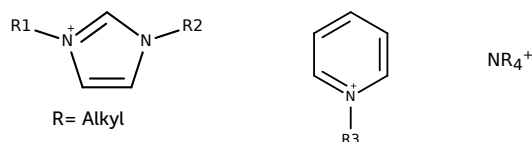


Typical anions:



Second generation of ILs

Typical cations:

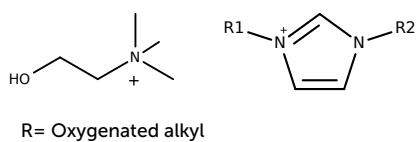


Typical anions:

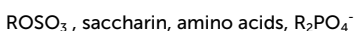


Third generation of ILs

Typical cations:

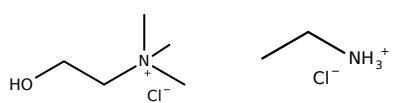


Typical anions:

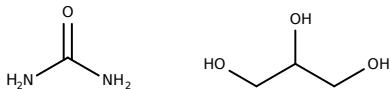


Deep eutectic solvents (DESs)

Typical quaternary ammonium salt:



Typical hydrogen bond donor (HBD):



Advanced Ionic Liquids

Fig. 1.1 Examples of ILs and DESs (adapted from Gorke *et al.*)^[9]

The first ionic liquid, ethylammonium nitrate $[\text{EtNH}_3]^+[\text{NO}_3]^-$ (melting point of 12 °C), was reported by Walden in 1914.^[10] However, it was not until the emergence of the first generation of ILs in 1960s that developments in the area started. Since then, many ILs with improved properties have been designed. The first generation of ILs were mainly composed of N,N' -dialkylimidazolium and N-alkylpyridinium cations with chloroaluminates and metal halide anions.^[2] Unfortunately, these ILs posed the disadvantage of being reactive with water and unstable on air. At the beginning of the '90s, the water reactive anions were replaced with halides or weakly coordinating anions such as BF_4^- , PF_6^- , NO_3^- , SO_4^{2-} and CH_3COO^- .^[11,12] The resulting ILs were stable toward water hydrolysis, presumably because strong inter-

action between the components reduced their reactivity. They exhibited moderate polarity (similar to ethanol) and most of them were hydrophobic. Despite the high cost of this generation of ILs (derived from the high cost of the components and purification required in the preparation), this type of ILs has became the most widely studied, particularly those based on 1-butyl-3-methylimidazolium $[\text{BMIM}]^+$ and 1-ethyl-3-methylimidazolium $[\text{EMIM}]^+$ cations.

Most recently, a third generation — called advanced ILs by Gorke *et al.* — has been developed.^[9] These liquids retain the moderate polarity, stability, and distributed negative charge of the second generation, but can be composed of biodegradable or less toxic cations (*e.g.*, choline derivatives) and/or anions (*e.g.*, sugars, amino or organic acids, and alkylsulfates or alkylphosphates). Moreover, they are more hydrophilic than previous ILs and miscible with water. Within this family of ILs are found the so called deep eutectic solvents (DESs), a new class of solvents that emerged around a decade ago.^[13] DESs share many of the characteristics of ILs, even though they cannot be considered as conventional ILs since are mixtures of organic salts with uncharged hydrogen bond donors such as amides, carboxylic acids and alcohols. Typical components of ILs and DESs are shown in Figure 1.1.

The following sections of this chapter will deepen on the topic of DESs, as they are used as multifunctional solvents throughout this work and are, in essence, the main component of every system described in this thesis. The “green” character of DESs will be discussed and an overview of the recent advances and applications of these solvents will also be presented.

1.1 Deep eutectic solvents

Deep eutectic solvents (DESs) are usually obtained by the complexation of a quaternary ammonium salt with a metal salt or hydrogen bond donor (HBD).^[14] The term DESs refers to liquids close to the eutectic composition of mixtures, *i.e.*, the molar ratio of the components which gives the lowest melting point.

In 2003 Abbott and collaborators^[13] reported that mixtures of substituted quaternary ammonium salts such as choline chloride ((2-hydroxyethyl)trimethylammonium chloride) with urea produce eutectics that are liquid at ambient tempera-

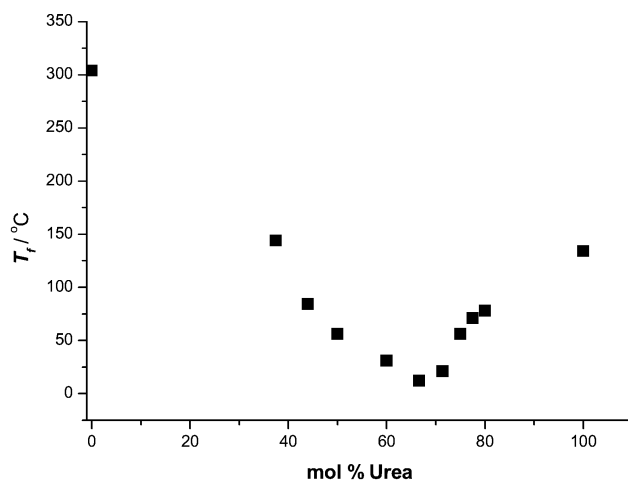


Fig. 1.2 Freezing point of choline chloride/urea mixtures as a function of composition.
Reproduced from Ref. [13] with permission from the Royal Society of Chemistry.

ture and have unusual solvent properties (Figure 1.2). It was shown that a mixture of choline chloride with urea in a molar ratio of 1:2 gives a liquid with a freezing point of 12 °C, which is considerably lower than that of either of the constituents (the melting point of choline chloride and urea are 302 and 133 °C, respectively). This decrease in the freezing point of the mixture, relative to the melting points of the individual components, is attributed to the charge delocalization occurring through hydrogen bonding between the halide anion and the amide hydrogen donor moiety.^[15] In that work, the term DESs was first used to differentiate these liquids from conventional ILs which contains only discrete ions.

DESs can be described by the general formula^[14]



where Cat^+ is in principle any ammonium, phosphonium, or sulfonium cation, and X is a Lewis base, generally a halide anion. The complex anionic species are formed between X^- and either a Lewis or Brønsted acid Y (z refers to the number of Y molecules that interact with the anion). Depending on the nature of the complexing agent used, DESs are classified according to Table 1.1. DESs formed from MCl_x and quaternary ammonium salts (type I) can be considered to be of an analogous type to the metal halide/imidazolium salt ILs.^[14] Given the limited range of nonhydrated metal halides which have a suitably low melting point to form type I DESs, the scope of DESs can be extended by using hydrated metal halides (type II). It has

Table 1.1 General formulae for the classification of DESs.^[14]

Type	General formula	Term
Type I	$\text{Cat}^+ \text{X}^- z \text{MCl}_x$	$\text{M} = \text{Zn, Sn, Fe, Al, Ga, In}$
Type II	$\text{Cat}^+ \text{X}^- z \text{MCl}_x \cdot y \text{H}_2\text{O}$	$\text{M} = \text{Cr, Co, Cu, Ni, Fe}$
Type III	$\text{Cat}^+ \text{X}^- z \text{RZ}$	$\text{Z} = \text{CONH}_2, \text{COOH}, \text{OH}$
Type IV	$\text{MCl}_x + \text{RZ} = \text{MCl}_{x-1}^+ \cdot \text{RZ} + \text{MCl}_{x+1}^-$	$\text{M} = \text{Al, Zn and Z} = \text{CONH}_2, \text{OH}$

been shown that also a range of transition metals can be incorporated into ambient temperature eutectics, and these have been termed type IV DES. While types I, II, and IV eutectics all contain metal salts with their innate toxicity, type III eutectics can be obtained from wide variety of environmental benign compounds.

Particularly, type III eutectics formed from choline chloride and HBDs have been of especial interest in the last years due to their ability to solvate a wide range of compounds. Moreover, choline chloride cation is non-toxic and biodegradable (it is indeed produced on large scale as an animal feed supplement) and has lower cost compared with imidazolium and pyridinium cations. As for the HBD, several compounds have been studied to date, with DESs formed using amines, amides, alcohols, carboxylic acids and sugars.^[16,17] (Figure 1.3) shows the chemical structures of the most common halide salts and hydrogen bond donors used to prepare type III eutectics.

DESs exhibit a low vapor pressure, relatively wide liquid-range and are non-flammable and non-reactive with water. Nevertheless, in contrast to conventional ILs, DESs offer several advantages that make them desirable for large scale applications. For instance, the ease of preparation in pure state (they are obtained by simple mixing of the components and do not require purification), and the easy availability from relatively low cost components.^[17] It is worth mentioning that price targets in 2010 from Solvent Innovation GmbH (Cologne, Germany) for ILs were approximately 10-20 USD/kg on the ton scale, which was at least 10 fold higher than many organic solvents.^[9] In comparison, the three most common DES (choline chloride/urea, choline chloride/ethylene glycol and choline chloride/glycerol) are priced at 200 £/kg, which is a fifth of the lowest cost ILs per kg.¹

¹Based on list prices from Scionix (<http://www.scionix.co.uk>) and Sigma-Aldrich® online catalogues as of April 2017.

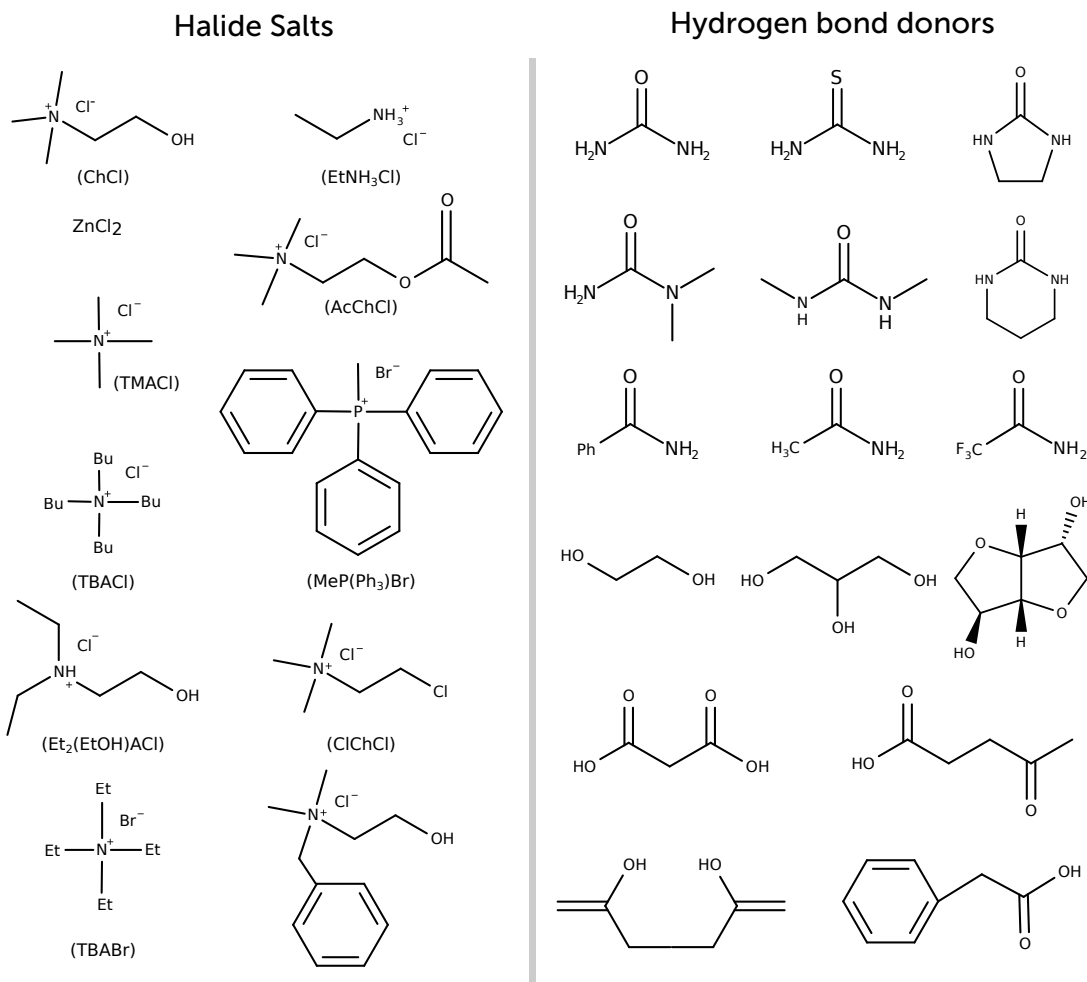


Fig. 1.3 Typical structures of the halide salts and hydrogen bond donors used for DES syntheses (adapted from Zhang *et al.*).^[16]

1.2 Physicochemical properties of DESs

Similar to ILs, one of the main features of DESs is that their properties can be easily tailored for specific applications by accurately combining various halide salts with different HBD. Hence, task-specific DESs with different physicochemical properties such as melting point, viscosity, ionic conductivity, and polarity, among others, can be obtained.^[16] Given the scope of applications, the physicochemical characterization of these solvents have been of paramount importance. In this section, the main physicochemical properties of DESs are described.

1.2.1 Melting point

As already mentioned, DESs are characterized by a melting point lower than that of each individual component. The steep depression in the melting point stems from an interaction between the halide anion and the HBD component. More precisely, the melting point of DESs depends on the lattice energies of both the halide salt and HBD, the anion-HBD interactions network and the changes in entropy when the liquid is formed.^[15] If the anion-hydrogen donor interaction is strong, the entropy of the system increases, resulting in a more disordered system, therefore offering a lower melting point. Even though, no clear correlation between the melting point of DESs and the melting point of the pure components has been found so far.

All reported DESs have melting points below 150 °C and most of them are liquid between ambient temperature and 70 °C.^[16] DESs with melting points lower than 50 °C are especially attractive for carrying out chemical processes at low temperatures or even ambient temperatures, thus reducing energy costs and making such processes safer. However, the number of known DESs which are liquid at ambient temperature is still limited. In the case of choline chloride it is possible to obtain room temperature DESs when HBD such as urea, trifluoracetamide, malonic acid, among others, are used. Table 1.2 lists the freezing points of various DESs described in the literature.

1.2.2 Viscosity and ionic conductivity

Most of the reported DESs are highly viscous (>100 cP) at room temperature^[9,16] (Table 1.3). These values are similar to glycerol or honey (for comparison, the viscosity of water is around 1 cP at 20 °C). The high viscosity of these systems has been attributed to the presence of a strong hydrogen bond network formed between the halide salt and the HBD, which reduces the mobility of free species within the DES. Other forces such as electrostatic or van der Waals interactions, the large ion size and very small free volume of DES may also contribute to their high viscosity.^[16,25]

DES's viscosity is strongly influenced by the chemical nature of the components (type of halide salt and HBDs), halide salt/HBD molar ratio, water content and

Table 1.2 Freezing point temperatures of some DESs and melting point temperatures of their individual components.

Halide salt	T_m (°C)	HBD	T_m (°C)	Salt:HBD (molar ratio)	DES T_f (°C)	Ref.
choline chloride	303	urea	134	1:2	12	[13]
choline chloride	303	thiourea	175	1:2	69	[13]
choline chloride	303	acetamide	80	1:2	51	[13]
choline chloride	303	benzamide	129	1:2	92	[13]
choline chloride	303	ethylene glycol	-12.9	1:2	-66	[18]
choline chloride	303	glycerol	17.8	1:2	-40	[19, 20]
choline chloride	303	xylitol	96	1:1	Liquid at RT	[21]
choline chloride	303	D-sorbitol	99	1:1	Liquid at RT	[21]
choline chloride	303	D-glucose	146-150	1:1	31	[22]
choline chloride	303	citric acid	149	1:1	69	[15]
choline chloride	303	malonic acid	134	1:1	10	[15]
choline chloride	303	oxalic acid	190	1:1	34	[15]
choline chloride	303	L-(+)-tartaric acid	171	1:0.5	47±3	[21]
ethylammonium chloride	107-108	acetamide	80	1:1.5		
ethylammonium chloride	107-108	2,2,2-trifluoroacetamide	73-75	1:1.5		
MeP(Ph ₃)Br	231-233	ethylene glycol	-12.9	1:3	-46	[23]
MeP(Ph ₃)Br	231-233	glycerol	17.8	1:3	-5.5	[23]
MeP(Ph ₃)Br	231-233	2,2,2-trifluoroacetamide	73-75	1:8	-69.3	[24]

MeP(Ph₃)Br = Methyltriphenylphosphonium bromide

temperature. For instance, selection of different HBDs in choline chloride-based DESs results in mixtures with notably different viscosity values. The viscosity of choline chloride/ethylene glycol (1:2) DES is reported to be 36 cP at 20 °C, whereas is slightly more than 10 times that of choline chloride/glycerol (1:2) DES at the same temperature (376 cP).^[25] Interestingly, it has been observed that addition of higher amounts of salt in choline chloride/glycerol DES decreases the viscosity of the mixture. Higher viscous choline chloride-based DESs can be obtained by using compounds with high density of HBD groups such as sugars (e.g. glucose, xylitol, sorbitol)^[21] or carboxylic acids (e.g. malonic acid).^[27]

Table 1.3 Viscosities and ionic conductivities of some DESs at specific temperatures.

Halide salt	HBD	Salt:HBD (molar ratio)	Viscosity (cP)	Conductivity (mS·cm ⁻¹)	Ref
choline chloride	urea	1:2	750 (25 °C)	0.20 (40 °C)	[13]
choline chloride	ethylene glycol	1:2	36 (20 °C)	7.61 (20 °C)	[25]
choline chloride	glycerol	1:2	376 (20 °C)	1.05 (20 °C)	[25]
choline chloride	glucose	1:1	9037 (25 °C)	—	[22]
choline chloride	1,4-butanediol	1:3	140 (20 °C)	1.65 (20 °C)	[25]
choline chloride	xylitol	1:1	5230 (30 °C)	—	[21]
choline chloride	D-sorbitol	1:1	12730 (30 °C)	—	[21]
choline chloride	malonic acid	1:2	1124 (25 °C)	—	[21]
ethylammonium chloride	2,2,2-trifluoroacetamide	1:1.5	256 (40 °C)	0.39 (40 °C)	[26]
ethylammonium chloride	acetamide	1:1.5	64 (40 °C)	0.69 (40 °C)	[26]
acetyl choline chloride	urea	1:2	2214 (40 °C)	0.02 (40 °C)	

Owing to their enormous potential as solvents, the design and development of DESs with low viscosities is highly desirable to minimize operational costs associated with stirring, mixing and pumping.

Table 1.3 also lists the ionic conductivity values of some DESs. Most of these solvents exhibit poor ionic conductivities (lower than $2 \text{ mS}\cdot\text{cm}^{-1}$ at room temperature) as a consequence of their generally high viscosity^[16] (or reduced ion mobility). As it can be expected, the conductivity values often increase significantly as the temperature increases owed to a decrease of DESs viscosity. Therefore, the ionic conductivity of these solvents depends also on the parameters that influence their viscosity.

1.2.3 Polarity

Polarity is a measure of a solvent's capability for solvating dissolved neutral (polar or apolar) and charged species,^[28] which in turn depends on the intermolecular interactions between solute ions or molecules and solvent molecules (excluding those interactions leading to chemical alteration).^[29] The most common indicator of polarity strength is the Reichardt's normalized scale E_T^N , which is based on the wavelength value of the maximum absorbance of betaine dye n°30 (Reichardt's dye) in a solvent, and can be calculated by means of the following expression^[29]

$$E_T^N = \frac{E_T(\text{solvent}) - E_T(\text{TMS})}{E_T(\text{water}) - E_T(\text{TMS})}, \quad (1.2)$$

where, for any solvent

$$E_T(\text{solvent}) = \frac{h \cdot c \cdot N_A}{\lambda_{\max}} \quad (1.3)$$

with h as the Planck constant, c the speed of light, N_A the Avogadro number and λ_{\max} the wavelength of the maximum absorption.

Notice, that in such normalized scale we have the reference values $E_T^N = 1.00$ for water and $E_T^N = 0.00$ for tetramethylsilane (TMS), as extreme polar and non-polar solvents, respectively.

Table 1.4 summarizes the E_T^N values for some common organic solvents, ILs and choline chloride-based DESs. It can be observed that DES's polarity values are

Table 1.4 E_T^N values of some common molecular solvents, ILs and DESs (adapted from Ruß *et al.*^[30])

Solvent	E_T^N	Ref	Solvent	E_T^N	Ref.
water	1.00	[29, 31]	dimethylformamide	0.40	[31]
glycerol	0.81	[29]	[BMIM][acetate]	0.61	[32]
ethylene glycol	0.78	[31]	[BMIM][propionate]	0.57	[32]
ethanol	0.65	[29]	choline chloride/glycerol	0.86	[33]
2-propanol	0.55	[31]	choline chloride/ethylene glycol	0.80	[33]
dimethylsulfoxide	0.44	[31]	choline chloride/urea	0.84	[33]

higher than those corresponding to short chain alcohols (ethanol and 2-propanol), some polar aprotic solvents (dimethylsulfoxide and dimethylformamide) and also some imidazolium-based ILs.

1.3 Assessing the greenness of DESs

Research into DESs is blooming. A web search² based on the words ‘deep eutectic solvents’ shows a total of 1068 publications in the topic since these solvents first appeared in 2003, and almost a third of them have been published in 2016. This burgeoning interest is associated to their low vapor pressure and the fact that can be obtained from natural and biodegradable compounds, which make DESs suitable substitutes for common industrial solvents. Owing to these features, DESs have been largely described in the literature as “green solvents”, but *can DESs really be considered green solvents?*

One major source of environmental pollution in the chemical industry is the emission of volatile organic compounds, primarily, from the use of solvents. Therefore, it is of great importance to reduce their use as they typically represent over 85% of mass utilization in a typical chemical manufacturing process.^[34] There are four principal strategies to avoid using conventional organic solvents: no solvent, water, supercritical fluids, and ILs.^[8] The solventless option would be the ideal situation, however, development of such strategies remains a challenge. The use of water can also be advantageous, but many organic compounds are difficult to dissolve in water, and disposing of contaminated aqueous streams its expensive. Supercritical fluids, which have both gas- and liquid-like properties, are highly versatile solvents

²According to Scopus as of December 15, 2016

for chemical synthesis, but high pressures are required to maintain the solvent in supercritical state. Together with ILs, these alternative solvent strategies provide a range of options to minimize the environmental impact of a chemical process.

DESs share many characteristics of conventional ILs, but offer certain advantages over the later. DESs can be easily prepared from biodegradable or low toxic compounds, offering a “greener” alternative to many traditional ILs, but they are not by definition “green”. However, as already mentioned, type III eutectics can be obtained from wide variety of environmental benign compounds. For instance, choline chloride has been of especial interest for DES preparation given its non-toxicity, biodegradability (it is classified as a provitamin in Europe and is produced on large scale as an animal feed supplement)^[14] and low cost. Regarding the HBD, amides an polyols such as urea, glycerol, and ethylene glycol are often employed.

More interestingly, DESs may also be consider biomimetic solvents. In 2011, Verpoorte *et al.*^[35] suggested the possibility that before the advent of green chemistry using ILs, nature maybe have engineered a kind of complex combinations of compounds to serve as solvents in various biochemical reactions and physiological functions. They realized that metabolites such as sugars, amino acids, choline and organic acids (*e.g.* malic acid, citric acid, lactic acid and succinic acid), which are present in considerable amounts in microbial, mammalian and plant cells, seemed perfect candidates for making DESs. Based on this observation, they discovered that more than 30 combinations of these major cellular constituents can form viscous liquids with a melting point much more lower than the counterparts themselves, and used the term natural deep eutectic solvents (NADES) to refer to these mixtures. This finding strongly suggest that water and lipids are indeed not the only solvents present in living organisms and would explain mechanisms and phenomena that are otherwise difficult to understand, such as cryo-protection, desiccation tolerance and biosynthesis of non-water-soluble small molecules and macromolecules.

To date, the majority of the applications of DESs have been focused in the areas of electrochemistry, organic synthesis, separation processes, biomass processing and materials synthesis. In most of these cases, DESs have been used as solvents, but it has been demonstrated that they can also act as all-in-one-solvent-template-reactant systems for the fabrication of a desired material with a defined morphology or chemical composition.^[17,34] In other words, DESs can be not only the solvent,

but also the precursor, template, and reactant medium, thus avoiding greater use of chemical compounds and production of waste products. Examples of materials prepared from all-in-one DESs include metal phosphates, zeolites, metal organic frameworks (MOFs) and polymers.

It is worth noting that even when the individual components of DESs can be nontoxic and are well toxicologically characterized, the mixtures of these components will not necessarily be nontoxic and inherently “green”. There are scarce reports about the toxicological properties of the mixtures,^[36–39] and this need to be further investigated by the scientific community before DESs can truly be claimed as nontoxic and biodegradable. Albeit DESs-assisted synthesis do not fully comply with the 12 Principles of Green Chemistry, the above mentioned features definitely make DESs attractive from the green chemistry point of view. Further research into the development of new synthetic strategies and enhancement of the features of these systems is needed, but DESs undoubtedly represents a big step towards truly green approaches to materials synthesis.

1.4 DESs applications

DESs have shown to be particularly versatile solvents, with numerous applications encompassing the fields of electrochemistry, organic synthesis, separation processes, biomass processing, catalysis and materials synthesis.

Herein, some applications of DESs will be introduced through selected examples. Focus will be on type III eutectics (formed from quaternary ammonium salts and HBDs) as this type of DESs was used in this research work.

1.4.1 Electrochemistry

DESs were first used in electrochemistry as electrolytes for electrodeposition of metals and as solvents for electropolishing and electrochemical reactions.

Abbott *et al.*^[40,41] showed that some metals oxides such as ZnO, PbO₂, CuO, NiO and Ag₂O dissolve in choline chloride/urea DES and investigated the ability to electrowin the metals from solution taking advantage of the ionic conductivity of this

mixture ($1\text{--}12 \text{ mS}\cdot\text{cm}^{-1}$ in a temperature interval of 20 to 100 °C). It was demonstrated that despite the relatively small potential window of choline chloride/urea on a platinum electrode (-1.2 to + 1.25 V vs Ag), metals can be reduced to the metallic state, with exception of CuO, and deposited from the mixed metal oxide matrix with high current efficiencies (> 95%). Compared with aqueous solutions, the considerably better current efficiencies obtained in this case derived from the fact that unlike water there is no electrolysis of DES at these potentials.

In a similar way, the electrolytic deposition of Zn, Sn and Zn/Sn alloys from a solution of the metal chloride salts (ZnCl_2 and SnCl_2) in choline chloride/urea and choline chloride/ethylene glycol DESs were also described by the same research group.^[42] The authors observed that deposition kinetics and thermodynamics in these systems completely differ from the aqueous processes. Particularly, it was found that is possible to obtain Zn/Sn alloys with different morphology and composition by only changing the DES.

One of the major drawbacks of carrying out electrodeposition of metals in aqueous solutions is the narrow electrochemical window of water, which restricts deposition of metals with redox potential higher than that of water. Although the electrochemical windows are significantly smaller in DESs than those for some imidazolium-based ILs, they are sufficiently wide to allow the deposition of metals such as Zn with high current efficiencies.

1.4.2 Dissolution and purification processes

DESs exhibit excellent solvent properties owing to its capacity of donating or accepting electrons or protons to form hydrogen bonds. It has been found that a wide variety of solutes are highly soluble in DESs. For example, in choline chloride/urea DES at 50 °C, high solubilities are observed for inorganic salts (e.g., $\text{LiCl} > 2.5 \text{ mol}\cdot\text{L}^{-1}$), salts sparingly soluble in water (e.g., AgCl solubility = $0.66 \text{ mol}\cdot\text{L}^{-1}$), aromatic acids (e.g., benzoic acid solubility = $0.82 \text{ mol}\cdot\text{L}^{-1}$) and amino acids (e.g. D-alanine solubility = $0.38 \text{ mol}\cdot\text{L}^{-1}$).^[13]

As previously mentioned, DESs have been employed for dissolution of metal oxides given the complexation abilities of ligands such urea and other HBD that can be part of these type of liquids. The idea of using DESs for this purpose was

first explored by Abbott *et al.*,^[13,15] by showing that it was possible to dissolve CuO in choline chloride/urea DES ($0.12 \text{ mol}\cdot\text{L}^{-1}$) and to achieve high solubilities for ZnO, CuO and Fe_3O_4 in mixtures composed of choline chloride and carboxylic acids (malonic acid, oxalic acid and phenylpropionic acid). Additionally, the solubility of each oxide was markedly different depending on the DES used, demonstrating that these solvents can preferentially extract one metal oxide from a mixed mineral source.

Although the studies of the dissolution properties of DES have been mainly focused on the dissolution of inorganic salts and metal oxides, there are few reports that describe the dissolution of organic compounds in these media. Morrison *et al.* showed that poorly soluble drugs such as danazol, griseofulvin, itraconazole and AMG517 (N-(4-(6-(4-(trifluoromethylphenyl)pyrimidin-4-yloxy)-1,3-benzothiazol-2-yl)acetamide) are highly soluble in choline chloride/urea and choline chloride/malonic acid DESs. For AMG517, the solubility of the drug was $0.01 \text{ mg}\cdot\text{mL}^{-1}$ and $0.4727 \text{ mg}\cdot\text{mL}^{-1}$ in choline chloride/urea and choline chloride/malonic acid, respectively, which correspond to an increase of 100 and almost 5000 fold with respect to its solubility in pure water ($<0.0001 \text{ mg}\cdot\text{mL}^{-1}$).

More interestingly, DES have been proven to be promising solvents for nucleic acids and some biopolymers. DNA powder was found to be soluble and stable, both chemically and structurally, in mixtures of choline chloride with glycerol and ethylene glycol after six months of storage.^[43] It was observed that concentrations up to $55 \text{ mg}\cdot\text{g}^{-1}$ and $25 \text{ mg}\cdot\text{g}^{-1}$ of DNA in choline chloride/ethylene glycol (1:2) and choline chloride/glycerol (1:2), respectively, resulted in the formation of transparent solutions. These were outstanding results considering the maximum solubility achieved of DNA in conventional ILs ($1 \text{ mg}\cdot\text{g}^{-1}$).

DESs have also been used for purification of raw biodiesel.^[20] The production of biodiesel from the transesterification reaction of vegetable oils with methanol or ethanol yields glycerol as by-product. Removal of glycerol from biodiesel must be performed before it can be used as fuel. Even though several methods have been proposed for its purification, these are associated with high costs and in some cases glycerol remains in non-negligible amount. Using ethylammonium chloride / glycerol DES it was possible to completely extract the residual glycerol given the

high affinity of the salt for this compound. The DES/biodiesel ratio was adjusted in order to obtain mixtures with a molar ratio of 1:2 after extraction of the polyol.

1.4.3 Catalytic processes

Examples of catalytic reactions where DESs have been used as solvents include base-, acid- and transition-metal-catalyzed reactions and even biocatalytic transformations.

Han and co-workers reported the conversion reaction of inulin, a natural oligosaccharide composed of glucose and fructose units, into 5-hydroxymethylfurfural (HMF) using choline chloride-based DESs as catalysts and solvents.^[44] HMF is a valuable molecular building block for the production of fuel additives and it is usually obtained from the acid-catalyzed dehydration of monosaccharides such as fructose. The authors found that inulin is highly soluble in choline chloride/oxalic and choline chloride/citric acid DESs, $150 \text{ mg}\cdot\text{g}^{-1}$ and $28 \text{ mg}\cdot\text{g}^{-1}$, respectively. The solubility of inulin in DESs made possible the combination of hydrolysis of this oligosaccharide and dehydration of fructose in one pot. It was found that using a high temperature favors the formation of HMF while a low temperature results in more fructose yield. Therefore, a two-temperature step reaction was proposed (inulin was first converted at 50°C for 2 h and then heated to 80°C for 2 h) to obtain a high yield (57%) and selectivity (65%). The reaction was also carried out in a biphasic system consisting of ethyl acetate and choline chloride/oxalic acid DES, where the product HMF is soluble in ethyl acetate and inulin and fructose are soluble in DES. The biphasic system allowed the extraction of HMF from the DES-rich phase continuously and reduction of by-products. Moreover, DESs were recycled 6 times. These results are interesting from the green chemistry point of view since harsh acidic conditions are avoided and recycling of the solvent/catalyst is possible.

The first biocatalytic reaction in DESs was reported by Gorke *et al.* in 2008.^[33] They investigated as a test reaction, the hydrolase-catalyzed transesterification of ethyl valerate with 1-butanol in choline chloride/urea and choline chloride/glycerol DESs, among others. It was found that *Candida antarctica lipase B* (CALB) and its immobilized form (*i*CALB) in DESs catalyze the transesterification reaction with

conversions comparable to that in toluene. Surprisingly, although urea is a well-known denaturant of proteins, the stability of CALB was at least 20 to 35-fold more in choline chloride/urea DES than in aqueous solution of the components (10 M urea or 5 M choline chloride). In addition, the initial specific activity of iCALB-catalyzed transesterification was comparable or higher in DESs than in typical ILs. Furthermore when choline chloride/glycerol DES was used, it was observed that glycerol was 4600-fold less reactive in transesterification reaction as a component of DES than the polyol itself, preventing less competition between glycerol and the product 1-butanol.

1.4.4 Materials synthesis

Up to now, the most studied and successful applications of DES have been in the field of electrochemistry as electrolytes or solvents for electrodeposition and electropolishing processes due to the high solubility of metal oxides in DESs and their high ionic conductivity compared to non-aqueous solvents. Notwithstanding, this situation is currently changing and the scope of the uses of DESs is now widening because, besides all the already mentioned interesting features, they can also play a template role for the preparation of materials with defined morphology.

In 2004, Morris *et al.*^[45] described the synthesis of a microporous crystalline zeolite by using an imidazolium-based IL and choline chloride-based DES. It was observed that IL and DES can act as both solvent and structure-directing agent (SDA, also known as template) around which the inorganic frameworks order, leading to four aluminophosphate zeotype frameworks under different experimental conditions from the commonly used (ambient pressure and no addition of structure-directing agent). Having found that DESs can play two roles simultaneously in the synthesis of metal phosphates, other research groups have extended this strategy to the preparation of metal-organic frameworks (MOFs),^[46] metal oxides, nanomaterials,^[47] carbon materials, among others, where DESs not only act as solvent and template, but also as a precursor.

One example of the use of DESs for the preparation of nanomaterials is the shape-controlled synthesis of gold nanoparticles.^[48] It is well-known that the presence of surfactants and stabilizers during the synthesis of nanoparticles is crucial

for controlling their shape and to avoid agglomeration. In this case, star-shaped Au nanoparticles were successfully obtained at room temperature by reduction of $\text{HAuCl}_4 \cdot 4\text{H}_2\text{O}$ by L-ascorbic acid using choline chloride/urea (1:2) DES as solvent and surfactant. Snowflake-like nanoparticles and nanothorns were also obtained by adjusting the content of water in DES.

Del Monte and collaborators have extensively studied the use of DESs for the preparation of carbon materials with hierarchical porosity for the sustainable capture of CO_2 and energy storage. The research group have reported the synthesis of different binary and ternary DESs (e.g., choline chloride/resorcinol, choline chloride/urea,^[49] choline chloride/resorcinol/3-hydroxypyridine)^[50] that, upon polycondensation with formaldehyde and subsequent carbonization of the obtained gels resulted in the formation of monolithic carbons with high surface areas. In case of choline chloride/resorcinol DES, one the components forming the DESs (resorcinol) acts as precursor of the polymer phase whereas the second (choline chloride) acts as SDA following a synthetic mechanism based on DES rupture and controlled delivery of the segregated SDA into the reaction mixture.

DESs have also shown promise as multifunctional solvents for the synthesis of polymeric materials. Since the work developed in this thesis was focused on this type of applications, a more detailed revision of the use of DESs in this area is given below and in the beginning of the following chapters.

1.4.4.1 Polymer synthesis

Despite the attractive features of DESs for materials preparations, only a few works describe the use of DESs in polymerization processes. These reports include free-radical polymerization, polycondensation and ring opening polymerization.

Poly(octanediol-co-citrate) (POC) elastomers containing lidocaine, a local anesthetic and anti-inflammatory compound, were synthesized by using DESs composed of one of the polymer precursors (1,8-octanediol) and the active pharmaceutical ingredient (lidocaine).^[51] DESs enabled solubilization of the second polymer precursor (citric acid) at temperatures below 100 °C, thus avoiding degradation of lidocaine and allowing its incorporation in high loadings. After solubilization of citric acid, DESs were used as reaction media for the polymerization reaction in

the absence of any further solvent. The ability of these polymers to locally deliver the drug was evaluated by release studies. Shortly after, the same research group reported the synthesis of POC elastomers by using DESs also composed of 1,8-octanediol but with different halide salts such as choline chloride, tetraethylammonium bromide, hexadecyltrimethylammonium bromide, and methyltriphenylphosphonium bromide with the aim to confer antibacterial properties to the polymer network.^[52] Quaternary ammonium compounds are well known as bactericidal compounds given their antiseptic and disinfectant activities. Hence, incorporation of these salts to the elastomeric polymers allowed them to behave in a dual manner, as inhibitors of bacterial growth and cellular supports. In both elastomer syntheses none of the used compounds was wasted as DESs played the role of precursor, solvent and pharmaceutical ingredient or bactericidal compound simultaneously.

Carranza *et al.*^[53] demonstrated the formation and polymerization of high internal phase emulsions (HIPEs) with acrylic monomers (methyl methacrylate, lauryl acrylate and stearyl methacrylate) as a continuous phase and choline chloride/urea DES as non-aqueous internal phase. HIPEs are defined as emulsions wherein the volume of the droplet (internal phase) is higher than 74% of the total emulsion volume. Introduction of a monomeric continuous phase and subsequent extraction of the internal phase after polymerization enables the synthesis of porous functional matrices, known as poly(HIPEs). The authors found^[53] that methacrylates provided the most desirable systems with high conversions, thermal stability, open porosity and consistent droplet diameter to pore diameter. They argued that in these cases methyl group possibly acts as an “anchor” allowing better monomer-surfactant interaction at the monomer-DES interphase and exposing all methacrylic groups for a more efficient polymerization. The absence of water in this synthetic process allows preparation of poly(HIPEs) at a wide range of temperatures and pressures, not possible when using water due to evaporation. Furthermore, it was possible to recover 82% to nearly 95% of DESs used.

Recently, the ring opening polymerization of ϵ -caprolactone using eutectic mixtures of methanesulfonic acid (MeSO_3H) and the guanidine 1,5,7-triazabicyclo-[4.4.0]dec-5-ene (TBD) as the catalyst was investigated. It was found that MeSO_3H and TBD, two organic compounds frequently used as catalysts for this type of reaction, are capable of forming eutectic mixtures at a certain molar ratio. The au-

thors evaluated the performance of the eutectic mixtures as bifunctional catalysts by carrying out the polymerization reaction in these media. Interestingly, neither further solvent nor initiators were required for the ring opening polymerization of ϵ -caprolactone. The polycaprolactones obtained were highly crystalline (87%) and exhibited an excellent capability to support the growth of mammalian cells.

1.5 Overview and aim of the thesis

Given all the interesting features of DESs is not hard to envisage some potential applications of these liquids in the area of material synthesis. Nonetheless, the use of DESs in this field has not been widespread so far, and particularly the literature regarding polymer synthesis is really scarce. In this context, the general aim of this work is to ponder DESs as versatile solvents for novel and sustainable synthesis of different types of polymers, where DESs not only play the role of solvent but also as precursor and compound with specific functionality (all at the same time), as well as to assess the possible advantages offered by these synthetic approaches over the conventional methods. In order to accomplish this goal, three different systems were devised going from the synthesis of hydrogels to enzyme-mediated polymerization to the synthesis of a conductive polymer. The research presented here encompasses the specific objectives listed below.

1. Synthesis and characterization of pH responsive poly(acrylic/methacrylic)-drug complexes from lidocaine hydrochloride-based DESs with applications as controlled drug delivery systems.
2. Elucidation of lidocaine hydrochloride transport mechanism and its release kinetics from the polymeric complexes.
3. Biocatalytic synthesis of polyacrylamide in nearly non-aqueous choline chloride-based DESs and study of the solvent effects on the structural conformation and thermal stability of the enzyme (horseradish peroxidase).
4. Characterization of polyacrylamide obtained in DESs (molecular weight and polydispersity index), and comparison of its properties with those attained for the polymer synthesized in totally aqueous media.

5. Design of novel aniline-hydrochloride based-DESs for the all-in-one synthesis of conductive polyaniline monoliths and determination of the electrical conductivity, oxidation state and “doping” level of the polymer.

Herein, the structure and content of this thesis is summarized. In chapter 2, a general overview of the existing challenges and difficulties for the incorporation of active pharmaceutical ingredients (APIs) to polymeric matrices (e.g., API polymorphism and solubility) is presented. Likewise, the most relevant breakthroughs in the topic involving the use of ILs and DESs are described, and how the already mentioned drawbacks can be overcome by incorporating ILs and DESs to the synthetic pathways of these materials. The use of DES formed by monomers as HBDs (acrylic and methacrylic acid) is proposed to carry out the polymerization reaction and *in situ* incorporation of the drug in the absence of any further solvent. The results and discussions derived from the research to achieve objectives 1 and 2 are embodied in this chapter, with emphasis in the advantages offered by this synthetic approach over the traditional methods from both, the environmental and process efficiency point of view.

In chapter 3, the use of DESs as reaction media to perform enzyme-mediated polymerizations is explored, based on the fact that some lipases shows good catalytic activity in choline chloride-based DESs despite the presence of HBDs such as urea, a well known protein denaturant. First, the chapter describes the advantages of employing enzymes in organic synthesis in contrast to the inorganic catalysts commonly used, as well as the limitations of using these biocatalysts in aqueous media. The purpose of this section is to clearly state the importance to explore alternative reaction media that are capable of providing better conditions to maintain or to improve the enzyme performance for some specific reactions. A few of the most relevant attempts of carrying out reactions with enzymes in non-conventional media are reviewed. To achieve objectives 3 and 4, two of the most well-studied choline chloride-based DES (choline chloride/urea and choline chloride/glycerol) were selected as solvents for polyacrylamide synthesis using the catalytic system horseradish peroxidase/H₂O₂/2,4-pentanodione. The study of the effects on the enzyme performance (catalytic activity and thermal stability) and the characterization of the polymer are also encompassed in this chapter. It is important to highlight that this work is the first report describing the use of enzymes in DESs for free-radical polymerization reactions.

In the first section of chapter 4, a basic introduction to conductive polymers is provided. The problems associated to the poor processability of this type of polymers derived from their low solubility in water and typical organic solvents are exposed. In addition, the existing synthetic strategies, specifically the ones for improving polyaniline processability, are reviewed. Although these approaches represent a solution to the processability issue, generally, the electrical conductivity of the polymer is compromised, yielding polyaniline of low electrical conductivity in most of the cases. This chapter also comprises the design of DESs for the all-in-one synthesis of polyaniline 3D structures (monoliths), and new aniline hydrochloride-based mixtures are reported for the first time. The determination of the electrical conductivity, oxidation state and doping level of the resulting materials is also included. It is noteworthy that the preparation of highly conductive 3D polymer structures is a non-trivial task, nonetheless, by this novel synthetic method it is possible to obtain polyaniline monoliths with the highest electrical conductivity values reported to date.

Bibliography

- [1] K. R. Seddon, *J. Chem. Tech. Biotechnol.* **1997**, *68*, 351–356.
- [2] J. S. Wilkes, *Green Chem.* **2002**, *4*, 73–80.
- [3] G. Laus, G. Bentivoglio, H. Schottenberger, V. Kahlenberg, H. Kopacka, T. Röder, H. Sixta, Ionic liquids: current developments, potential and drawbacks for industrial applications, en, Article, **2005**.
- [4] T. Welton, *Chem. Rev.* **1999**, *99*, 2071–2084.
- [5] M. Antonietti, D. Kuang, B. Smarsly, Y. Zhou, *Angew. Chem. Int. Ed.* **2004**, *43*, 4988–4992.
- [6] M. Armand, F. Endres, D. R. MacFarlane, H. Ohno, B. Scrosati, *Nat. Mater.* **2009**, *8*, 621–629.
- [7] F. van Rantwijk, R. A. Sheldon, *Chem. Rev.* **2007**, *107*, 2757–2785.
- [8] R. D. Rogers, K. R. Seddon, *Science* **2003**, *302*, 792–793.
- [9] J. Gorke, F. Srienc, R. Kazlauskas, *Biotechnology and Bioprocess Engineering* **2010**, *15*, 40–53.
- [10] P. Walden, *Bull. Acad. Imper. Sci. (St. Petersburg)* **1914**, *8*, 405–422.
- [11] J. S. Wilkes, M. J. Zaworotko, *J. Chem. Soc. Chem. Commun.* **1992**, 965–967.
- [12] J. Fuller, R. T. Carlin, H. C. De Long, D. Haworth, *J. Chem. Soc. Chem. Commun.* **1994**, 299–300.
- [13] A. P. Abbott, G. Capper, D. L. Davies, R. K. Rasheed, V. Tambyrajah, *Chem. Commun.* **2003**, 70–71.
- [14] E. L. Smith, A. P. Abbott, K. S. Ryder, *Chem. Rev.* **2014**, *114*, 11060–11082.
- [15] A. P. Abbott, D. Boothby, G. Capper, D. L. Davies, R. K. Rasheed, *J. Am. Chem. Soc.* **2004**, *126*, 9142–9147.
- [16] Q. Zhang, K. De Oliveira Vigier, S. Royer, F. Jerome, *Chem. Soc. Rev.* **2012**, *41*, 7108–7146.

- [17] D. Carriazo, M. C. Serrano, M. C. Gutierrez, M. L. Ferrer, F. del Monte, *Chem. Soc. Rev.* **2012**, *41*, 4996–5014.
- [18] K. Shahbaz, F. S. Mjalli, M. Hashim, I. M. Al-Nashef, et al., *J. Appl. Sci.* **2010**, *10*, 3349–3354.
- [19] M. Hayyan, F. S. Mjalli, M. A. Hashim, I. M. AlNashef, *Fuel Process. Technol.* **2010**, *91*, 116–120.
- [20] A. P. Abbott, P. M. Cullis, M. J. Gibson, R. C. Harris, E. Raven, *Green Chem.* **2007**, *9*, 868–872.
- [21] Z. Maugeri, P. Dominguez de Maria, *RSC Adv.* **2012**, *2*, 421–425.
- [22] A. Hayyan, F. S. Mjalli, I. M. AlNashef, Y. M. Al-Wahaibi, T. Al-Wahaibi, M. A. Hashim, *J. Mol. Liq.* **2013**, *178*, 137–141.
- [23] K. Shahbaz, F. S. Mjalli, M. A. Hashim, I. M. AlNashef, *Energy Fuels* **2011**, *25*, 2671–2678.
- [24] M. A. Kareem, F. S. Mjalli, M. A. Hashim, I. M. AlNashef, *J. Chem. Eng. Data* **2010**, *55*, 4632–4637.
- [25] A. P. Abbott, R. C. Harris, K. S. Ryder, *J. Phys. Chem. B* **2007**, *111*, 4910–4913.
- [26] A. P. Abbott, G. Capper, S. Gray, *ChemPhysChem* **2006**, *7*, 803–806.
- [27] C. D'Agostino, R. C. Harris, A. P. Abbott, L. F. Gladden, M. D. Mantle, *Phys. Chem. Chem. Phys.* **2011**, *13*, 21383–21391.
- [28] A. Pandey, R. Rai, M. Pal, S. Pandey, *Phys. Chem. Chem. Phys.* **2014**, *16*, 1559–1568.
- [29] C. Reichardt, *Chem. Rev.* **1994**, *94*, 2319–2358.
- [30] C. Ruß, B. König, *Green Chem.* **2012**, *14*, 2969–2982.
- [31] G. Imperato, S. Hoger, D. Lenoir, B. Konig, *Green Chem.* **2006**, *8*, 1051–1055.
- [32] Y. Wu, T. Sasaki, K. Kazushi, T. Seo, K. Sakurai, *J. Phys. Chem. B* **2008**, *112*, 7530–7536.
- [33] J. T. Gorke, F. Srienc, R. J. Kazlauskas, *Chem. Commun.* **2008**, 1235–1237.

- [34] F. del Monte, D. Carriazo, M. C. Serrano, M. C. Gutiérrez, M. L. Ferrer, *ChemSusChem* **2014**, *7*, 999–1009.
- [35] Y. H. Choi, J. van Spronsen, Y. Dai, M. Verberne, F. Hollmann, I. W. Arends, G.-J. Witkamp, R. Verpoorte, *Plant Physiol.* **2011**, *156*, 1701–1705.
- [36] M. Hayyan, M. A. Hashim, A. Hayyan, M. A. Al-Saadi, I. M. AlNashef, M. E. Mirghani, O. K. Saheed, *Chemosphere* **2013**, *90*, 2193–2195.
- [37] Q. Wen, J.-X. Chen, Y.-L. Tang, J. Wang, Z. Yang, *Chemosphere* **2015**, *132*, 63–69.
- [38] K. Radošević, M. C. Bubalo, V. G. Srček, D. Grgas, T. L. Dragičević, I. R. Redovniković, *Ecotoxicol. Environ. Saf.* **2015**, *112*, 46–53.
- [39] B. Kudłak, K. Owczarek, J. Namieśnik, *Environ. Sci. Pollut. Res.* **2015**, *22*, 11975–11992.
- [40] A. P. Abbott, G. Capper, D. L. Davies, R. K. Rasheed, P. Shikotra, *Inorg. Chem.* **2005**, *44*, 6497–6499.
- [41] A. P. Abbott, G. Capper, D. L. Davies, K. J. McKenzie, S. U. Obi, *J. Chem. Eng. Data* **2006**, *51*, 1280–1282.
- [42] A. P. Abbott, G. Capper, K. J. McKenzie, K. S. Ryder, *J. Electroanal. Chem.* **2007**, *599*, 288–294.
- [43] D. Mondal, M. Sharma, C. Mukesh, V. Gupta, K. Prasad, *Chem. Commun.* **2013**, *49*, 9606–9608.
- [44] S. Hu, Z. Zhang, Y. Zhou, J. Song, H. Fan, B. Han, *Green Chem.* **2009**, *11*, 873–877.
- [45] E. R. Cooper, C. D. Andrews, P. S. Wheatley, P. B. Webb, P. Wormald, R. E. Morris, *Nature Aug.* **2004**, *430*, 1012–1016.
- [46] J. Zhang, T. Wu, S. Chen, P. Feng, X. Bu, *Angew. Chem. Int. Ed.* **2009**, *48*, 3486–3490.
- [47] D. V. Wagle, H. Zhao, G. A. Baker, *Acc. Chem. Res.* **2014**, *47*, 2299–2308.
- [48] H.-G. Liao, Y.-X. Jiang, Z.-Y. Zhou, S.-P. Chen, S.-G. Sun, *Angew. Chem. Int. Ed.* **2008**, *47*, 9100–9103.
- [49] D. Carriazo, M. C. Gutiérrez, M. L. Ferrer, F. del Monte, *Chem. Mater.* **2010**, *22*, 6146–6152.

- [50] M. C. Gutierrez, D. Carriazo, C. O. Ania, J. B. Parra, M. L. Ferrer, F. del Monte, *Energy Environ. Sci.* **2011**, *4*, 3535–3544.
- [51] M. C. Serrano, M. C. Gutierrez, R. Jimenez, M. L. Ferrer, F. d. Monte, *Chem. Commun.* **2012**, *48*, 579–581.
- [52] S. García-Argüelles, M. C. Serrano, M. C. Gutiérrez, M. L. Ferrer, L. Yuste, F. Rojo, F. del Monte, *Langmuir* **2013**, *29*, 9525–9534.
- [53] A. Carranza, J. A. Pojman, J. D. Mota-Morales, *RSC Adv.* **2014**, *4*, 41584–41587.

But still try, for who knows what is possible?

— Michael Faraday

2

Controlled release of lidocaine hydrochloride from polymerized deep eutectic solvents

Polymers have been used extensively in the development of smart drug delivery systems by which the active pharmaceutical ingredient (API) can be administered with prolonged and good control.^[1–3] Currently, major attention has been paid to the polymorphism of APIs because, aside from the economic issues derived from patenting, it can have a profound impact on the way the API is processed, stored and delivered.

Formation of API-based eutectics is a well-known strategy to enhance the pharmacological performance of a given API, favoring their processability and allowing the synthesis of mixtures where a synergistic effect^[4,5] can be obtained (e.g., lidocaine/prilocaine eutectic cream).^[6] More recently, API transformation into ILs has proven to be useful to overcome polymorphism, opening new paths of already commercialized APIs and tuning their lipophilicity/hydrophobicity in order to enhance their transmembrane transport.^[7–10]

APIs require the aid of excipients to protect them from degradation before reaching their target and to modulate their release profiles. The incorporation of drugs into excipients has restrictions dictated by the physicochemical properties of each system.^[11] Polymers are frequently used as excipients owing to their compositional versatility, thermal properties and ease of storage.^[12] The main advantage of amorphous molecular level dispersions of APIs in polymers is that they prevent the crys-

tallization of low T_g amorphous APIs over pharmaceutically relevant time scales. Also they improve the dissolution rate, and hence possibly the bioavailability of the API. Nevertheless the amount of drug that can be efficiently dispersed in these systems requires time-consuming techniques such as directly mixing the two molten components, melt extrusion, and dissolution of each component in a mutual solvent followed by solvent removal.^[13] For these reasons, the *in situ* incorporation of APIs to polymeric matrices has been proposed. The advantages offered by using this strategy are mentioned in the next section through some examples.

2.1 Background

In contrast to solid blends of drugs and polymers, the direct polymerization of monomers in the presence of drugs allows synthesizing *in situ* polymers with a specific molecular weight or architectures required for the intended drug delivery systems. In addition, the drugs are homogeneously integrated into the matrix, and their release can be controlled depending on their “phase stability” in the pre-polymerized mixture and more importantly in the resulting polymer.^[14] In this regard different methods of polymerization have been explored, which include interfacial polymerization,^[15–17] anionic polymerization,^[18] free-radical polymerization^[19–21] and frontal polymerization.^[22] Polycondensation of silica precursors in the presence of an ibuprofenate-based ionic liquid has proven to be an efficient technique to produce drug-releasing systems with kinetics controlled by the nature of the silica wall.^[23] Whereas in another approach, the synthesis of the poly(diol-co-citrate) polyester by polycondensation was carried out under mild conditions, thanks to the formation of deep eutectic solvents with lidocaine or ammonium salts and one of the precursors of the polyester.^[24] Thus the lidocaine and ammonium salts integrated in the polyester were released depending on the biodegradable character of the resulting elastomer.^[25] The more obvious advantage that those approaches offer is the creation of drug delivery systems in one step such that the chance of losing drug activity by processing is minimized.

Recently our group showed that it is possible to control the exothermicity of frontal polymerization of highly reactive monomers such as acrylic acid, methacrylic acid and acrylamide by means of their complexation with ammonium salts and

transformation into DESs.^[26,27] Frontal polymerization is a way to produce polymers in unstirred reactors where localized thermal initiation generates a polymerization front that propagates through the reactor.^[28,29] Convective instabilities that interfere with front propagation can be avoided using inert fillers which increase the viscosity of the reaction mixture.^[30,31] The bubbles due to boiling of monomers are also avoided using solvents having high boiling points (e.g., DMSO or DMF).^[32] In our case, the ammonium salts (the active fillers) pose a dual role considering that they can modify the viscosity of the monomers by forming DESs and they are also the releasable molecules from the polymer after full conversion under solventless conditions.^[33]

Frontal polymerization of this type of polymerizable DES containing lidocaine hydrochloride was first described by our group.^[27] In the current work frontally polymerized DESs containing lidocaine hydrochloride as a drug delivery system were studied. For that, two DESs containing acrylic acid and methacrylic acid as hydrogen bond donors (HBDs), and lidocaine hydrochloride as the ammonium salt, were polymerized by free-radical frontal polymerization. After polymerization, the effects of pH and ionic strength on the kinetics of drug release were studied. This work expands the types of drug delivery systems that can be prepared exploiting DES chemistry, since the monomers (HBDs and crosslinkers) can be selected and copolymerized depending on the desired properties of the final drug delivery system suitable for transdermal technologies.

2.2 Materials and experimental methods

Lidocaine hydrochloride monohydrate, acrylic acid, methacrylic acid, 1-bis(*tert*-butylperoxy)-3,3,5-trimethylcyclohexane, ethylene glycol dimethacrylate, pentaerythritol triacylate, monosodium phosphate ($\text{NaH}_2\text{PO}_4 \cdot 2\text{H}_2\text{O}$) and disodium phosphate ($\text{Na}_2\text{HPO}_4 \cdot \text{H}_2\text{O}$) were purchased from Sigma-Aldrich and used as received. Phosphate buffer solutions at different molar concentrations and pH were prepared from both sodium phosphate salts.

2.2.1 Deep eutectic solvent synthesis

Deep-eutectic mixture counterparts were mixed together in an appropriate ratio and heated at 80 °C until a homogeneous liquid was obtained. For example, 1 mL (14.57 mmol) of acrylic acid and 1.4 g (43.71 mmol) of lidocaine hydrochloride monohydrate were mixed in a vial and placed in an oven at 80 °C for 1 h.

2.2.2 Polymerization of DESs

Frontal polymerization was carried out by dissolving 1,1-bis(*tert*-butylperoxy)-3,3,5-trimethylcyclohexane (Luperox 231®), as a thermal initiator and ethylene glycol dimethacrylate (EGDMA) or pentaerythritol triacrylate (PETA), as a cross-linker, in the different DESs. The resulting solutions after stirring were transferred to a long test tube (70 mm length and 6 mm diameter), and bubbled with N₂. The reactor was covered for thermal isolation. Then, the bottom part of the tube was heated with an electrical resistance (*ca.* 200 °C) for thermal initiation, whereas the upper end of the reactor remained open to atmospheric pressure (Figure A.1). After initiation, the exothermic nature of acrylic polymerizations promoted an increase in the temperature at the bottom portion of the reactor such that polymerization occurred upwards through the entire reactor without buoyancy-driven convection and with constant velocity.

2.2.3 Release experiments

The monoliths were soaked in deionized water until all the API was washed out, and the medium was then lyophilized. The solid residue was analyzed by proton-nuclear magnetic resonance (¹H NMR) to identify the API entrapped in the polymer during the polymerization. The controlled release of the drugs from the polymers was carried under sink conditions at 24 °C. The effect of pH and ionic strength on the release was tested in phosphate buffer solution (PBS) at pH 6 and 7 with two different ionic strengths (0.5 and 0.1 M). At predetermined time intervals, samples were withdrawn and immediately replaced with an equal volume of dissolution medium to keep the volume constant. Lidocaine hydrochloride concentration was determined by UV-vis spectroscopy at 263 nm (Figure A.2).

2.2.4 DESs characterization

The viscosity of the different DESs was measured with a Brookfield Digital Rheometer DV-III at 24 °C. Modulated differential scanning calorimetry (MDSC) was performed with a TA Instruments Model DSC Q-100 system, under a N₂ atmosphere on an aluminium pan in a sealed furnace, and at a scan rate of 5 °C min⁻¹ from -120 to 100 °C for AA–LidHCl DES and from -70 to 100 °C for MAA–LidHCl DES. The thermograms showed the melting point (T_m) and the glass transition temperature (T_g) of the DESs. TGA was performed with a Hi-Res Modulated TGA 295 thermogravimetric analyzer under a N₂ atmosphere on an aluminium pan, and at a heating rate of 10 °C min⁻¹ in a temperature range from 23 to 600 °C. FTIR spectra were collected on a Perkin–Elmer spectrophotometer using an ATR accessory with a diamond crystal in the range of 4000–650 cm⁻¹ at room temperature with a resolution of 4 cm⁻¹. The spectra shown are an average of 32 scans and were displaced along the y-axis for clarity. For the measurement, the sample was completely grind and an amount of it was placed on the ATR accessory.

2.2.5 Polymer-drug characterization

Once the polymerization front reached the top of the DES in the reactor, the conversion was calculated by dividing the dry polymer weight after soaking in distilled water (to wash out unreacted acrylates and the API) by the theoretical weight of the polymer that would result from full monomer-crosslinker polymerization. Those results were further verified by the loss of weight of the monomer (unreacted acrylic acid or methacrylic acid) in the temperature range between 140 and 200 °C following the derivative weight curve in a thermogravimetric analysis, and by the disappearance of the bands related to the monomer in FTIR spectra. The specific interactions between the components of the DESs were studied by FTIR and the spectra were displaced along the y-axis for clarity. The polymer-APIs were subjected to the same characterization.

The API released was characterized by ¹H NMR spectroscopy using a Bruker DRX-500 spectrometer.

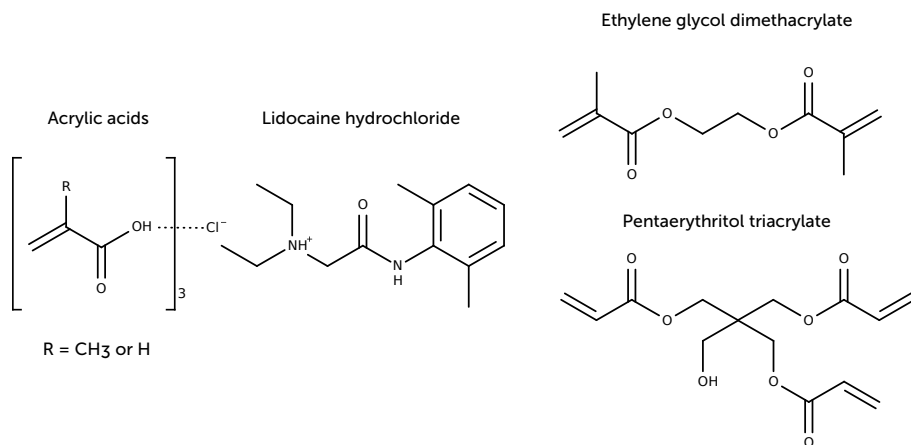


Fig. 2.1 Structures of the polymerizable LidHCl-based DESs and crosslinkers used in this work.

2.3 Results and discussion

2.3.1 Drug-based DESs

ILs have been used in pharmaceutical sciences for tuning the polarity of the active pharmaceutical ingredient (API) in such a way that the concentrations of sparingly soluble APIs are enhanced in aqueous media or lipophilic membranes.^[10] In the current work the transformation of APIs into DESs is used as a strategy to control the reactivity of acrylate monomers in free-radical polymerization^[34] to obtain drug delivery systems. Recently our group reported that the complexation of monomers by ammonium salts results in control over the exothermicity of free-radical polymerization of acrylates in the bulk, *e.g.*, in frontal polymerization (Figure A.3).^[26] It is therefore crucial to ensure that the mixtures of APIs and monomers — the polymerizable DESs — exhibit the characteristic properties of DESs. For that, modulated DSC was used to study the thermal properties of mixtures of monomers and APIs, namely acrylic acid (AA), methacrylic acid (MAA) and lidocaine hydrochloride (LidHCl), respectively (Figure 2.1).

The compositions of the DESs were optimized such that the viscosity and the density of double bonds exhibited by DESs were adequate to sustain frontal polymerization.^[27,35] This means that even when the mixtures used in this work might not correspond to the eutectic point, the combination of viscosity and density of

Table 2.1 Viscosity and melting point (T_m) of polymerizable the LidHCl-based DESs and their components.

DES	HBD:QAS (molar ratio)	Viscosity (MPa·s)	DES T_m (°C)	HBD T_m (°C)	QAS T_m (°C)
AA–LidHCl	3:1	231	-78.4	13	80-82
MAA–LidHCl	3:1	315	6.8	16	80-82

QAS: Quaternary ammonium salt

double bonds (monomer/salt ratio) was selected to achieve frontal polymerization (Table 2.1). However, API-based eutectic mixtures still show melting points or glass transitions below the melting points of their pure components, (Figure A.4), and so they match one of the principal characteristics of a DES;^[36,37] thus, they will be referred to as DESs throughout.

Fourier transform infrared (FTIR) spectra of DESs disclose the intermolecular hydrogen-bond interaction between the HBD and the quaternary ammonium salt (QAS) mainly in the carbonyl region. For instance, in AA–LidHCl DES, the carbonyl band of AA was originally located at 1696 cm⁻¹ in pure AA, it shifts and broadens as a result of the disruption of the AA dimer by creating a new type of hydrogen bond. The bands at 1688 and 1722 cm⁻¹ are related to the carbonyl group in the DES and the free form respectively, as described elsewhere.^[27] Also the band at 1432 cm⁻¹, which corresponds to CH₂, shifts toward lower wave numbers because of the HBD nature of AA. In the case of MAA–LidHCl the carbonyl band notably decreases its intensity and becomes broader, revealing its association into a DES complex (Figure 2.2). It is worth noting that the N–H bending vibration and C–N stretching at 1543 cm⁻¹ from LidHCl do not shift after forming DESs with acrylic acids. This suggests that DESs association is mainly due to an anion–HBD complex (Figures A.5, A.6 and 2.3).^[38,39]

2.3.2 Polymerization of DESs

The main drawback of free-radical polymerization in the bulk of API-monomer mixtures is that undesirable side-reactions between the API and the monomer can occur due to the high temperatures. On the other hand, the presence of remaining monomers (that might be toxic) and the need for post-purification steps make this approach difficult to perform. Thus, complete conversion is necessary. In this re-

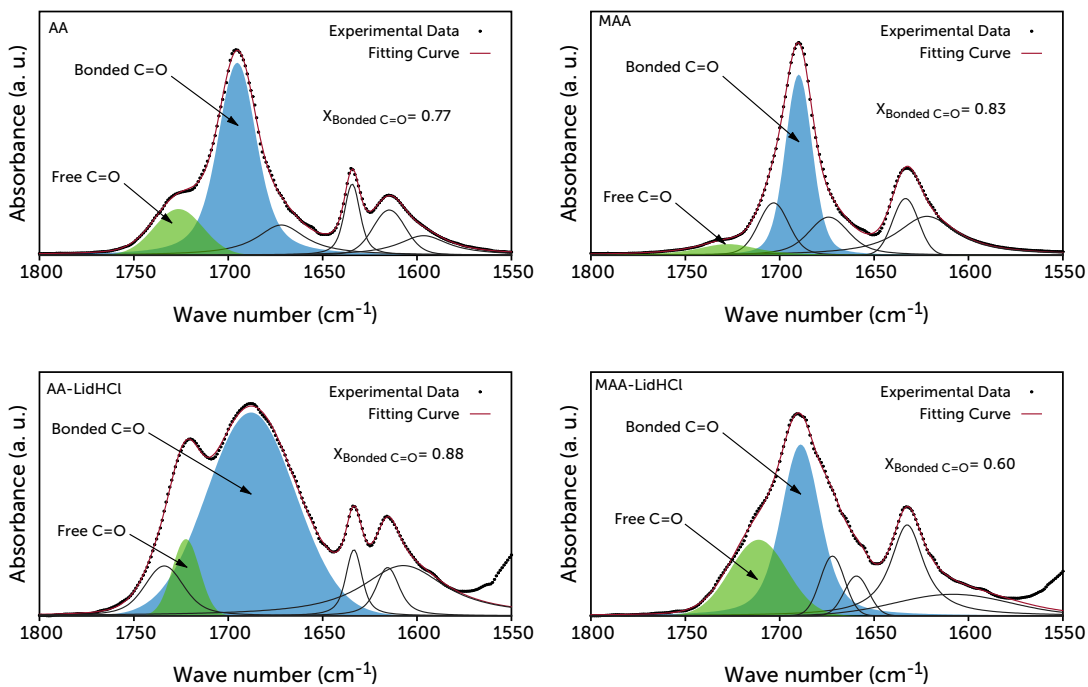


Fig. 2.2 Analysis of carbonyl region in AA, MAA, and AA–LidHCl and MAA–LidHCl DESs. The spectra were deconvoluted using the Fityk software.^[40]

gard, mixtures of acrylamide and diclofenac sodium salt frontally polymerized in water with high conversion have been reported.^[22] The resultant drug delivery systems showed a heterogeneous appearance due to the poor control of the exothermicity of the reaction that led to boiling of the water causing irregular surfaces; hence the release of diclofenac was difficult to control, unless a high amount of crosslinker was added (up to 40 wt%).

It has already been pointed out that the presence of the non-polymerizable counterpart helps to reduce the temperature of the acrylate polymerization, but it is also plausible that the formation of DESs through hydrogen-bonding prevented eventual degradation of the API caused by high temperatures during polymerization.^[24]

Frontal polymerization of DESs containing LidHCl was performed as previously reported.^[26] The high viscosity of the polymerizable DESs allowed ascending frontal polymerization without buoyancy-driven convection. The experimental setup and results from polymerization of DESs are listed in Table 2.2.

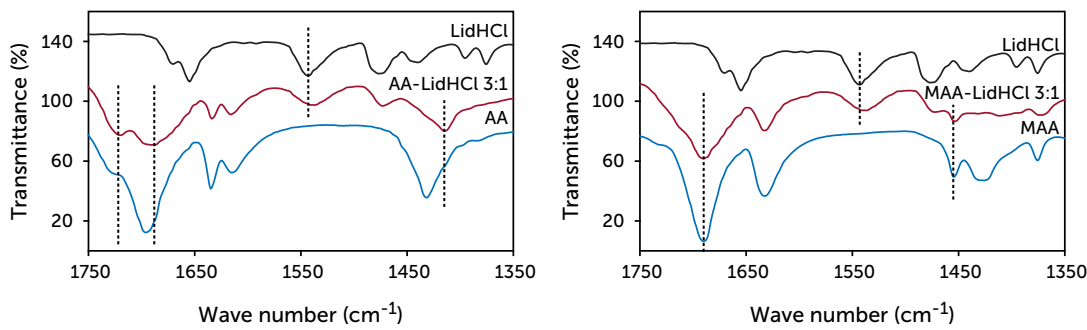


Fig. 2.3 ATR-FTIR spectra of polymerizable LidHCl-based DESs and their components in the range of 1350 to 1750 cm⁻¹.

The rapid polymerization coupled with the DES nature of the components produced homogeneous and solid monoliths, *i.e.*, no segregation of LidHCl occurred during polymerization (Figure 2.4).

Figure 2.5 shows that the spectrum of pure poly(acrylic acid) (PAA) does not match the corresponding bands of PAA in the spectrum of the PAA–LidHCl monolith in the carbonyl region; the same occurred for poly(methacrylic acid) (PMAA). Thus, the resultant polymer-API can be considered as complexes due to the strong interactions between their components,^[41–43] which are shown by the FTIR spectra. See for instance the band at 1700 cm⁻¹ in PAA in Figure 2.5 (left) that corresponds to the C=O group. It is shifted because it is involved in a polymer-API complex through H-bonding (*e.g.* it splits and shifts to 1722 cm⁻¹ in the PAA–LidHCl complex), resembling the DES precursor;^[35] the same occurs with PMAA–LidHCl. However the band at 1157 cm⁻¹ that corresponds to bending in the plane of CH₂^[44] does not change in shape or intensity compared with bare PAA due the lack of any interaction with LidHCl during its polymerization. It is also clear the disappearance of the bands related to monomers (acrylate double bond) in the polymer complexes due to complete polymerization of DESs, in accordance with gravimetric and thermo-

Table 2.2 Experimental setup and polymerization results.

DES	Initiator (% mol to monomer)	Crosslinker (% mol to monomer)	Front temperature (°C)	Front velocity (mm·s ⁻¹)
AA-LidHCl	1	0.7	138	0.49
MAA-LidHCl	2	0.7	135	0.22
AA-LidHCl/MAA-LidHCl	2	0.7	131	0.19



Fig. 2.4 Photograph of the polymer-drug monoliths.

gravimetric analyses (Figure A.7). Those bands are located at 1634 and 1613 cm^{-1} in AA, and at 1637 cm^{-1} in MAA.

2.3.3 Kinetics of LidHCl release

From Figure 2.6 it can be seen that both polymer systems — PMAA and PAA — under every condition studied (pH and ionic strength), released the maximum theoretical amount of API present in the DES within *ca.* 30 hours or less. The ^1H NMR spectra of the released compounds reveal that only LidHCl was released (Figure A.8), and it remained unaffected by the polymerization process since comparing the signals of the spectra corresponding to the supernatant recovered after release of LidHCl from the polymer complexes in PBS to those appearing in the spectrum of

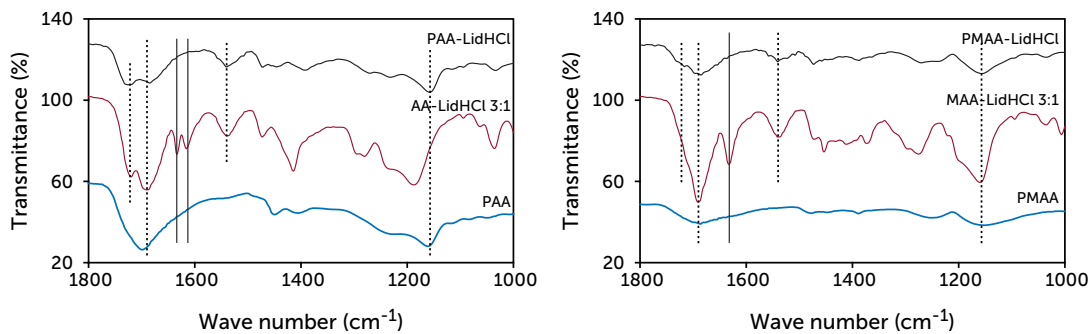


Fig. 2.5 ATR-FTIR spectra of polymerizable DESs, the polymer complexes resulting after polymerization of DESs, and the pure polymers. Some important bands are indicated with dashed lines while the related to monomer with solid lines.

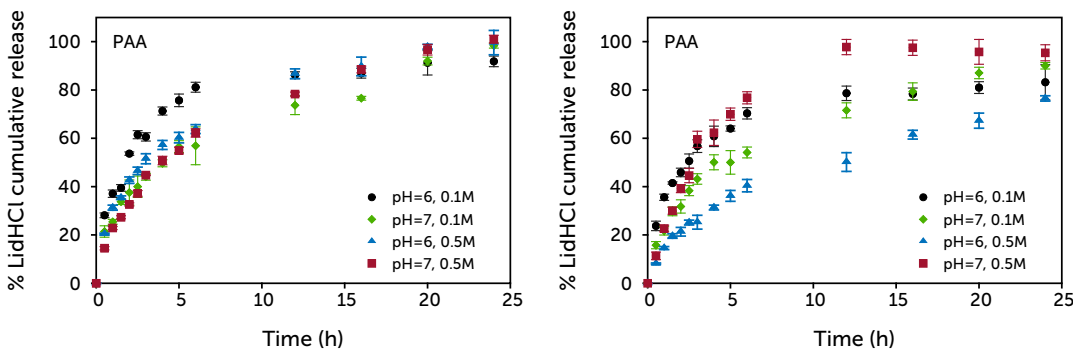


Fig. 2.6 Kinetics of the release of LidHCl from PAA and PMAA crosslinked with EGDMA in phosphate buffer at different pH and ionic strength under sink conditions at 24 °C. Experiments were at least triplicated and the standard deviation error bars for each point are shown.

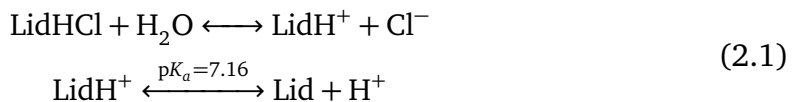
pure LidHCl monohydrate in D₂O (reference), they are located at the same position and no other signals appear.

Poly(acrylic acids) are a well-known class of polyelectrolytes that are pH responsive. As hydrogels, their swelling depends on the protonation state of the pendant COOH groups. In consequence, swelling in these systems is due to electrostatic repulsion. The pK_a of PAA is around 4.8–6.7 constrained by the molecular weight and the crosslinking degree,^[45] while for PMAA it is between 6.4–7.^[46] Regarding the ionic strength, the general behavior is that increasing the salt concentration in the hydrogel increases the degree of electrostatic screening. Therefore, the electrostatic repulsion between hydrogel charges, which causes swelling, is prevented by the presence of the counterions of the salt.^[47]

Herein, the experiments were conducted at pH 6 and pH 7 to show how the amount of drug release can be controlled by the pH of the medium.

It is expected that both the pH and the ionic strength would have a strong impact on the kinetics of the release of APIs. The release of drugs from this class of hydrogels has been well studied, and it is generally accepted that diffusion and swelling are the phenomena that govern the drug release from the hydrogels.^[48] LidHCl, a local anesthetic, is the type of API whose degree of ionization is also pH dependent, *i.e.*, the efficiency of dissolution and delivery varies with pH. Such dependence means that, in the case of LidHCl ($pK_a = 7.16$), an increase in the pH of the medium

results in conversion of positively charged molecules into electrically neutral species, reducing their solubility in aqueous media (Equation 2.1).^[49]



In the present case, the kinetics of the API release involves not only the simultaneous absorption of water and desorption of the drug via swelling-controlled diffusion, but also API dissolution that is pH-dependent. Thus the kinetics depicted in Figure 2.6 are the result of the competition of different mechanisms operating at the same time, although under certain pH and ionic strength some phenomena become more relevant and are the predominant mechanisms. By comparing the kinetics of swelling and the drug release, the overall kinetics can be dissected into two regimens depending on polymer swelling and drug solubility, which will be discussed below.

The first stage of the release involves the swelling of the polymer-API complex from the glassy state to the swollen state, which is accompanied by the diffusion of the API. In the case of PAA–LidHCl, 60% of the cumulative release of LidHCl occurs within the first 3 to 6 hours depending on the pH and the ionic strength of the media; whereas it takes 4 to 16 hours for PMAA–LidHCl depending on the pH and ionic strength. The first stage of the release fits well to the Fickian model for all cases ($R^2 > 0.9$, Figure A.9), such that the process can be considered mainly as a swelling-controlled mechanism following Equation 2.2.^[50,51]

$$\frac{M_t}{M_\infty} = kt^n \quad (2.2)$$

where M_t and M_∞ are the amounts of drug released at time t , and at equilibrium, respectively; k is the proportionality constant and n is the diffusional exponent, which is 0.5 for the Fickian model.

It is worth noting that the amount of LidHCl released at pH 6 is higher than at pH 7, irrespective of ionic strength in the PAA case, and at low ionic strength in the PMAA case. This could be considered as an anomalous behavior due to the fact that polyacrylic acids swell more in basic than acid media, and in consequence the

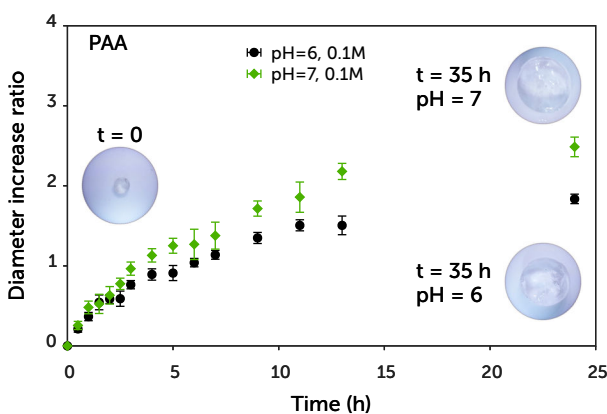


Fig. 2.7 Swelling behavior of PAA crosslinked with EGDMA in phosphate buffer at different pH values. Experiments were at least triplicated and the standard deviation error bars for each point are shown.

release should be higher at pH 7 than 6. In order to disregard this mechanism, the diameter of cylinders of PAA–LidHCl (as a function of volume) was measured over time at pH 6 and 7 at a fixed ionic strength (Figure 2.7). It is clear that the swelling follows Fickian behavior ($R^2 > 0.99$), which indicates that the incorporation of the API does not interfere with the macroscale swelling of PAA hydrogels containing LidHCl (Figure A.10).

However, the dissolution of the API in aqueous media, and hence its ionization, plays a crucial role in the release. As mentioned above, the pK_a of LidHCl makes the molecule soluble at pH 6 due to its ionization to LidH^+ and Cl^- ions (see Equation 2.1). During the onset of swelling, the dissolution rate of LidHCl becomes more relevant to finally being the controlling factor due to the high concentration of the drug in the network.^[52] The ionic strength also affects the trend of the first stage of the release by diminishing the swelling of PAA and also increasing the solubility of LidHCl via the diverse ion effect (Figure 2.8, top).^[53] This double effect is notable in Figure 2.8 (top right) in which both phenomena seem to nullify themselves in a sort of “buffering effect”.^[54] On the other hand, the release of LidHCl from PMAA is higher at pH 6 only with low ionic strength (Figure 2.8, bottom left). At 0.5 M the charge screening causes the release to be controlled by the swelling rather than by the API dissolution; as a result, the release rate is considerably higher at pH 7 (close to the pK_a of PMAA) enhanced by the diverse ion effect (Figure 2.8, bottom right).^[47]

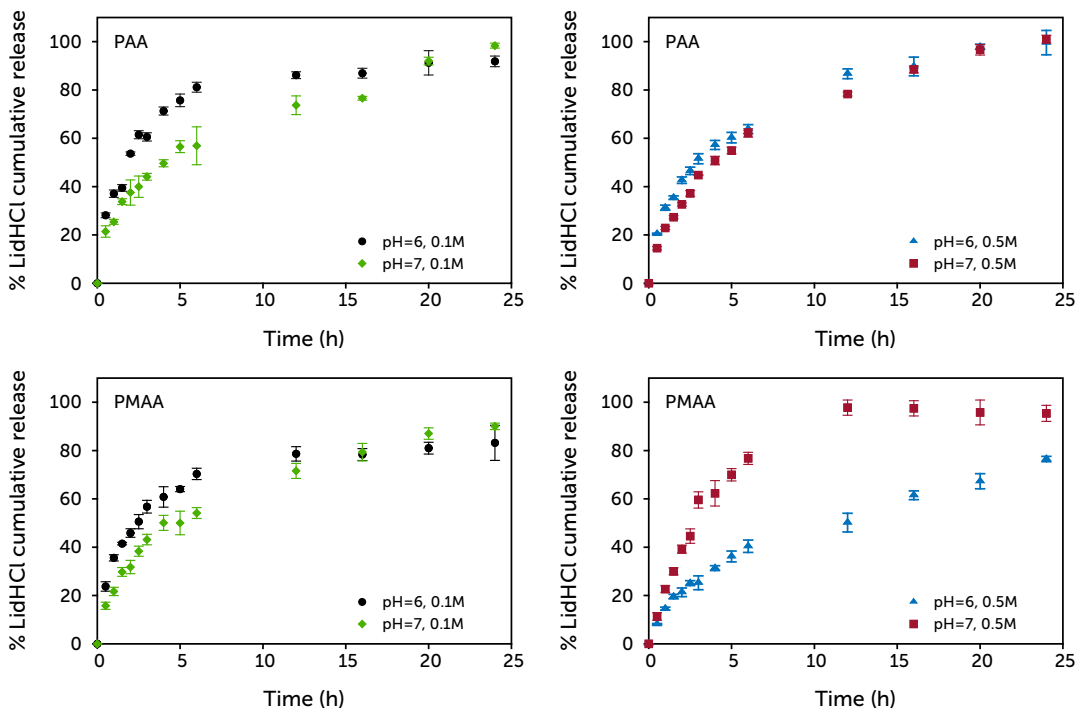


Fig. 2.8 Effect of pH and ionic strength on the release of LidHCl from PAA and PMAA hydrogels crosslinked with EGDMA in phosphate buffer under sink conditions at 24 °C. Experiments were at least triplicated and the standard deviation error bars for each point are shown.

Nevertheless, in all cases after 10–12 hours the swelling reaches a constant rate, and the amount of LidHCl released seems to follow zero-order kinetics, as previously reported for drug delivery systems based on PAA.^[55–57] This second stage in the release is associated with a diffusion-controlled process of the API from the already swelled matrix.^[58,59]

In order to further control the swelling of the polymers, two types of crosslinkers with different functionalities were used, and their effect on the release was studied. Ethylene glycol dimethacrylate (EGDMA) possesses two methacrylate groups, whereas pentaerythritol triacrylate (PETA) possesses three acrylate groups; both are able to undergo free-radical polymerization to form networks (Figure 2.1). The amount of crosslinker used in this work is very low (0.7% mol to monomers), though adequate to form hydrogels. Since PETA is a trifunctional monomer, the degree of crosslinking of the resultant hydrogel is higher compared with the hydrogel crosslinked with EGDMA, and then the swelling in the former case is slower at fixed pH and ionic strength. Hence the release is controlled during the first stage

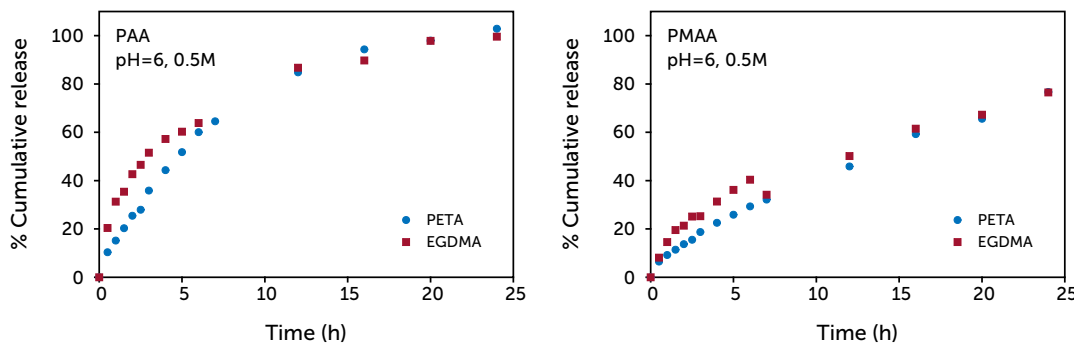


Fig. 2.9 Effect of crosslinkers on the release of LidHCl from PAA (left) and PMAA (right) in phosphate buffer under sink conditions at 24 °C.

by modifying the relaxation of the network, *i.e.*, its swelling by water absorption (Figure 2.9).

Another way to control the relaxation of the polymer is through copolymerization. In this way different functionalities can control different properties yielding a tailored performance. Although, it can be seen in Figure 2.10 that the random copolymerization of AA and MAA in a 1:1 ratio results in a copolymer whose release kinetics resembles more the PAA homopolymer than the PMAA one at pH 6. Interestingly the use of PETA gives rise to the case II transport mechanism at pH 6 and 0.5 M, *i.e.*, $n=1$ in Equation 2.2 and hence controlled by the rate of polymer relaxation, which follows zeroth order kinetics.^[48]

Furthermore, by the appropriate combination of PAA and PMAA,^[45,60] a series of copolymers with tailored surface properties that ultimately control their bioactivity and release mechanisms can be easily envisaged by the use of polymerizable DESs.

2.4 Conclusions

This work showed that by taking advantage of the DES chemistry, the exothermicity of acrylate free-radical polymerization in the bulk (*e.g.* frontal polymerization) can be controlled by means of its complexation with the API (quaternary ammonium salt). Polymer-API complexes can be easily synthesized in a one-pot synthesis with minimum consumption of energy, full conversion and under solventless conditions,

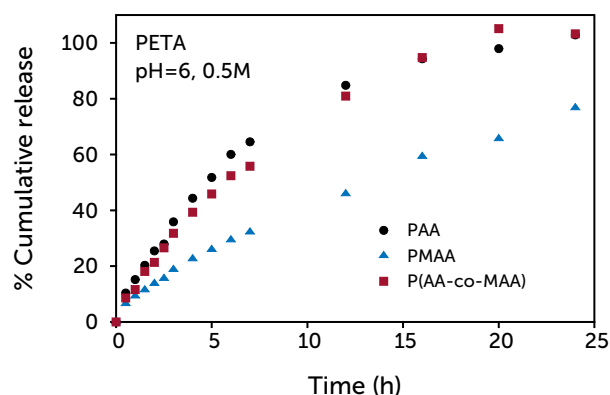


Fig. 2.10 Release of lidocaine HCl from PAA, PMMA and P(AA–co–MAA), all crosslinked with PETA in phosphate buffer under sink conditions at 24 °C.

preserving the API from degradation. The tailored composition of DESs allowed designing of polymer and copolymer complexes that are pH responsive at pH 6 and 7 such that the entrapped API can be released in a controlled manner.

With *in vitro* experiments, the sustained release of LidHCl (as a model drug) was controlled by the pH, ionic strength and solubility of the drug in the medium. During the initial stages, the mechanism governing the release is the dissolution and diffusion of the API through the polymer. However, as the swelling develops, the mechanism turns into a sustained release controlled by diffusion. Those mechanisms can be tuned by the appropriate combination of monomers (*i.e.*, different DESs) and crosslinkers.

The amount of LidHCl homogeneously integrated in the stable polymer complexes is, to the best of our knowledge, the highest ever reported for PAA and PMMA. This is due to the fact that the API is one of the components of the polymerizable DESs. Therefore the specific interactions between the components that are formed and maximized in the DES precursor result in homogeneous polymer complexes.

Finally, it was demonstrated that acrylic monomers such as acrylic acid and methacrylic acid, can play the role of a hydrogen bond donor and by means of their copolymerization a new type of polymerizable DES was achieved. These results significantly expand the possibilities of drug delivery system preparation by exploiting the DES chemistry.

Bibliography

- [1] P. Gupta, K. Vermani, S. Garg, *Drug Discov. Today* **2002**, *7*, 569–579.
- [2] D. Schmaljohann, *Adv. Drug Deliver. Rev.* **2006**, *58*, 1655–1670.
- [3] A. Bajpai, S. K. Shukla, S. Bhanu, S. Kankane, *Prog. Polym. Sci.* **2008**, *33*, 1088–1118.
- [4] S. Cherukuvada, A. Nangia, *Chem. Commun.* **2014**, *50*, 906–923.
- [5] P. W. Stott, A. C. Williams, B. W. Barry, *J. Control. Release* **1998**, *50*, 297–308.
- [6] M. M. Buckley, P. Benfield, *Drugs* **1993**, *46*, 126–151.
- [7] J. Stoimenovski, D. R. MacFarlane, K. Bica, R. D. Rogers, *Pharm. Res* **2010**, *27*, 521–526.
- [8] M. Moniruzzaman, Y. Tahara, M. Tamura, N. Kamiya, M. Goto, *Chem. Commun.* **2010**, *46*, 1452–1454.
- [9] K. Bica, J. Shamshina, W. L. Hough, D. R. MacFarlane, R. D. Rogers, *Chem. Commun.* **2011**, *47*, 2267–2269.
- [10] J. L. Shamshina, P. S. Barber, R. D. Rogers, *Expert Opin. Drug Del.* **2013**, *10*, 1367–1381.
- [11] K. E. Uhrich, S. M. Cannizzaro, R. S. Langer, K. M. Shakesheff, *Chem. Rev.* **1999**, *99*, 3181–3198.
- [12] O. Pillai, R. Panchagnula, *Curr. Opin. Chem. Biol.* **2001**, *5*, 447–451.
- [13] P. J. Marsac, S. L. Shamblin, L. S. Taylor, *Pharm. Res.* **2006**, *23*, 2417.
- [14] N. Ngwuluka, *AAPS PharmSciTech* **2010**, *11*, 1603–1611.
- [15] H.-J. Krause, A. Schwarz, P. Rohdewald, *Drug Dev. Ind. Pharm.* **1986**, *12*, 527–552.
- [16] K. Krauel, N. Davies, S. Hook, T. Rades, *J. Control. Release* **2005**, *106*, 76–87.

- [17] J. Yang, H. Lee, W. Hyung, S.-B. Park, S. Haam, *J. Microencapsul.* **2006**, *23*, 203–212.
- [18] M. S. Mesiha, M. B. Sidhom, B. Fasipe, *Int. J. Pharm.* **2005**, *288*, 289–293.
- [19] S. Lu, K. S. Anseth, *J. Control. Release* **1999**, *57*, 291–300.
- [20] R. A. Scott, N. A. Peppas, *Biomaterials* **1999**, *20*, 1371–1380.
- [21] C. Mukesh, J. Bhatt, K. Prasad, *Macromol. Chem. Physic.* **2014**, *215*, 1498–1504.
- [22] E. Gavini, A. Mariani, G. Rassu, S. Bidali, G. Spada, M. C. Bonferoni, P. Giunchedi, *Eur. Polym. J.* **2009**, *45*, 690–699.
- [23] L. Viau, C. Tourne-Peteilh, J.-M. Devoisselle, A. Vioux, *Chem. Commun.* **2010**, *46*, 228–230.
- [24] M. C. Serrano, M. C. Gutierrez, R. Jimenez, M. L. Ferrer, F. d. Monte, *Chem. Commun.* **2012**, *48*, 579–581.
- [25] S. García-Argüelles, M. C. Serrano, M. C. Gutiérrez, M. L. Ferrer, L. Yuste, F. Rojo, F. del Monte, *Langmuir* **2013**, *29*, 9525–9534.
- [26] J. D. Mota-Morales, M. C. Gutierrez, I. C. Sanchez, G. Luna-Barcenas, F. del Monte, *Chem. Commun.* **2011**, *47*, 5328–5330.
- [27] J. D. Mota-Morales, M. C. Gutiérrez, M. L. Ferrer, I. C. Sanchez, E. A. Elizalde-Peña, J. A. Pojman, F. D. Monte, G. Luna-Bárcenas, *J. Polym. Sci. Part A: Polym. Chem.* **2013**, *51*, 1767–1773.
- [28] J. A. Pojman, *J. Am. Chem. Soc.* **1991**, *113*, 6284–6286.
- [29] J. A. Pojman, G. Curtis, V. M. Ilyashenko, *J. Am. Chem. Soc.* **1996**, *118*, 3783–3784.
- [30] L. Chen, T. Hu, H. Yu, S. Chen, J. A. Pojman, *J. Polym. Sci. Part A: Polym. Chem.* **2007**, *45*, 4322–4330.
- [31] D. I. Fortenberry, J. A. Pojman, *J. Polym. Sci. Part A: Polym. Chem.* **2000**, *38*, 1129–1135.
- [32] R. P. Washington, O. Steinbock, *J. Am. Chem. Soc.* **2001**, *123*, 7933–7934.
- [33] F. del Monte, D. Carriazo, M. C. Serrano, M. C. Gutiérrez, M. L. Ferrer, *ChemSusChem* **2014**, *7*, 999–1009.

- [34] S. Bednarz, M. Fluder, M. Galica, D. Bogdal, I. Maciejaszek, *J. Appl. Polym. Sci.* **2014**, *131*, n/a–n/a.
- [35] J. D. Mota-Morales, M. C. Gutierrez, M. L. Ferrer, R. Jimenez, P. Santiago, I. C. Sanchez, M. Terrones, F. Del Monte, G. Luna-Barcenas, *J. Mater. Chem. A* **2013**, *1*, 3970–3976.
- [36] A. P. Abbott, G. Capper, D. L. Davies, R. K. Rasheed, V. Tambyrajah, *Chem. Commun.* **2003**, 70–71.
- [37] A. P. Abbott, D. Boothby, G. Capper, D. L. Davies, R. K. Rasheed, *J. Am. Chem. Soc.* **2004**, *126*, 9142–9147.
- [38] H. Sun, Y. Li, X. Wu, G. Li, *J. Mol. Model.* **2013**, *19*, 2433–2441.
- [39] S. L. Perkins, P. Painter, C. M. Colina, *J. Phys. Chem. B* **2013**, *117*, 10250–10260.
- [40] M. Wojdyr, *J. Appl. Cryst.* **2010**, *43*, 1126–1128.
- [41] Z. S. Nurkeeva, G. A. Mun, V. V. Khutoryanskiy, A. B. Bitekenova, A. B. Dzhusupbekova, *J. Biomat. Sci. Polym. E* **2002**, *13*, 759–768.
- [42] W. Musial, V. Kokol, B. Voncina, *Chem. Pap.* **2009**, *64*, 84.
- [43] Y. Cui, S. G. Frank, *J. Pharm. Sci.* **2006**, *95*, 701–713.
- [44] M. A. Moharram, S. M. Rabie, H. M. El-Gendy, *J. Appl. Polym. Sci.* **2002**, *85*, 1619–1623.
- [45] H. Park, J. R. Robinson, *Pharm. Res.* **1987**, *4*, 457–464.
- [46] A. Katchalsky, P. Spitznik, *J. Polym. Sci.* **1947**, *2*, 432–446.
- [47] J. Ostroha, M. Pong, A. Lowman, N. Dan, *Biomaterials* **2004**, *25*, 4345–4353.
- [48] P. I. Lee, *J. Control. Release* **1985**, *2*, 277–288.
- [49] H. Sjöberg, K. Karami, P. Beronius, L.-O. Sundelöf, *Int. J. Pharm.* **1996**, *141*, 63–70.
- [50] N. Peppas, P. Bures, W. Leobandung, H. Ichikawa, *Eur. J. Pharm. Biopharm.* **2000**, *50*, 27–46.
- [51] S. W. Kim, Y. H. Bae, T. Okano, *Pharm. Res.* **1992**, *9*, 283–290.
- [52] P. Lee, *Polym. Commun.* **1983**, *24*, 45–47.

Bibliography

- [53] C. Valenta, U. Siman, M. Kratzel, J. Hadgraft, *Int. J. Pharm.* **2000**, *197*, 77–85.
- [54] N. Dan, *Colloid. Surface. B.* **2003**, *27*, 41–47.
- [55] M. Glavas-Dodov, K. Goracinova, K. Mladenovska, E. Fredro-Kumbaradzi, *Int. J. Pharm.* **2002**, *242*, 381–384.
- [56] B. Das, A. K. Nayak, U. Nanda, *Int. J. Biol. Macromol.* **2013**, *62*, 514–517.
- [57] T. Ozeki, H. Yuasa, Y. Kanaya, *J. Control. Release* **2000**, *63*, 287–295.
- [58] C.-C. Lin, A. T. Metters, *Adv. Drug Deliver. Rev.* **2006**, *58*, 1379–1408.
- [59] E. L. Cussler, *Diffusion: Mass Transfer in Fluid System*, 3rd, Cambridge University Press, **2009**.
- [60] V. V. Khutoryanskiy, Z. S. Nurkeeva, G. A. Mun, A. D. Sergaziyev, Z. Ryskalieva, J. M. Rosiak, *Eur. Polym. J.* **2003**, *39*, 761–766.

An expert is a person who has made all the mistakes that can be made in a very narrow field.

— Niels Bohr

3

Enzyme-mediated free-radical polymerization of acrylamide in deep eutectic solvents

Currently, the concept of green chemistry has become more relevant in organic, inorganic and polymer synthesis due to the fact that many synthetic pathways involve the use of toxic and non-biodegradable compounds as precursors, reaction media and catalysts. In pursuit of green and sustainable alternatives, the use of enzymes for materials synthesis has been proposed as a replacement for inorganic catalysts aside from advantages such as their high specificity and the fact that they can readily be immobilized.^[1] Enzymes have been employed successfully in the synthesis of small molecules to large polymers.^[2] These biocatalysts usually work in aqueous solution under mild conditions of temperature and pH.^[3] Although it is well-known that an aqueous environment, the natural medium of enzymes, is preferred to maintain their activity, there are many enzymatic reactions that are difficult to carry out in water, either because of poor solubility of the substrate/product or because undesirable hydrolytic side-reactions can occur. Such restrictions have led to the use of alternative media capable of providing better conditions to maintain or improve the enzyme performance for those specific reactions.^[3,4]

Attempts of carrying out reactions with enzymes in non-conventional media range from aqueous solutions of acetone/ethanol and biphasic mixtures to nearly non-aqueous or even anhydrous organic solvents,^[5] but it still remains challenging. Interestingly, some enzymes are able to maintain their catalytic activity and

show remarkable novel properties when in organic media;^[6] sometimes exhibiting faster rates and higher selectivity and stability than in water. Further, in some cases it is possible to recover or recycle them easily. Among the solvents used for this goal, ILs have shown promise for application in biocatalytic processes due to their high chemical and thermal stability, negligible vapor pressure and tuneable properties.^[7]

3.1 Background

In 2000 Erbeldinger and co-workers reported the first enzymatic reaction carried out in ILs.^[8] They described the thermolysin-catalyzed synthesis of Z-aspartame using $[\text{BMIM}]^+[\text{PF}_6]^-/\text{H}_2\text{O}$ (95/5% v/v) as solvent, where the enzyme exhibited higher stability than in ethylacetate/ H_2O with comparable reaction rates. Shortly after, other research groups showed that it is possible to catalyze a variety of transesterification, ammoniolysis, epoxidation^[9] and enantioselective reactions^[10,11] using a lipase B in anhydrous imidazolium-based ILs with better reaction rates and higher yield and selectivity than those observed in conventional organic media. Since enzymes seem to better tolerate ILs than conventional organic solvents, imidazolium-based ILs, mainly $[\text{BMIM}]^+[\text{BF}_4]^-$ and $[\text{BMIM}]^+[\text{PF}_6]^-$,^[7] have been employed as co-solvents with water, as a secondary phase or non-aqueous solvents for a number of enzymatic reactions.

The vast majority of research on enzymatic reactions in ILs to date has focused on hydrolases.^[7,9] Nevertheless, there has also been an increasing number of studies using oxidoreductases in these media due to their wide application range in organic synthesis, *e.g.*, synthesis of chiral alcohols from aldehydes/ketones,^[12,13] polymer synthesis^[14–17] and oxidative degradation of pollutants.^[18,19] In particular, horseradish peroxidase (HRP) has shown good activity in $[\text{BMIM}]^+[\text{BF}_4]^-$ in the presence of small amount of water (4.53% v/v), and high stability in this IL upon immobilization in agarose hydrogels for biosensing applications.^[20] The activity of HRP was reported to increase 30 to 240-fold in a tailor made IL (tetrakis (2-hydroxyethyl) ammonium trifluoromethanesulfonate) compared to that in conventional ILs, and more than 10 times greater than that in methanol.^[21] This enzyme has also been used in water-in-IL microemulsions for the oxidation of pyrogal-

lol by H_2O_2 and a significant increase of the reaction rate was obtained in contrast with that in oil microemulsions.^[22]

Despite all of these seemingly attractive scenarios, ILs' toxicity, and the high costs derived from their synthesis and post-purification limit their use in large-scale applications. Fortunately, DESs offers an alternative to overcome the previously mentioned drawbacks. As mentioned in chapter 1, DESs have proved to be very good solvents for a great variety of substances and they have shown potential use in biocatalysis,^[23,24] dissolution of proteins and natural polymers,^[25,26] polymer synthesis^[27,28] and materials preparation.^[29] Herein, the use of DESs as non-volatile solvents coupled with enzymes as catalysts as a further step towards greener alternatives in polymer synthesis by free-radicals is proposed.

Recently, the work of Yang and collaborators^[30] suggested that HRP activity is favored in highly diluted solutions of DES's constituents (*ca.* below 8% w/w). Motivated by this and the fact that some oxidoreductases, such as HRP, can induce polymerization of vinyl monomers,^[14–16] the effect of these solvents containing small amounts of water on the HRP performance was studied in this work. Furthermore, the enzyme-mediated polymerization of acrylamide in DES-aqueous mixtures was carried out in order to demonstrate for the first time, that it is not only possible for HRP to retain catalytic activity at relatively high temperatures and low pressure, but also to initiate the free-radical polymerization of an acrylate in these non-conventional media with similar average molecular weights of the polymer compared to those obtained in aqueous buffered solution.

3.2 Materials and experimental methods

3.2.1 Materials

Choline chloride, urea, glycerol, phenol, 4-aminoantipyrine, 2,4-pentanodione, monosodium phosphate ($\text{NaH}_2\text{PO}_4 \cdot 2\text{H}_2\text{O}$), disodium phosphate ($\text{Na}_2\text{HPO}_4 \cdot \text{H}_2\text{O}$), acrylamide and horseradish peroxidase were purchased from Sigma Aldrich, and H_2O_2 (30% solution) from J. T. Baker. Phosphate buffer solutions (PBS) at different molar concentrations and pH were prepared from both sodium phosphate salts. Except for choline chloride all reagents were used without further purification.

3.2.2 Deep eutectic solvent synthesis

Prior to DESs synthesis, choline chloride was recrystallized from absolute ethanol and completely dried. Choline chloride/urea (CCl–U) and choline chloride/glycerol (CCl–Gly) were prepared by heating the two corresponding components in a 1:2 molar ratio at 90 °C and stirring until a homogeneous liquid was formed.

3.2.3 Enzymatic activity assays

The enzyme activity was measured using an Ocean Optics USB4000 UV-Vis spectrometer following a standard colorimetric method.^[31] The assay was carried out at RT and the reaction was initiated by the addition of 5 mL of HRP (type I, 52 U · mg⁻¹ using pyrogallol) solution (1 mg·mL⁻¹) to a cuvette with 995 mL of PBS (0.1 M, pH 7.0) containing phenol, 4-aminoantipirine and H₂O₂ at a final concentration of 10 mM, 0.2 mM and 2.4 mM, respectively. Upon addition of the enzyme solution, the cuvette was capped and inverted three times prior to being placed in the spectrometer. The change in absorbance over time was monitored at 510 nm during the first minute. The slope of the linear increase of absorbance and a molar extinction coefficient of 7100 L · mol⁻¹ · cm⁻¹ were used to determine the catalytic activity. The activity of HRP in DESs-aqueous mixtures at different DES concentrations (v/v%) was determined following the same procedure. The measurements were at least triplicated and the average is reported.

3.2.4 Thermal stability tests

For the thermal stability tests, 100 mL of HRP solution (145.7 U·mg⁻¹, 10 mg·mL⁻¹) were added to 900 mL of PBS (0.1 M, pH 7.0) and to DESs-aqueous mixtures, respectively. The samples were incubated at 50 °C and the final concentration of DESs-aqueous mixtures was 80% v/v DES. During a period of 6 hours, aliquots of 5 mL were taken at different times for the activity assay as mentioned above. For each enzyme solution $t_{1/2}$ was calculated from the time-dependent loss in activity. All thermal stability experiments were at least triplicated and the average of HRP activity after incubation in the reaction media is reported.

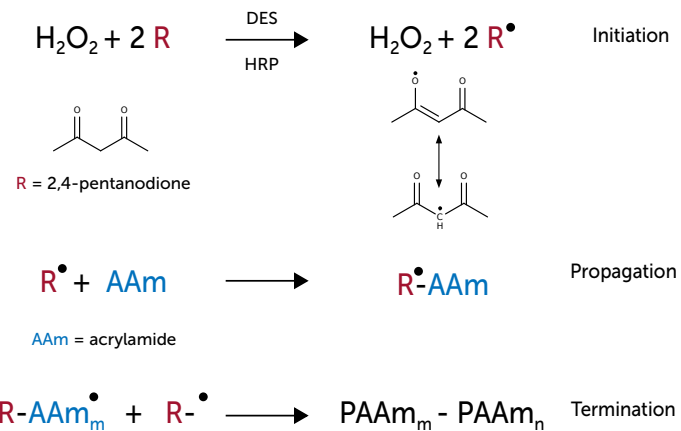


Fig. 3.1 Reaction scheme of HRP-mediated free-radical polymerization of AAm in water^[15] (the same reaction mechanism is believed to occur when using DES since DES appeared to be an inert solvent during polymerization).

3.2.5 HRP-mediated free-radical polymerization

HRP-mediated polymerization of acrylamide (AAm) was carried out in three different solvents, two DES-aqueous mixtures composed of choline chloride and either urea (CCl-U) or glycerol(CCl-Gly), both in a 1:2 molar ratio at 80% v/v DES (20% of water and 80% v/v of the corresponding DES), and one consisting of pure water as reference. For all these systems, initiation by free-radical species was generated by the catalytic system $\text{HRP}/\text{H}_2\text{O}_2/2,4\text{-pentanodione}$ as reported by Emery *et al.* for polyacrylamide (PAAm) synthesis in water (Figure 3.1).^[15] As in their experiments, no polymer was formed in absence of enzyme, of H_2O_2 , and of 2,4-pentanodione, further confirming that the combination of the three components is the sole responsible of initiation.

Prior to the addition of the catalytic system to the solvents, water and DESs-aqueous mixtures containing AAm were degasified by N_2 bubbling. HRP (145.7 U mg^{-1} , 37.5 mL, 10 mg mL^{-1}), H_2O_2 (10 mL, 0.82 M) and 2,4-pentanodione (12.84 mL) were added into a flask containing 6.25 mL of 0.64 M aqueous AAm solution. In the case of the DES containing systems, AAm (284.4 mg) was first dissolved in CCl-U or CCl-Gly , and the same amount of the remaining reagents was subsequently introduced into each DES-AAm solution. In the final solutions, 80% of the total H_2O volume was replaced by DES. After 72 h of reaction at RT (24 h under vacuum), the solutions were added dropwise to a large excess of methanol to precipitate the

PAAm, filtered off and washed several times to ensure complete removal of the DES. PAAm samples were dried under vacuum at 50 °C. The experimental procedure for AAm polymerization at 50 and 4 °C was the same followed at RT. The reaction yield was determined gravimetrically and corresponds to the weight of PAAm recovered compared to the weight of AAm used initially.

3.2.6 DESs characterization

DESs-aqueous mixtures with various water contents (20–90% v/v) were freshly prepared. The thermodynamic water activity (a_w) was determined at 25.5 °C using an AquaLab CX-2.

3.2.7 Enzyme characterization

The fluorescence of the tryptophan residue of HRP was measured using a steady-state FluoroMax-3 spectrofluorometer by Jobin Yvon Horiba. For the assays, 5 mM HRP solutions were prepared in PBS (0.1 M, pH 7.0) and DESs-aqueous mixtures (80% v/v DES), respectively. The spectra were acquired at RT and 90 ° with an excitation wavelength of 295 nm to avoid the contribution of the tyrosine residues of HRP. A quartz cuvette with a path length of 10 mm was used for the experiments. Fluorescence intensity of the corresponding solvent was subtracted from each spectrum that contained HRP to eliminate the contributions of the solvents on the fluorescence measurements and only the deconvoluted tryptophan signal is shown (see Figure B.1 for the raw fluorescence spectra).

Absorbance spectra of HRP were determined with 5 mM enzyme in PBS (0.1 M, pH 7.0) and DESs-aqueous mixtures (80% v/v DES), respectively. The enzymes solutions were equilibrated for 30 min at RT before collection of the spectra on an Agilent 8453 UV-Vis spectrophotometer.

3.2.8 Polymer characterization

ATR-FTIR spectra of PAAm samples were acquired at RT using a Perkin-Elmer Spectrum GX FTIR spectrometer in the range from 4000 to 650 cm⁻¹ with a resolution of 4 cm⁻¹ and an average of 32 scans.

¹H NMR spectra were conducted in a 500 MHz Bruker Avance III using a 5 mm direct broad band with Z-grad (PABBO-1H/D Z-GRAD) probe at RT and with D₂O as solvent. The spectra were recorded with the presaturation mode. The chemical shifts in the spectra were referenced to residual no deuterated solvent.

The number average molar mass (M_n), mass average molar mass (M_w) and molecular weight distribution of polymers were measured using an Agilent 1260 Infinity HPLC-GPC size exclusion chromatograph (SEC) equipped with an auto sampler and a differential refractive index detector. The SEC equipment was fitted with three PL aqua-gel-OH columns; 30 (8 mm, 300 x 7.5 mm, range molecular weight 100–30 000), 40 (15 mm, 300 x 7.5 mm, range molecular weight 10 000–200 000) and 50 (15 mm, 300 x 7.5 mm, range molecular weight 50 000–1 000 000); and one aqua-gel-OH (15 mm, 50 x 7.5 mm) guard column (Polymer Laboratories). PBS (pH 7) was used as eluent at 0.5 mL min⁻¹ and 40 °C. The molecular weights were determined relative to polyacrylic acid standards (100 to 1 000 000 Da).

3.3 Results and discussion

3.3.1 Catalytic activity and enzyme conformation

Prior to polymerization experiments, the specific activity and thermal stability of HRP in PBS (0.1 M, pH 7) and DES-aqueous mixtures at different DES concentrations were determined. Figure 3.2 shows that HRP activity is higher in CCl–Gly than CCl–U aqueous mixtures, whereas in both media the activity decreases with increasing DES concentration. Given the large difference in viscosity between water and DESs (Table 3.1),^[32–37] the drop on the enzyme activity may be related to some extent to diffusional and mass transfer limitations of the reagents in both reaction media. It is important to consider that although the viscosity of CCl–Gly in its pure state is almost three times lower than that of CCl–U, CCl–Gly has a higher

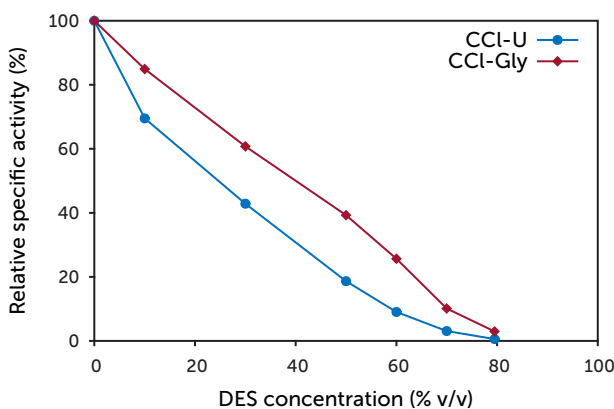


Fig. 3.2 Relative specific activity of HRP in DESs-aqueous mixtures at RT and different DES concentration (experiments were at least triplicated, see Figure B.2 in Appendix B for standard deviation.)

viscosity than CCl-U in aqueous mixtures with more than 6% w/w of water.^[38] If this were the only factor involved, it would be expected that the catalytic activity of HRP would be higher in CCl-U than CCl-Gly aqueous mixtures with less than 90% v/v DES concentration. This is clearly not the main factor for the drop on HRP activity.

Changes on the enzyme conformation, triggered either by the solvent or temperature effects, can also significantly affect the catalytic activity of enzymes. The impact of the solvents on the enzyme conformation was investigated by fluorescence spectroscopy of the tryptophan residue of HRP in PBS and DES-aqueous mixtures at a high DES concentration (Figure 3.3, left). Alterations of the environment surrounding the tryptophan residue, reflected on shifts and intensity variations of the amino acid fluorescence peak, can be used to infer changes on the tertiary structure of the enzyme. By comparing the fluorescence emission spectra of HRP in CCl-Gly

Table 3.1 Freezing temperature and viscosity of the used DESs and DESs-aqueous mixtures.

QAS	HBD	QAS : HBD (molar ratio)	T_f (°C)	Viscosity (cP)		
				Pure	80 v/v% DES ^a (20 °C)	80 v/v% DES ^a (50 °C)
		1:2	12 [32]	750 (25 °C) [34]	17.6 [35]	6.5 [36]
		1:2	-40 [33]	376 (20 °C) [34]	41.2 [37]	13.3 [35]

^aViscosity values were taken from the corresponding references by looking up the wt% equivalent concentrations.

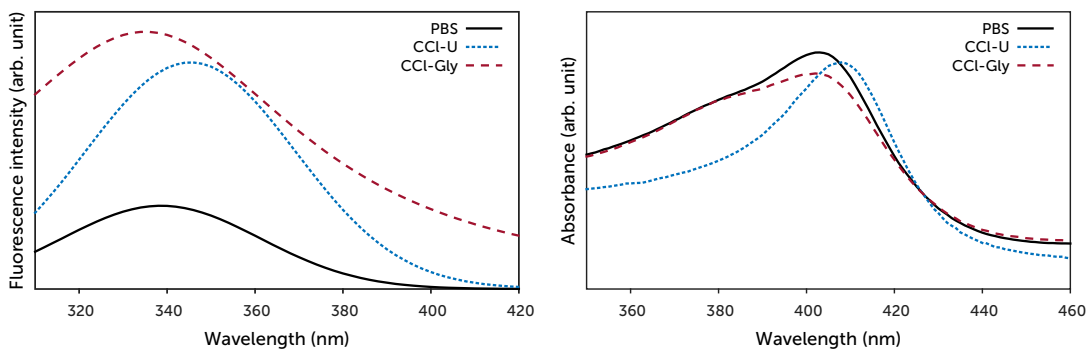


Fig. 3.3 Tryptophan fluorescence emission spectra of HRP (excitation wavelength 295 nm) (left), and UV-Vis spectra of the Soret region of HRP (right) in PBS (0.1 M, pH 7) and DESs-aqueous mixtures (80% v/v DES) at RT.

and CCl-U to that obtained in PBS, an intensification of the tryptophan fluorescence signal can be observed. In heme proteins, this has been attributed to an increase of the distance between the tryptophan residue and the heme group upon protein denaturation.^[39]

The spectra of HRP in CCl-Gly displayed also a slight blue shift of the maximum intensity (λ_{max}), which may indicate a rearrangement of the enzyme structure in this medium, where the heme group partially dissociates from the active site.^[39,40] On the other hand, in the CCl-U aqueous mixture, an evident red shift of λ_{max} is observed as a result of the HRP unfolding and exposition of the indole ring to the polar solvent.^[41,42] These results are in agreement with the absorbance measurements of the Soret region of HRP. Figure 3.3 (right) shows that DESs induced a decrease in the Soret band absorption with respect to the same band in aqueous solution. For CCl-Gly no detectable shift in wavelength for the band is observed as it has been seen earlier for inactivation of HRP in presence of sodium azide due to partial degradation of the heme group.^[43] HRP absorption spectra in CCl-U showed a red shift that coincides with that observed for heme non-covalently bonded proteins such as hemoglobin and myoglobin, where this has been attributed to the expulsion of the prosthetic group into solution.^[44] As it can be seen from Figure 3.2, the partial denaturation of HRP in CCl-U due to unfolding accompanied by expulsion of the heme group into solution seems to have a greater negative impact on the catalytic activity than the partial dissociation of the prosthetic group in CCl-Gly.

Regardless of this decrease on the activity at higher DES concentrations, CCl-U and CCl-Gly concentrations in the reaction media for AAm polymerization were

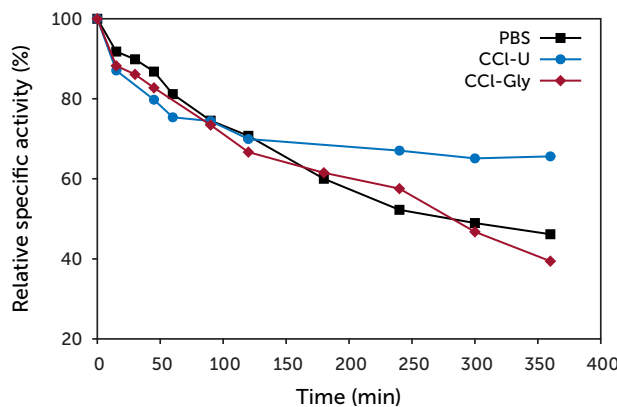


Fig. 3.4 Thermal stability of HRP in PBS (0.1 M, pH 7) and DES aqueous mixtures (80% v/v DES) at 50 °C (experiments were at least triplicated).

fixed to 80% v/v mainly for two reasons: (*i*) to preserve the halide–HBD supramolecular complexes characteristic of DES, which integrate water within up to certain threshold;^[38,40,45–47] and (*ii*) to lower the viscosity of these solvents and thus, facilitating its handling and homogeneous stirring during the reaction,^[48,49] taking also into account that the viscosity of these reaction systems increases as soon as the polymerization starts.

3.3.2 Thermal stability

As for the thermal stability of the enzyme at 80% v/v DES, it was notably higher in CCl–U and comparable in CCl–Gly to that in PBS at 50 °C (Figure 3.4). The half-life time ($t_{1/2}$) obtained from Figure 3.4 for each enzyme solution is shown in Table 3.2. The enhanced thermal stability of enzymes generally observed in conventional ILs has been mainly ascribed to the high viscosity of these solvents, which according to some authors slows the migration of the protein domain from the active conformation into the inactive one;^[7] and to the ability of ILs to compact the native structural conformation of the enzyme.^[50]

Although the underlying causes of this stabilization effect are not completely well elucidated in DES, a recent study based on molecular dynamic simulations confirmed the last assumption, and lead us to believe that in the case of CCl–U a similar phenomenon occurs. Monhemi *et al.* showed that the compactness of a lipase remains constant in CCl–U DES even at high temperatures (*i.e.* 100 °C), which

Table 3.2 Half-life time values ($t_{1/2}$) for HRP obtained in PBS and DESs-aqueous mixtures (80% v/v DES) at 50 °C.

Reaction medium	PBS	CCl–U	CCl–Gly
$t_{1/2}$ (min)	281	>360	283

means that the enzyme has a rigid structure in this solvent.^[51] Moreover, it was found that urea, choline and chloride ions form hydrogen bonds with the surface residues of the enzyme and that these rigid structures formed in the enzyme surface help to promote the protein stability. This may explain the high thermal stability of HRP in CCl–U where the enzyme, in spite of exhibiting a partially unfolded structure, retains higher catalytic activity than buffered aqueous solutions and CCl–Gly for a prolonged period of time. Otherwise, in the case of CCl–Gly, the presence of glycerol as the HBD in the DES structure has a different influence on the thermal stability of HRP. It seems that the interactions between CCl–Gly molecules with the surface residues of the enzyme are not strong enough to maintain the enzyme structure “docked” upon heating, leading to a behavior similar to that observed in the aqueous environment.

3.3.3 HRP-mediated free-radical polymerization

Polymerizations of AAm were successfully achieved with very high reaction yields in all cases (Table 3.3). PAAm solutions and the corresponding polymers recovered after precipitation are shown in Figure 3.5. Despite the low catalytic activity

Table 3.3 Yield and M_n of PAAm samples obtained by HRP-mediated initiation in H_2O and DESs-aqueous mixtures (80% v/v DES).

Reaction medium	T (°C)	^a Yield (wt%)	M_n (g·mol ⁻¹)	M_w (g·mol ⁻¹)	PDI
H_2O	RT	99	1.61×10^5	3.92×10^5	2.4
	50	96	1.23×10^5	4.39×10^5	3.6
CCl–U	RT	100	1.60×10^5	3.28×10^5	2.1
	50	90	7.79×10^4	2.16×10^5	2.8
CCl–Gly	RT	100	2.27×10^4	9.85×10^4	4.3
	50	99	8.33×10^3	6.96×10^4	8.3
	4	99	3.00×10^4	1.47×10^5	5.0

^aThe yield corresponds to the weight of PAAm recovered after precipitation, filtration and drying, to the weight of AA used initially.

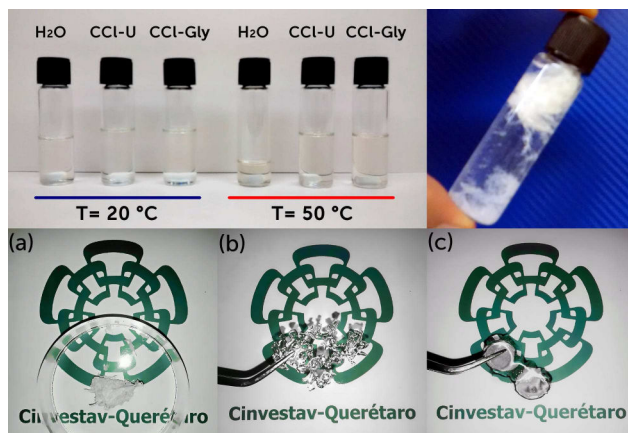


Fig. 3.5 Top left: PAAm solutions in H₂O and DESs-aqueous mixtures (80% v/v DES). Top right: PAAm precipitated with methanol. Bottom: PAAm synthesized in (a) H₂O, (b) CCl-U aqueous mixture, and (c) CCl-Gly aqueous mixture at RT after precipitation and drying.

of the enzyme at high DES concentration, it proved to be enough to initiate the polymerization reaction. ATR-FTIR and ¹H NMR spectra of all samples showed the characteristic bands and signals for PAAm (Figures B.3 and 3.6). The bands at 3335 cm⁻¹ and 3196 cm⁻¹ correspond to the stretching modes of the NH₂ group, and bands at 1660 cm⁻¹ and 1620 cm⁻¹ to the stretching of C=O and bending of NH₂ groups, respectively.^[52] The proton spectrum of PAAm samples showed two signals for methylene proton between 2.35 to 2.1 ppm and other two signals with small multiplicity for methylene protons between 1.8 to 1.4 ppm (Figure B.3). The splitting observed for these two groups is due to tacticity splitting in small range, as results of the low viscosity associated to the relativity low molecular weight. The integral relation between methylene and methyne proton is 2/1 in accordance to the expected value. The NH₂ groups are missed, due to exchange with deuterium from water. No signals for free monomer were detected. Depending on the protocol of PAAm synthesis the corresponding spectrum shows: CCl, CCl-U or CCl-Gly in low quantities as contaminants coming from the solvent (note the narrow and well defined signals of the solvents vs the broad signals of PAAm).

The different reaction systems yielded PAAm samples with a number-average molar mass (M_n) and polydispersity index (PDI) ranging from 161 000 to 8 330 g·mol⁻¹ and 2.1 to 8.3, respectively. Notwithstanding the significantly reduced catalytic activity of HRP in CCl-U (almost 170 times lower to that in PBS, see Figure B.2), this solvent allowed the synthesis of PAAm with similar M_n and even

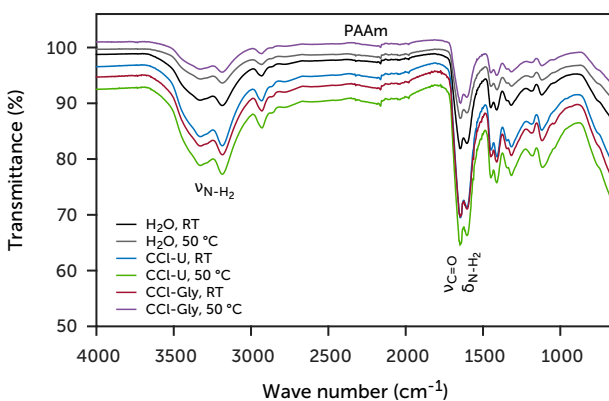


Fig. 3.6 FTIR spectra of PAAm synthesized in H_2O and DESs aqueous mixtures of CCl-U and CCl-Gly, respectively.

slightly narrower polydispersity to the corresponding experiment in water at RT. Actually the PDI in CCl-U is close to 2, which is the theoretical limit of conventional polymerization via free-radicals,^[53] *i.e.* contribution from intra- and intermolecular chain transfer reactions during polymerization is minimized. In this regard, although AAm has proven to form DES with choline chloride,^[54] the ATR-FTIR spectra of the reaction mixture and the resulting PAAm solution in DES (80% v/v) after polymerization do not show noticeable changes in the bands of the DES constituents, thus reflecting no significant changes in the H-bonding network of DES^[55,56] at any stage of polymerization at the concentrations tested (Figures B.4 and B.5). In addition ¹H NMR spectra of the polymers synthesized in DES reveal small amounts of the corresponding solvent (Figure B.6) but not taking part of the polymer structure, confirming the inertness of the DES towards free-radical polymerization of AAm.

Contrary to these results, replacement of water by CCl-Gly in the polymerization reaction does not offer any benefit in terms of molecular weight or PDI. For instance, PDI increases two-fold or more compared with water and CCl-U; M_n also decreases *ca.* one order of magnitude. A decrease in the catalytic activity of HRP in CCl-Gly coupled with a thermal stability similar to that in the buffered aqueous media at 50 °C resulted in PAAm with the lowest M_n values. High polydispersity in CCl-Gly can be explained on the same basis than in CCl-U case, actually chain transfer during spontaneous polymerization of AAm has been reported to occur in glycerol alone.^[57]

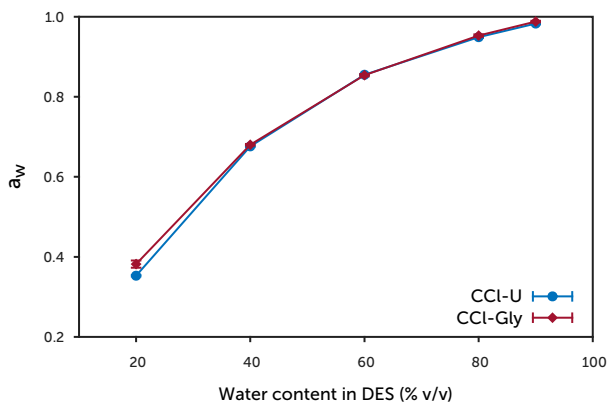


Fig. 3.7 Thermodynamic activity of water (a_w) as a function of water content in CCl-U and CCl-Gly aqueous mixtures. Note: error bars are almost all within the size of the plot symbols.

Another interesting feature resulting from the use of DES as solvent, in this case with “hydrated” DES, is the lower water activity (a_w) of these systems (Figure 3.7). Derived of this, the rather narrow conditions of pH (5.4–8) for the polymerization of AAm in water are circumvented,^[58,59] since DES provide a unique environment where acid-base equilibrium is different in nature than in water.^[60,61] DES containing up to 20% v/v of water as co-solvent demonstrated to be stable (e.g. no weight lost) under vacuum at 50 °C or RT during the course of the experiments. The possibility of applying vacuum to the systems during the first stages of polymerization was exploited in order to minimize the effect of oxygen,^[62] which is a well-known factor that reduces the efficiency of propagation in free-radical polymerization; therefore helped in obtaining 100% of conversion.

Taking advantage of the low freezing point of CCl-Gly in its pure state (-40 °C)^[63,64] we carried out an additional polymerization experiment at 4 °C in this solvent and water. As it was expected, given the low temperature of the system, no polymer precipitated from the AAm solution when water was used as solvent. However, in CCl-Gly, PAAm with M_n of 30 000 g·mol⁻¹ was obtained (Table 3) which suggests that the enzyme conformation is not drastically disrupted at this temperature. It is also worth noting that M_n of PAAm synthesized at 4 °C was slightly higher than those obtained in the same solvent at RT and 50 °C. Undoubtedly, this intriguing behaviour of HRP in CCl-Gly deserves a deeper study, but showed the potential use of these solvents to carry out biocatalytic reactions in a wide range of temperatures.

3.4 Conclusions

In summary, the use of hydrated DESs as alternative solvents for enzyme-mediated free-radical polymerizations under conditions of temperature and pressure inaccessible for PAAm synthesis in water has been described. HRP retained enough catalytic activity to initiate the polymerization of AAm in hydrated DES owed to its high thermal stability regardless exhibiting a partially unfolded structure. Resulting polymers showed comparable M_n values to those obtained in water for CCl–U system with complete conversion. The slightly enhancement in polydispersity obtained in the CCl–U 80% v/v system reflects the suitable environment provided for AAm propagation that minimize contributions from intra- and intermolecular chain transfer reactions during polymerization.

Several properties of the polymer such as M_n , M_w and PDI can be potentially tuned by taking advantage of the solvent properties of the DES. Furthermore, the conditions provided by CCl–Gly DES allowed the exploration of the polymerization reaction at lower temperatures (4 °C), at which no polymer was formed in aqueous medium. In addition, the increase of the enzyme thermal stability in CCl–U DES enabled the polymerization of AAm with similar M_n despite the low catalytic of HRP in this medium. Finally, access to low temperatures for polymerization in the CCl–Gly system paves the way for unprecedented possibilities in materials synthesis, for instance through enzyme-mediated free-radical cryo-polymerization in nearly non-aqueous media.

Bibliography

- [1] P. T. Anastas, L. B. Bartlett, M. M. Kirchhoff, T. C. Williamson, *Catal. Today* **2000**, *55*, 11–22.
- [2] S. Kobayashi, K. Kashiwa, T. Kawasaki, S. Shoda, *J. Am. Chem. Soc.* **1991**, *113*, 3079–3084.
- [3] G. M. Whitesides, C.-H. Wong, *Angew. Chem. Int. Ed.* **1985**, *24*, 617–638.
- [4] A. M. Klibanov, *Trends Biotechnol.* **1997**, *15*, 97–101.
- [5] A. M. Klibanov, *Trends Biochem. Sci.* **1989**, *14*, 141–144.
- [6] A. Zaks, A. M. Klibanov, *J. Biol. Chem.* **1988**, *263*, 3194–3201.
- [7] F. van Rantwijk, R. A. Sheldon, *Chem. Rev.* **2007**, *107*, 2757–2785.
- [8] M. Erbeldinger, A. J. Mesiano, A. J. Russell, *Biotechnol. Prog.* **2000**, *16*, 1129–1131.
- [9] R. Madeira Lau, F. Van Rantwijk, K. R. Seddon, R. A. Sheldon, *Org. Lett.* **2000**, *2*, 4189–4191.
- [10] K.-W. Kim, B. Song, M.-Y. Choi, M.-J. Kim, *Org. Lett.* **2001**, *3*, 1507–1509.
- [11] S. Park, R. J. Kazlauskas, *J. Org. Chem.* **2001**, *66*, 8395–8401.
- [12] W. Hummel, *Trends Biotechnol.* **1999**, *17*, 487–492.
- [13] K. Goldberg, K. Schroer, S. Lütz, A. Liese, *Appl. Microbiol. Biotechnol.* **2007**, *76*, 237.
- [14] R. A. Derango, L.-c. Chiang, R. Dowbenko, J. G. Lasch, *Biotechnol. Tech.* **1992**, *6*, 523–526.
- [15] O. Emery, T. Lalot, M. Brigodiot, E. Maréchal, *J. Polym. Sci. Part A: Polym. Chem.* **1997**, *35*, 3331–3333.
- [16] B. Kalra, R. A. Gross, *Biomacromolecules* **2000**, *1*, 501–505.
- [17] B. Kalra, R. A. Gross, *Green Chem.* **2002**, *4*, 174–178.
- [18] J. Karam, J. A. Nicell, *J. Chem. Technol. Biotechnol.* **1997**, *69*, 141–153.

- [19] N. Durán, E. Esposito, *Appl. Catal. B-Environ.* **2000**, *28*, 83–99.
- [20] S.-F. Wang, T. Chen, Z.-L. Zhang, D.-W. Pang, *Electrochim. Commun.* **2007**, *9*, 1337–1342.
- [21] D. Das, A. Dasgupta, P. K. Das, *Tetrahedron Lett.* **2007**, *48*, 5635–5639.
- [22] M. Moniruzzaman, N. Kamiya, M. Goto, *Langmuir* **2009**, *25*, 977–982.
- [23] J. T. Gorke, F. Srienc, R. J. Kazlauskas, *Chem. Commun.* **2008**, 1235–1237.
- [24] D. Lindberg, M. de la Fuente Revenga, M. Widersten, *J. Biotechnol.* **2010**, *147*, 169–171.
- [25] M. Sharma, C. Mukesh, D. Mondal, K. Prasad, *RSC Adv.* **2013**, *3*, 18149–18155.
- [26] J. Parnica, M. Antalik, *J. Mol. Liq.* **2014**, *197*, 23–26.
- [27] D. Carriazo, M. C. Gutiérrez, M. L. Ferrer, F. del Monte, *Chem. Mater.* **2010**, *22*, 6146–6152.
- [28] J. D. Mota-Morales, M. C. Gutierrez, I. C. Sanchez, G. Luna-Barcenas, F. del Monte, *Chem. Commun.* **2011**, *47*, 5328–5330.
- [29] D. V. Wagle, H. Zhao, G. A. Baker, *Acc. Chem. Res.* **2014**, *47*, 2299–2308.
- [30] B.-P. Wu, Q. Wen, H. Xu, Z. Yang, *J. Mol. Catal. B: Enzym.* **2014**, *101*, 101–107.
- [31] J. A. Nicell, H. Wright, *Enzym. Microb. Technol.* **1997**, *21*, 302–310.
- [32] A. P. Abbott, G. Capper, D. L. Davies, R. K. Rasheed, V. Tambyrajah, *Chem. Commun.* **2003**, 70–71.
- [33] M. Hayyan, F. S. Mjalli, M. A. Hashim, I. M. AlNashef, *Fuel Process. Technol.* **2010**, *91*, 116–120.
- [34] C. D'Agostino, R. C. Harris, A. P. Abbott, L. F. Gladden, M. D. Mantle, *Phys. Chem. Chem. Phys.* **2011**, *13*, 21383–21391.
- [35] A. P. Abbott, R. C. Harris, K. S. Ryder, *J. Phys. Chem. B* **2007**, *111*, 4910–4913.
- [36] A. Yadav, S. Pandey, *J. Chem. Eng. Data* **2014**, *59*, 2221–2229.
- [37] A. Yadav, S. Trivedi, R. Rai, S. Pandey, *Fluid Phase Equilib.* **2014**, *367*, 135–142.

- [38] C. D'Agostino, L. F. Gladden, M. D. Mantle, A. P. Abbott, E. I. Ahmed, A. Y. M. Al-Murshedi, R. C. Harris, *Phys. Chem. Chem. Phys.* **2015**, *17*, 15297–15304.
- [39] A. S. L. Carvalho, E. P. e Melo, B. S. Ferreira, M. T. Neves-Petersen, S. B. Petersen, M. R. Aires-Barros, *Arch. Biochem. Biophys.* **2003**, *415*, 257–267.
- [40] R. Esquembre, J. M. Sanz, J. G. Wall, F. del Monte, C. R. Mateo, M. L. Ferrer, *Phys. Chem. Chem. Phys.* **2013**, *15*, 11248–11256.
- [41] K. Chattopadhyay, S. Mazumdar, *Biochemistry* **2000**, *39*, 263–270.
- [42] T. E. Huntley, P. Strittmatter, *J. Biol. Chem.* **1972**, *247*, 4641–4647.
- [43] M. A. Ator, S. K. David, P. R. Ortiz de Montellano, *J. Biol. Chem.* **1987**, *262*, 14954–60.
- [44] T. T. Herskovits, B. Gadegbeku, H. Jaillet, *J. Biol. Chem.* **1970**, *245*, 2588–2598.
- [45] M. C. Gutierrez, D. Carriazo, C. O. Ania, J. B. Parra, M. L. Ferrer, F. del Monte, *Energy Environ. Sci.* **2011**, *4*, 3535–3544.
- [46] E. Durand, J. Lecomte, B. Barea, E. Dubreucq, R. Lortie, P. Villeneuve, *Green Chem.* **2013**, *15*, 2275–2282.
- [47] D. Shah, F. S. Mjalli, *Phys. Chem. Chem. Phys.* **2014**, *16*, 23900–23907.
- [48] Y. Dai, J. van Spronsen, G.-J. Witkamp, R. Verpoorte, Y. H. Choi, *Anal. Chim. Acta* **2013**, *766*, 61–68.
- [49] Y. Dai, G.-J. Witkamp, R. Verpoorte, Y. H. Choi, *Food Chem.* **2015**, *187*, 14–19.
- [50] T. De Diego, P. Lozano, S. Gmouh, M. Vaultier, J. L. Iborra, *Biotechnol. Bieng.* **2004**, *88*, 916–924.
- [51] H. Monhemi, M. R. Housaindokht, A. A. Moosavi-Movahedi, M. R. Bozorgmehr, *Phys. Chem. Chem. Phys.* **2014**, *16*, 14882–14893.
- [52] R. Murugan, S. Mohan, A. Bigotto, *J. Korean Phys. Soc.* **1998**, *32*, 505–512.
- [53] G. Odian, *Principles of polymerization*, John Wiley & Sons, **2004**, pp. 198–398.
- [54] J. D. Mota-Morales, M. C. Gutiérrez, M. L. Ferrer, I. C. Sanchez, E. A. Elizalde-Peña, J. A. Pojman, F. D. Monte, G. Luna-Bárcenas, *J. Polym. Sci. Part A: Polym. Chem.* **2013**, *51*, 1767–1773.

- [55] K. Bica, J. Shamshina, W. L. Hough, D. R. MacFarlane, R. D. Rogers, *Chem. Commun.* **2011**, *47*, 2267–2269.
- [56] R. J. Sánchez-Leija, J. A. Pojman, G. Luna-Barcenas, J. D. Mota-Morales, *J. Mater. Chem. B* **2014**, *2*, 7495–7501.
- [57] A. I. Bol'shakov, D. P. Kiryukhin, *Polym. Sci. Ser. A* **2007**, *49*, 975–980.
- [58] A. Durand, T. Lalot, M. Brigodiot, E. Maréchal, *Polymer* **2001**, *42*, 5515–5521.
- [59] H.-R. Lin, *Eur. Polym. J.* **2001**, *37*, 1507–1510.
- [60] A. Pandey, R. Rai, M. Pal, S. Pandey, *Phys. Chem. Chem. Phys.* **2014**, *16*, 1559–1568.
- [61] A. Pandey, S. Pandey, *J. Phys. Chem. B* **2014**, *118*, 14652–14661.
- [62] A. Carranza, J. A. Pojman, J. D. Mota-Morales, *RSC Adv.* **2014**, *4*, 41584–41587.
- [63] A. P. Abbott, P. M. Cullis, M. J. Gibson, R. C. Harris, E. Raven, *Green Chem.* **2007**, *9*, 868–872.
- [64] Q. Zhang, K. De Oliveira Vigier, S. Royer, F. Jerome, *Chem. Soc. Rev.* **2012**, *41*, 7108–7146.

Imagination will often carry us to worlds that never were. But without it we go nowhere.

— Carl Sagan

4

Synthesis of conductive polyaniline monoliths from deep eutectic solvents

The discovery of conductive polymers by Alan J. Heeger, Alan G. MacDiarmid and Hideki Shirakawa in 1977 came to change the notion that polymers could not conduct electricity and brought the field to the forefront.^[1] They found that polyacetylene can be made conductive almost like a metal by treating it with a halogen (chlorine, bromine or iodine vapour).^[2,3] After this treatment, which is called “doping”, polyacetylene reached a conductivity of $10^5 \text{ S}\cdot\text{cm}^{-1}$, the highest value obtained so far for a polymer (as comparison, silver and cooper have a conductivity of $10^8 \text{ S}\cdot\text{cm}^{-1}$). This novel finding and years of subsequent research in the field earned these scientists the 2000 Nobel Prize in Chemistry.¹

Since the discovery of conductive polyacetylene, there have been many research efforts for the study and development of other conductive polymers (CPs), being polythiophene,^[4–6] polypyrrole^[7,8] and polyaniline^[9–12] the most promising types.^[4] The unique combination of properties that these materials can offer, *i.e.*, electrical and optical properties as metals or semiconductors and mechanical properties and processing advantages of polymers,^[13] has made them attractive for a wide variety of applications, especially for the development of flexible electronic devices.

¹“The Nobel Prize in Chemistry 2000”. Nobelprize.org. Nobel Media AB 2014. Web. 8 Feb 2017. http://www.nobelprize.org/nobel_prizes/chemistry/laureates/2000/

Today, there is a vast amount of studies on the synthesis, characterization and applications of polyaniline (PANI).^[14,15] In contrast to other CPs, PANI is an electrochromic material, chemically stable, low cost and easy to synthesize.^[16] On top of this, the nitrogen atoms occupying the bridging positions in PANI structure confer it reversible acid/base (doping/dedoping) chemistry, allowing the control of its electrical conductivity (up to the order of 10^2 S·cm⁻¹).^[17,18] All these properties make PANI attractive for numerous potential applications in electronic devices (displays,^[19–21] sensors,^[22–26] light-emitting diodes,^[27–29] energy-storage^[30–32]), antistatic materials,^[33–35] corrosion inhibition,^[36–38] gas separation,^[39] catalysis^[40–42] and medicine.^[43–45] Unfortunately, as for many others CPs, the commercial applications of PANI are still limited due to its poor processability, mainly ascribed to its insolubility in water and most common organic solvents.

The inert chemical nature of this family of polymers renders challenging its preparation as fibers, films and 3D-networks without the need of harsh reaction conditions and complex synthetic and post-synthesis processes. Therefore, development of novel and eco-friendly synthetic pathways that either simplify or shorten the process to obtain CPs with targeted morphologies, suitable electrical conductivity values and mechanical properties for specific applications, is highly valuable.

4.1 Background

PANI is commonly prepared by chemical or electrochemical oxidative polymerization of aniline.^[14,15] Chemical oxidation is usually carried out in acidic aqueous medium using ammonium persulfate as the oxidant,^[46] and is often preferred over the electrochemical method because of its simplicity and scalability. By this method, short-length chain PANI powders difficult to process are obtained owed to its non-solubility in water and also in most typical organic solvents.^[20]

To date intense research efforts in the field have been focused to overcome this drawback, with approaches encompassing either new synthetic methods to obtain soluble PANI, or post-synthesis processes that enable preparation of PANI with suitable morphologies, electrical and mechanical properties for an specific application.^[14,15] Unfortunately, although some of these approaches have helped to sort

out the problem, PANI of low electrical conductivity is obtained in most of the cases, thus still limiting its applications.

Among the attempts to improve PANI's solubility, introduction of functional groups (e.g., $-\text{CH}_2\text{R}$ & $-\text{OCH}_3$,^[47] $-\text{SO}_3\text{H}$,^[48] $-\text{COOH}$ ^[49]) into the polymer backbone by polymerization of substituted anilines or their copolymerization with aniline has been proposed. In particular, the introduction of groups such as sulfonic acids has been the most successful for the preparation of aqueous soluble self-doped PANI. Sulfonation of PANI can also be achieved by treating the polymer with acids as fuming sulfonic acid after polymerization.^[50,51] More interestingly, it has been found that using functionalized sulfonic acids such as dodecylbenzene sulfonic acid (DBSA) or camphor sulfonic acid (CSA) to dope the polymer, results in a PANI–complex soluble in organic solvents (toluene, xylene, chloroform, *m*-cresol, etc.).^[17,18] The functionalized counterion allows processing of doped PANI from solution to fabricate films, fibers, etc. with significantly high electrical conductivity ($100\text{--}400 \text{ S}\cdot\text{cm}^{-1}$).^[17,27]

PANI synthesis as colloidal particles and nanostructures have also been useful to enhance its processability.^[52] Colloidal PANI dispersions with nanosphere morphology are frequently obtained by dispersion polymerization in aqueous medium using stabilizers such as poly(vinyl alcohol), poly(N-vinylpyrrolidone)^[53] and other water-soluble polymers.^[54] Other PANI nanostructures can be prepared employing organic solvents — protic, aprotic, polar, non-polar — and their homogeneous and heterogeneous mixtures with water.^[55\text{--}59] For instance, while the classic synthetic method yields granular PANI, the use of aqueous solutions of alcohols such as methanol,^[60] ethanol,^[61] 1-propanol^[62] and 1,6-hexanediol,^[63] or biphasic mixtures such as water/chloroform,^[64,65] and water/methylene chloride^[64] enable preparation of PANI nanotubes and nanofibers. Hard template-based methods have been an effective way to prepare PANI nanostructures with controllable diameter, length and orientation. These methods employ a physical template as a scaffold for the growth of conductive polymers.^[66] The hard template includes colloidal particles and some templates with a nanosized channel (e.g., zeolite,^[67] anodic alumina oxide^[68] and polycarbonate templates^[69]). Nonetheless, template solubilization may result difficult and can lead to sample destruction during its removal, making these methods laborious in some cases.

An alternative strategy has been the preparation of composites, usually obtained either by polymerizing aniline onto existing non-conductive polymer matrix (e.g., poly(acrylic acid),^[70] poly(methyl methacrylate),^[71] polystyrene^[72]), or carbon support (e.g., graphene,^[73] graphene oxide^[74]); or by simply mixing of PANI with insulating polymers, *i.e.*, polymer blends.^[75] This alternative offers the advantage of yielding materials with better mechanical properties derived from the polymeric matrix, but the presence of an insulating material results in the deterioration of the electrical properties.

Conductive polymeric networks with PANI as the continuous phase are highly desirable since higher electrical conductivity values can be achieved. Attempts to prepare this type of materials have included the synthesis of 3D-interconnected PANI structures (aero- and hydrogels),^[76–78] where a crosslinker agent, usually phytic acid, is essential for obtaining 3D architectures. PANI hydrogels provide an excellent processability as can be easily cast into thin films and can also be ink-jet printed or screen printed into micro-patterns.^[79] Although it is true that the electrical conductivity of these materials can be higher than that of PANI–polymer blends regardless the existence of crosslinking sites along the conductive polymer backbone, the mechanical properties of the material are compromised.^[80] Consequently, the synthesis of flexible and highly conductive 3D-interconnected polymer structures is not an easy task. Further research must be done to develop novel synthetic pathways that enable to obtain materials with a suitable combination of these properties, where avoiding harsh reaction conditions and complex synthetic and post-synthesis processes represents an appealing gain.

Herein, the novel synthesis of conductive 3D-porous interconnected PANI monoliths from aniline hydrochloride-based DESs in one-pot, and in the absence of water is reported.

4.2 Materials and experimental methods

Aniline hydrochloride, *p*-phenylenediamine, ethylene glycol, glycerol, L-lactic acid, glycolic acid, ammonium persulfate, glutaraldehyde, phytic acid, H₂SO₄ and HCl were purchased from Sigma-Aldrich and used as received without further purifica-

tion. Glutaraldehyde and phytic acid solutions were obtained with initial concentrations of 25 and 50% w/w, respectively.

4.2.1 Deep eutectic solvents synthesis

DESSs were prepared by mixing aniline hydrochloride (AHCl, 1.5 mmol, 194.39 mg) with either ethylene glycol (Egly, 4.5 mmol, 279.32 mg), glycerol (Gly, 4.5 mmol, 414.41 mg), L-lactic acid (LAc, 6 mmol, 540.48 mg) or glycolic acid (GlyAc, 6 mmol, 456.30 mg) at 90 °C until a homogeneous liquid was formed. AHCl-based DESSs are, from here on, referred as AHCl–Egly, AHCl–Gly, AHCl–LAc and AHCl–GlyAc.

4.2.2 Polymerization of aniline hydrochloride-based DESSs

PANI monoliths were obtained by chemical oxidative polymerization of AHCl. Two different sets of samples, PANI–S and PANI–P, were prepared from AHCl-based DESSs.

PANI–S samples were synthesized as follows. Prior polymerization, N₂ was bubbled through the eutectic mixtures to remove oxygen from the reaction media. Afterwards, ammonium persulfate (APS) was added to AHCl-based DESSs in an equimolar ratio to AHCl to initiate the polymerization. As soon as the oxidant was added, the eutectic mixtures were vigorously stirred using a vortex at 2500 rpm until a homogeneous dark green color was observed (*ca.* 1-2 min). Due to the high reaction exothermicity observed in the case of AHCl–Egly DES, the reaction system was placed in a jacketed bath at 4 °C for 30 min after stirring to avoid overheating. After 24 h, the vials containing the polymer were broken to obtain monolithic samples. PANI monoliths were then washed with 0.1 M H₂SO₄ for 24 h and two or three times with acetone to remove residual compounds and oligomers. Finally, samples were dried for 24 h in air and 24 h in a vacuum oven at RT.

PANI–P samples were prepared by first adding *p*-phenylenediamine (PPDA) to DESSs in a relation of 2 % mol relative to AHCl. Once PPDA was completely dissolved, AHCl-based DESSs were polymerized following the experimental procedure described above.

Table 4.1 Experimental procedures to obtain crosslinked PANI–P monoliths from AHCl–Egly DES.

Sample	DES precursor	First wash (HBDs removal)	Crosslinking process	Second wash (redoping)
PANI–P			—	Acetone
PGA–HCl	AHCl–Egly, PPDA	0.10 M H ₂ SO ₄	0.014 M GA (72 h)	0.10 M HCl
PGA–PA			0.014 M GA (72 h)	0.05 M PA
PPA–HCl			0.013 M PA (72 h)	0.10 M HCl

4.2.3 Crosslinking of polyaniline monoliths

Glutaraldehyde (GA) and phytic acid (PA) were used as crosslinkers to improve the mechanical properties of monoliths. PANI–P samples obtained from AHCl–Egly DES were selected for the crosslinking process. The experimental procedure to prepare crosslinked monoliths was the same as for previous samples up to washing with 0.1 M H₂SO₄, that is, no acetone washing was performed. Instead, PANI–P monoliths were immediately placed in 15 mL of 0.014 M GA solution or 15 mL of 0.013 M PA solution for 3 days at 37 °C. After this, the samples were washed again for a couple of hours for redoping the polymer (as some counterions could have been lost during the later step), this time with 0.1 M HCl or 0.05 M PA for samples using GA as crosslinker (named PGA–HCl and PGA–PA, respectively), or with 0.1 M HCl for samples using PA as crosslinker (referred as PPA–HCl). Finally, monoliths were dried for 24 h at 37 °C and 24 h at 37 °C in a vacuum oven.

Table 4.1 summarizes the experimental procedures followed to obtain cross-linked PANI–P monoliths. Non-crosslinked PANI–P monoliths were used as reference.

4.2.4 DESs characterization

DSC analysis was performed with a TA Instruments Discovery system, under a N₂ atmosphere on an aluminium pan in a sealed furnace, and at a scan rate of 5 °C·min⁻¹ during the whole process. For data acquisition, the eutectic mixtures were cooled from room temperature to -90 °C and kept at this temperature for 10 min before starting the heating/cooling cycle, which consisted of heating the sample to 100 °C

and then cooling it again to -90 °C. This cycle measurement was repeated two times and the sample was cooled to room temperature at the end of the analysis. DSC scans showed the glass transition temperature (T_g) of DESs.

4.2.5 Polymer characterization

The **electrical conductivity** (σ) of PANI samples was determined by using a digital multimeter Fluke 8840A in a four-probe collinear configuration, where two outer probes source current, while two inner probes sense the resulting voltage drop across the sample.² The four probes were equally spaced, placed in the center of the material and brought into contact with the sample. The electrical resistance (R) values obtained were used to calculate the conductivity using Equation 4.1 for compressed PANI powders (pellets of 13 mm diameter and *ca.* 1 mm thick), and Equation 4.2 for PANI monoliths.^[81,82]

$$\sigma = \frac{\ln 2}{\pi} \cdot \frac{1}{R \cdot w \cdot k_1} \quad (4.1)$$

$$\sigma = \frac{1}{2\pi} \cdot \frac{1}{R \cdot s \cdot k_2} \quad (4.2)$$

With w as the thickness of the sample (cm), s as the distance between probes (cm) and k_1 and k_2 as correction factors based on the ratio of sample thickness to probe spacing.

XPS surface analysis was performed in a VG ESCALAB 200R electron spectrometer equipped with a hemispherical electron analyser and an Al K α ($h\nu = 1486.6$ eV, 1 eV = 1.63×10^{-19} J) 100 Watts X-ray source. Samples were carbon glued on 8 mm diameter stainless steel troughs mounted on a sample rod placed in the pretreatment chamber and degassed for 30 min prior to being transferred to the analysis chamber. The base pressure in the analysis chamber was maintained below 3×10^{-9} mbar during data acquisition. The pass energy of the analyser was set at 50 eV. The binding energies were referenced to the binding energy of the C1s core-level spectrum at 284.8 eV. Data processing was performed with the XPS peak program,

²<http://www.tek.com/sites/tek.com/files/media/document/resources/2615%204%20Point%20Probe%20AN.pdf>

the spectra were decomposed with the least squares fitting routine provided with the software with Gaussian/Lorentzian (90/10) product function and after subtracting a Shirley background. Atomic fractions were calculated using peak areas normalized on the basis of sensitivity factors provided by the manufacturer.

UV-Vis spectrometry analysis were performed in a Varian Cary 4000 spectrophotometer. For the measurements, the samples were dispersed in *N*-methylpyrrolidone (NMP) and 1 M HCl, respectively, with an initial concentration of 1 mg·mL⁻¹, and placed in an ultrasonic bath for a few minutes before recording their absorption spectra.

FTIR spectra were collected on a Bruker Model IFS60 spectrophotometer in the range of 4000–550 cm⁻¹ at room temperature with a resolution of 4 cm⁻¹, and the spectra shown are an average of 250 scans. Some spectra were displaced along the *y*-axis for clarity.

SEM was carried out to study the morphology of the resulting PANI monoliths. SEM micrographs of PANI-S monoliths were acquired at 1500x with a Hitachi S-3000N system operated at 20 kV, whereas the micrographs corresponding to PANI-P monoliths were obtained at 800x with a Hitachi S-4700 equipment operated at 15 kV.

4.3 Results and discussion

4.3.1 AHCl-based DESs characterization

As mentioned in the corresponding section, new AHCl-based DESs were formed by mixing AHCl with the HBDs in a molar ratio of 1:3 for AHCl-Egly and AHCl-Gly, and 1:4 for AHCl-LAc and AHCl-GlyAc DESs. Table 4.2 shows the chemical structure and the melting point temperature (T_m) of the pure components of DESs. The DSC scans revealed that all DESs but AHCl-Egly exhibit a glass transition and that the corresponding T_g values are much lower than the melting points of the components themselves, thus confirming the eutectic nature of the mixtures (Figure 4.1).

Table 4.2 Melting point of polymerizable AHCl-based DESs and their individual components.

DES	Quaternary ammonium salt (QAS)	Hydrogen bond donor (HBD)	QAS : HBD (molar ratio)	QAS T_m (°C)	HBD T_m (°C)	DES T_g (°C)
AHCl-Egly			1:3	196-198	-13	ND
AHCl-Gly			1:3	196-198	20	-71.1
AHCl-LAc			1:4	196-198	53	-57.6
AHCl-GlyAc			1:4	196-198	75-80	-58.0

ND: No detectable melting point temperature in the range of -90 to 100 °C by DSC.

4.3.2 PANI monoliths characterization

PANI in its conductive form was successfully prepared by oxidative polymerization of AHCl-based DESs with APS in the absence of water (Figure 4.2). The dual role of DES — as monomer and reaction medium — allowed, after addition of the oxidant, the synthesis of doped PANI in one-pot without further addition of solvent. After HBDs removal by washing, samples were drying and conductive PANI monoliths were obtained with electrical conductivities ranging from 0.11 to 0.40 S·cm⁻¹ for PANI-S monoliths, being PANI from AHCl-Gly DES the most conductive. The electrical conductivity of PANI-S samples as pressed powders was also determined as reference (Table 4.3).

It has been reported that small additions of PPDA to aniline result in an increase of the electrical conductivity of the polymer.^[83] Accordingly, PANI samples with 2% mol of PPDA relative to the AHCl (added to DESs prior polymerization) were also prepared (PANI-P monoliths) as a step to further increase this property, yielding conductivities up to 10 times higher, 0.94 and 1.21 S·cm⁻¹ when using AHCl-Gly and AHCl-Egly DESs, respectively. As opposed to the previous samples, the PANI-P monolith from AHCl-Egly was the most conductive in this case (Table 4.3).

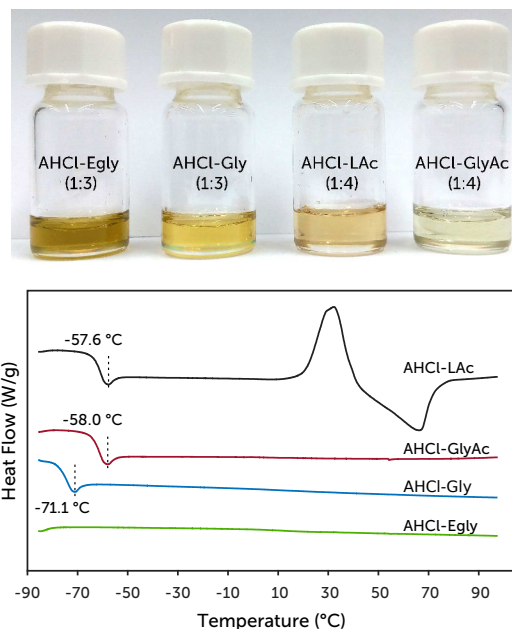


Fig. 4.1 AHCl-based DESs (top) and DSC scans of the eutectic mixtures (bottom).

It is well-known that the electrical conductivity of PANI is mainly function of the oxidation state and degree of “protonation” or “doping” level of the conjugated- π polymer, thus determination of both factors is crucial. Polyanilines are a family of polymers with the general formula shown at the top of Figure 4.3, containing y reduced (amine) and $(1 - y)$ oxidized (imine) repeated units, where $0 \leq y \leq 1$. Depending upon its oxidation state, PANI can exist in three basic structures; leucomeraldine (fully reduced, $y = 0$), emeraldine (half reduced/half oxidized, $y = 0.5$)



Fig. 4.2 Synthesis procedure to obtain conductive PANI-S monoliths from AHCl-based DESs (picture shows the particular case of PANI from AHCl-Egly DES).

Table 4.3 Electrical conductivity of PANI–S and PANI–P monoliths.

Sample set	DES precursor	Electrical conductivity (S·cm ⁻¹)	
		Monolith	Pellet
PANI–S	AHCl–Egly	0.11	0.93
	AHCl–Gly	0.40	2.08
	AHCl–LAc	*	1.29
	AHCl–GlyAc	0.15	1.36
PANI–P (DESSs additionally contained 2% mol of PPDA relative to AHCl)	AHCl–Egly	1.21	—
	AHCl–Gly	0.94	—
	AHCl–LAc	**	—
	AHCl–GlyAc	***	—

* Monolith fractured during measurement manipulation.

** DES solidified as soon as PPDA was added.

*** Monolith fractured during drying process.

— No determined data.

and pernigraniline (fully oxidized, $y = 1$).^[16,84] Each basic PANI structure is referred as base when in its undoped state or salt when in its doped state (e.g., leucoemeraldine base or leucomeraldine salt). Among these, PANI emeraldine salt (PANI–ES), named like this due to its characteristic green color, is the most conductive.

The chain structure of emeraldine base (PANI–EB) is the most stable and contains more than 95% of *para*–substituted aniline units linked in a “head-to-tail” configuration.^[16] Formation of delocalized orbitals by a regularly alternating pattern of single (nitrogen-containing groups) and double bonds (phenyl rings) provides polyconjugation to the polymer backbone, resulting in an electron mobility path. Existence of an electron mobility path, albeit necessary for charge transport, is not sufficient. In addition, a current stabilizer agent is needed (counterion) to facilitate electron mobility, being strong acids the most effective ones. Only after doping with an acid, PANI–EB becomes effectively conductive (PANI–ES).^[86] The doping process essentially changes the number of the electrons in the polymer by either removing or adding electrons to the atoms. Removing electrons creates empty spaces (holes) in the outermost orbital of the atom allowing the remaining electrons to move around more freely. Adding electrons, forces an atom to allocate another orbital and so long as this orbital is not full, the electrons have more space to move around and hop from atom to atom. Therefore, the insulating PANI–EB polymer

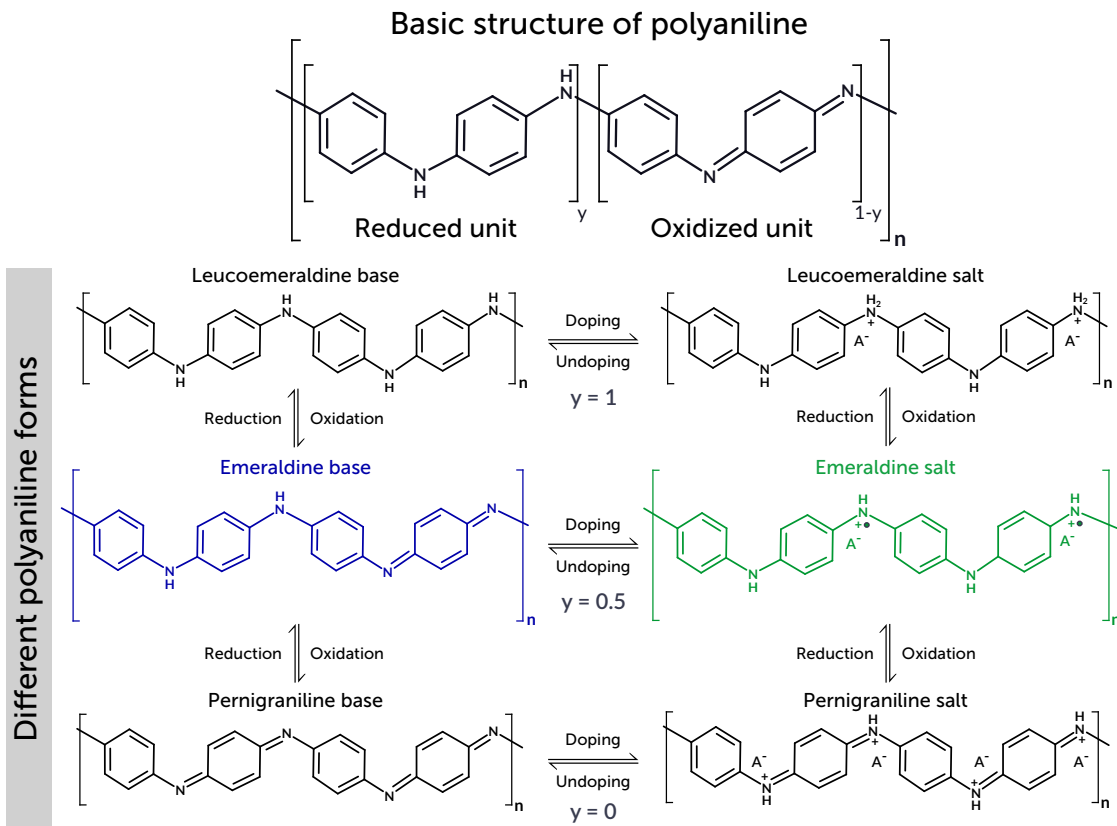


Fig. 4.3 Polyaniline forms (adapted from Dhand *et al.*).^[85]

is converted into a conductive ionic complex consisting of a polymeric cation and a counterion.

XPS analysis was employed to identify the chemical nature of PANI. Figure 4.4 shows the deconvoluted N1s core-level spectra of PANI-S and PANI-P samples from AHCl–Egly, further discussion will be made on samples prepared from this eutectic mixture as it yielded the most conductive PANI monoliths. The lowest energy peak at 398.5 eV corresponds to neutral imine atoms in the polymer network, $-N=(N_1)$, while the peak at 1 eV higher to neutral amine atoms $-NH-(N_2)$. The two peaks at higher binding energies, 400.8 and 402.2 eV, are assigned to the positively charged nitrogen species $-N^+H-(N_3)$ and $-N^+H=(N_4)$, respectively.^[87–89] From these data, the oxidation state and doping level of PANI monoliths were determined by using the equations below^[87,89] (Table 4.4).

$$\text{Oxidation state} = \frac{N_1 + N_3 + N_4}{N_{total}} \quad (4.3)$$

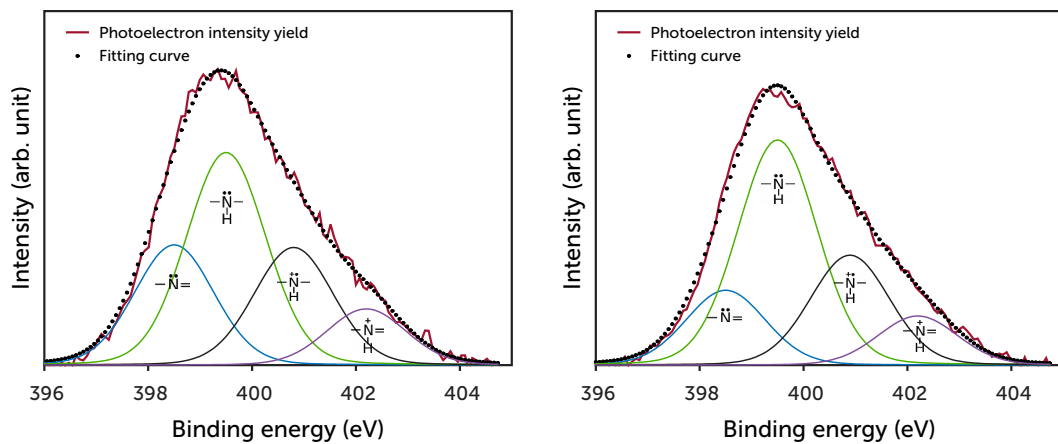


Fig. 4.4 Deconvoluted N1s core-level spectra of PANI-S (left) and PANI-P (right) samples from AHCl–Egly DES.

$$\text{Doping level} = \frac{N^+}{N_{total}} \quad (4.4)$$

It can be seen from Table 4.4 that oxidation state of PANI samples with and without PPDA was basically the same and close to $y = 0.5$, which means that resulting PANI chains are constituted of approximately one-half of oxidized units ($y = 0.5$). Hence, PANI in its emeraldine form was successfully obtained. Regarding the extent of protonation or doping level, 34 and 35 % of the nitrogen containing groups were found doped for both samples. It is believed that protonation of PANI–EB occurs preferably over the imine nitrogen atoms,^[90,91] thus if fully doped, 50 % of the nitrogen species must be protonated to maximize charge transport.^[84] In this case, polymerization from the anilinium cation promoted the formation of conductive PANI chains even in the absence of water, suggesting that the doping level right after DESs polymerization may be near to the maximum possible value due to an excess of counterions (each monomeric unit contained a HCl moiety). However, the degree of protonation of the final PANI monoliths was somewhat below, possibly due to dedoping or withdrawal of counterions during drying of the samples.

In accordance with other reports, electrical conductivity of PANI monoliths also increased after addition of PPDA.^[83,92] Particularly, an increase from 0.11 to 1.21 S·cm⁻¹ was observed for PANI monoliths from AHCl–Egly DES despite both samples exhibited an oxidation state close to $y = 0.5$ and almost the same doping level. As previously mentioned, the oxidation state and percentage of doping are the most

Table 4.4 Binding energies (eV) of N1s core-level of PANI–S and PANI–P samples from AHCl–Egly DES.

Reaction system	N1s	PANI oxidation state (N ₁ +N ₃ +N ₄ /N _{Total})	Doping level (%) (N ⁺ /N _{Total})	Electrical conductivity (S·cm ⁻¹)
AHCl–Egly	398.5 (24)	0.53	34	0.11
	399.5 (42)			
	400.8 (23)			
	402.2 (11)			
AHCl–Egly, PPDA	398.5 (19)	0.54	35	1.21
	399.5 (46)			
	400.8 (23)			
	402.2 (12)			

important factors of which electrical conductivity of PANI depends. Notwithstanding, the molecular weight of the polymer and its degree of crystallinity may also have influence on this physical property.^[14] It is known that PPDA increase the growth rate of polymer and possibly favor formation of longer linear *para*-coupled PANI chains^[83] owed to the presence of two sites in *para* positions, which promotes chain growth at both ends. Thus, the resulting extension of the conjugated- π system derived from an increase on the molecular weight may explain the improvement in conductivity when PPDA is added to AHCl-based DESs.^[92]

Interestingly, incorporation of high concentrations of AHCl through DES formation, enabled the facile synthesis of PANI monolithic structures in one-pot and in the absence of water. The morphology of the resulting PANI–S monoliths consisted in a porous network built of globular PANI that aggregates into a interconnected structure (Figure 4.5), whereas for PANI–P monoliths, the network was formed by aggregates of different morphology including fibers, coral-like and rice-like morphologies (Figure 4.6). It is clear that morphology is greatly influenced by addition of PPDA and, depending upon DES precursor, has a different effect on the nucleation and growth mechanism of the polymer.

It is noteworthy that the synthesis of highly conductive 3D-interconnected porous PANI structures poses a great challenge. This type of materials is often prepared as composites formed by PANI and non-conductive polymers or carbon supports; or as PANI aero- and hydrogels where the use of crosslinkers is essential for obtaining 3D architectures.^[76,77,79] Unfortunately, the presence of an insulating material in the former case and crosslinking sites in the later has as immediate consequence a remarkable decrease in conductivity. Particularly, existence of crosslinking sites

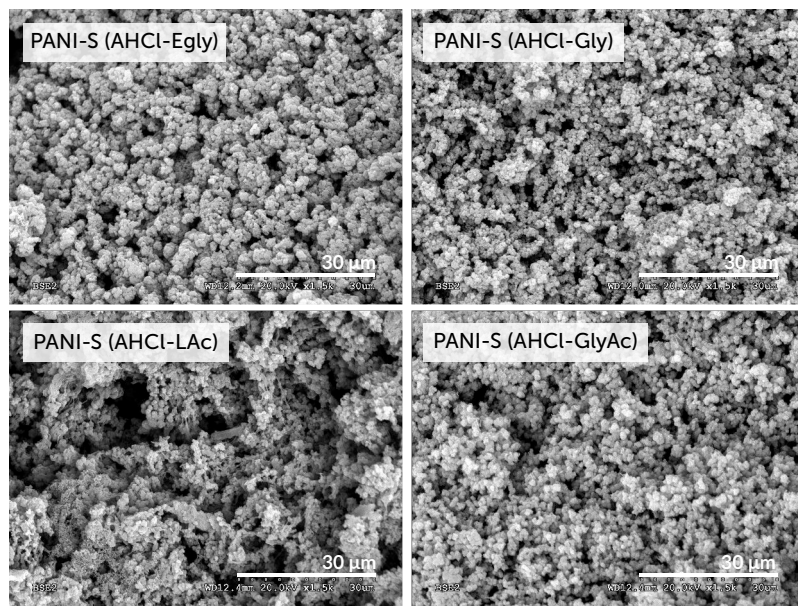


Fig. 4.5 SEM micrographs of PANI-S monoliths.

along the conductive polymer backbone introduces chain defects that break the conjugation and leads to a drop in electrical conductivity.^[80]

In 2015, Guo *et al.* first reported the preparation of porous PANI 3D hydrogels and aerogels from AHCl without the use of any crosslinker in aqueous media, but the electrical conductivity values of the self-crosslinked PANI were not given by the authors.^[76] Similarly, in this work, the synthesis of 3D-interconnected porous PANI structures was possible in the absence of any crosslinker. However, based on earlier reports where GA has been employed for functionalization of PANI surfaces to incorporate bioactivity to this polymer,^[93,94] and PA as a common gelating agent for the synthesis of PANI hydrogels,^[77] the use of these bidentate and multidentate

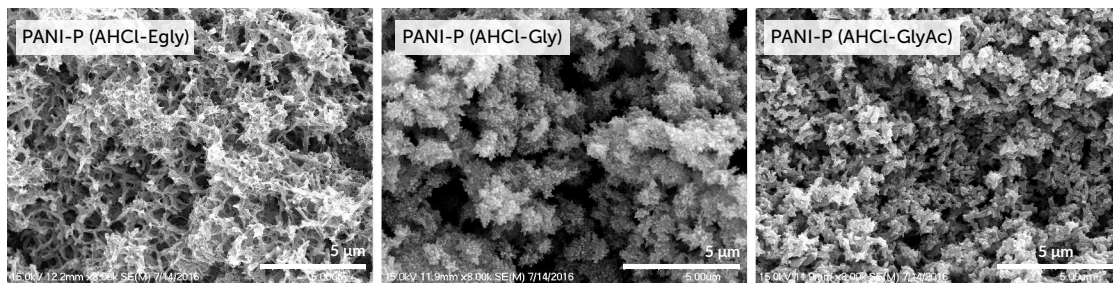


Fig. 4.6 SEM micrographs of PANI-P monoliths showing fibers (AHCl-Egly), coral-like (AHCl-Gly) and rice-like (AHCl-GlyAc) morphologies.

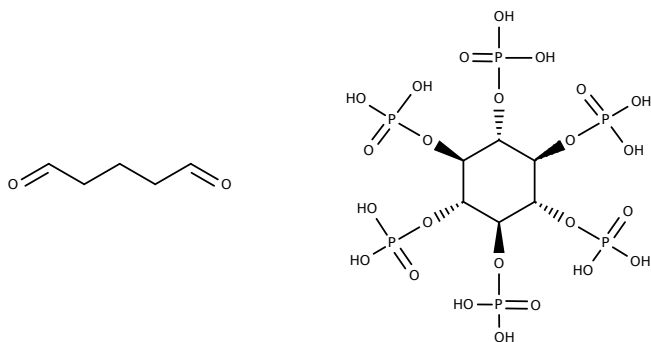


Fig. 4.7 Chemical structures of glutaraldehyde (left) and phytic acid (right) crosslinkers.

crosslinkers (Figure 4.7) was explored as a mean to reinforce the polymeric network and provide mechanical stability to the monoliths. The most conductive samples, PANI–P monoliths from AHCl–Egly, were selected to study the effect of crosslinking on the electrical conductivity. Table 4.5 shows the resulting conductivity values after PANI–P monoliths were subjected to different crosslinking procedures and redoped either with HCl or PA. The non-crosslinked monolith is referred for simplicity as PANI–P from here on, while crosslinked monoliths are labelled as PGA–HCl, PGA–PA and PPA–HCl depending upon crosslinker and redopant acid used (see also Table 4.1 for a detailed sample description).

Remarkably, PGA–PA and PPA–HCl crosslinked samples showed only a slight decrease in conductivity, from 1.21 S·cm⁻¹ (non-crosslinked monolith) to 1.17 S·cm⁻¹ and 1.00 S·cm⁻¹, respectively, probably because PA not only acts as crosslinker in the gelation, but also as an inter-chain dopant (*i.e.*, PA can interact with more than one PANI chain).^[78,79] In contrast to previous attempts of preparing conductive porous 3D-interconnected structures with PANI as the continuous phase, where electrical conductivities of 0.11 S·cm⁻¹ (hydrated hydrogel) and 0.23 S·cm⁻¹ (dehydrated hydrogel, pressed powder) has been the highest achieved so far,^[77] in this work a

Table 4.5 Electrical conductivity of crosslinked PANI–P monoliths from AHCl–Egly DES.

Sample	DES precursor	Crosslinker	Second wash (redoping)	Electrical conductivity (S·cm ⁻¹)
PANI–P		—	Acetone	1.21
PGA–HCl	AHCl–Egly, PPDA	GA	HCl	0.72
PGA–PA		GA	PA	1.17
PPA–HCl		PA	HCl	1.00

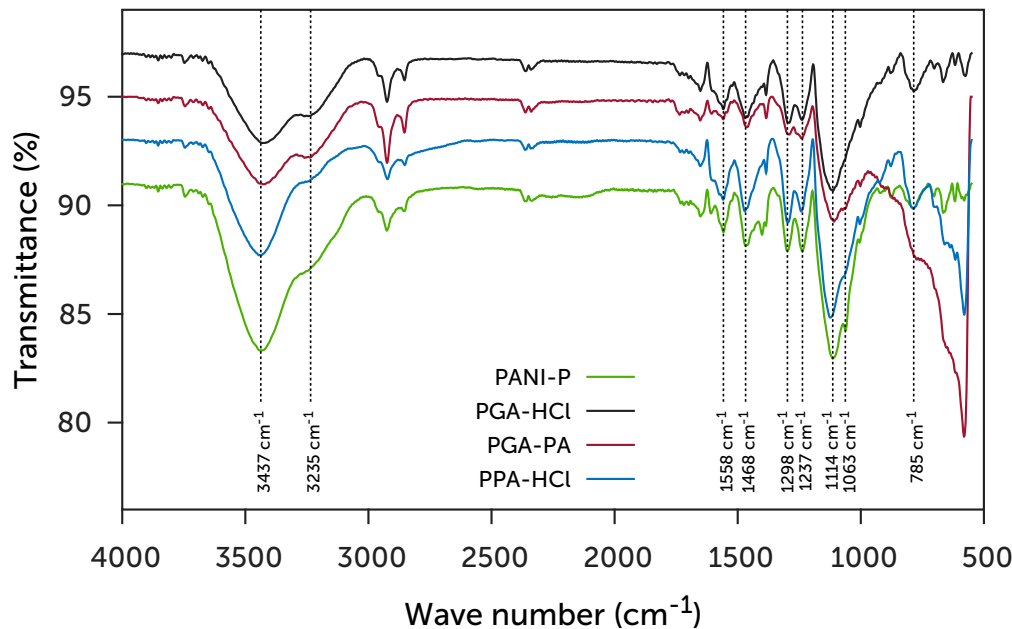


Fig. 4.8 FTIR spectra of PANI-P and crosslinked PANI samples.

10-fold higher value was obtained even for crosslinked samples. Despite the conductivity values attained and the enhancement of the mechanical stability, PANI monoliths were stiff and further work must be done to develop flexible PANI monoliths.

The chemical structure of pristine PANI and its changes after crosslinking were studied by FTIR and UV-Vis spectroscopies. The FTIR spectra of crosslinked PANI monoliths are shown in Figure 4.8. The spectrum of PANI-P sample also appears for comparison. The characteristic bands of doped emeraldine form of PANI (PANI-ES) can be observed in all spectra.^[59,95,96] The broad band of PANI-P at 3437 cm^{-1} is assigned to the N–H stretching vibration. Comparing the spectrum of PANI-P sample to those of GA crosslinked samples, PGA-HCl and PGA-PA, this band shifted to around 3427 cm^{-1} in both cases, which may reveal intermolecular hydrogen bonding between amine and hydroxyl groups of the cyclic hemiacetal form of GA.^[94] The band at 3235 cm^{-1} is assigned to the N–H⁺ (indicative of doping), while the bands at 1558 and 1468 cm^{-1} are ascribed to the C=C stretching vibration of quinoid and benzenoid rings, respectively. The band associated to the C–N stretching of the quinoid ring appears at 1298 cm^{-1} and the one associated to C–N^{•+} in the doped

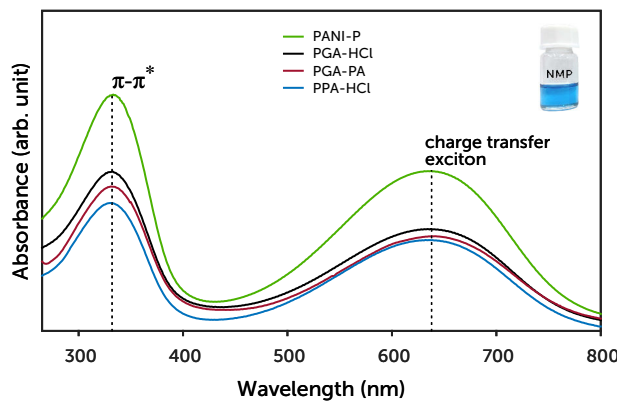


Fig. 4.9 Absorption spectra of PANI–P and crosslinked PANI samples in NMP.

structure at 1237 cm^{-1} . Besides, a broad band between 1000 and 1200 cm^{-1} can also be observed, encompassing contributions from the vibrations of $-\text{N}-\text{H}^+=$ at around 1144 cm^{-1} , C–H in plane bending at 1114 cm^{-1} and S=O stretching at 1063 cm^{-1} . The band at 785 cm^{-1} is related to the out-of-plane vibration in the 1,4-disubstituted benzene ring, that is, the *para*-coupled structure. Unlike PANI–P spectrum, PGA–PA and PPA–HCl spectra showed an evident broad band between 600 and 850 cm^{-1} associated to some of PA vibrations. In this region, the O=P–O bending appears at 642 and 678 cm^{-1} , while the P–O–P stretching at 780 cm^{-1} ,^[97] confirming the presence of PA in both samples, which crosslinks PANI by protonation of the imine nitrogen groups. The characteristic bands of PA assigned to P–O at 1003 cm^{-1} and P=O at 1163 cm^{-1} stretching vibrations^[98] possibly overlap with the corresponding PANI bands appearing in this region.

Figure 4.9 displays the UV-Vis absorption spectra of undoped PANI–P and cross-linked PANI samples obtained after dispersion in NMP. The two absorption bands, typical of the undoped blue emeraldine form of PANI (PANI–EB), were found in all spectra.^[99] This means that PANI chains that constitute the monolithic structures effectively possess polyconjugation. The band located at 330 nm is attributed to the $\pi - \pi^*$ transition of the benzenoid rings and the band at 632 nm to the charge transfer exciton transition.^[100] Likewise, the absorption spectra of the doped samples dispersed in 1 M HCl appear in Figure 4.10. For an accurate assignment, the spectrum of PANI–P sample was decomposed into individual absorption bands by Voigt curve-fitting. The deconvoluted spectrum showed the corresponding bands of PANI–ES. The bands at 273 and 345 nm are assigned to $\pi - \pi^*$ transitions, while

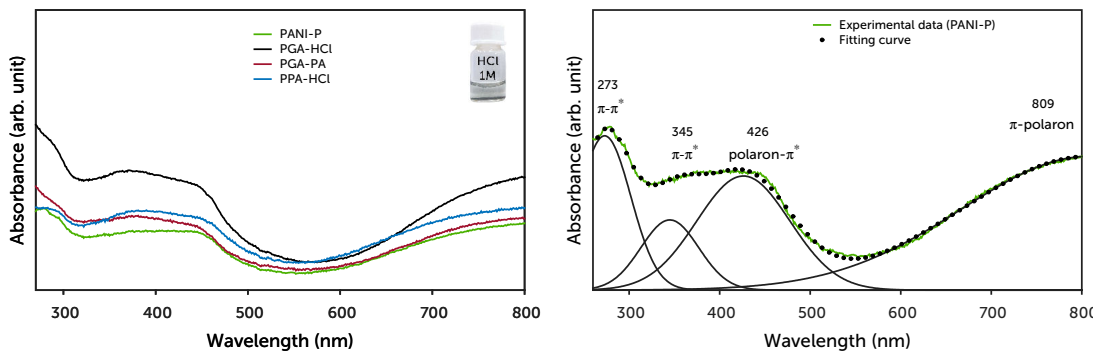


Fig. 4.10 Absorption spectra of PANI-P and crosslinked PANI samples in 1M HCl.

the bands at 426 and 809 nm are ascribed to polaron- π^* and π - polaron transitions, respectively.^[101,102] The polaronic transitions indicate the presence of charge carriers in the polymer, and the $\pi - \pi^*$ transitions arise from the aromatic rings. Only the PANI-P spectrum was deconvoluted as similar spectra were found for the remaining samples.

It is important to highlight that the absence of water during PANI synthesis can be favorable for subsequent applications in electrochemistry or catalysis since PANI prepared by the classic method can retain water molecules that are difficult to remove by drying. Moreover, synthesis of PANI in non-aqueous media might also be useful for preparation of conductive PANI blends with other insulating polymers via the solution polymerization technique.

The literature regarding non-aqueous chemical synthesis of PANI is scarce, with only a couple of works describing PANI synthesis in purely organic solvents. Konyushenko and co-workers reported the polymerization of aniline and AHCl in ethylene glycol and glycerol.^[57] The synthesis of PANI from aniline resulted in poor conversions and yielded only non-conducting oligomers with irregular structure owed to the low effective acidity of reaction mixture and oxidation of the non-protonated monomer. In case of AHCl polymerization, the miscibility of the salt in these organic compounds led to products of granular and packed layers morphologies with electrical conductivities up to $8.3\text{ S}\cdot\text{cm}^{-1}$. Nevertheless, the conductivity values of samples were determined as pressed powders since PANI was only obtained in this form. For comparison, in this work, the electrical conductivity of a monolithic sample of $0.40\text{ S}\cdot\text{cm}^{-1}$ increased to $2.08\text{ S}\cdot\text{cm}^{-1}$ when measured as a pressed powder,

this may lead to believe that the highest conductive sample (PANI-P, $1.21\text{ S}\cdot\text{cm}^{-1}$) would probably exhibit a higher conductivity as pressed sample.

Shortly after, the same research group reported the suspension polymerization of AHCl in purely organic solvents, where the monomer and the oxidant (APS) were not completely soluble.^[58] PANI was formed in acetone, methanol and toluene. In solvents such as chloroform and *n*-butylacetate only aniline oligomers were obtained, while in DMSO and NMP no interaction of the monomer and the oxidant was observed and the reaction did not proceed. The electrical conductivity of the final products was of the order of $0.01 - 1\text{ S}\cdot\text{cm}^{-1}$.

With regard to ILs, reports have been mainly focused on their use as an alternative media to enhance the operational performance of PANI devices as degradation of the polymer occurs after only a few cycles in some aqueous electrolytes due to nucleophilic attack on, and hydrolysis of PANI.^[103,104] Indeed, synthesis of this conductive polymer in ILs (mostly imidazolium-based) has been described just in a few works, and has been exclusively restricted to the synthesis of films and colloidal particles.^[105-108]

As alternative reaction media, DESs have shown promise in organic synthesis given their remarkable solvent properties, and PANI synthesis has not been the exception. To date, there is only a handful of reports describing the synthesis of this polymer in DESs and are limited to the electropolymerization of aniline using DESs as electrolytes.^[109,110] Recently, Silva and co-workers reported the electrochemical synthesis of PANI films in choline chloride-based DESs using fluorine-doped tin oxide electrodes. The electrical conductivities achieved were 10 times higher (up to $50\text{ S}\cdot\text{cm}^{-1}$) than those obtained either by chemical or electrochemical methods where aqueous solvents or aqueous electrolytes have been used. According to the authors, the high conductivity values were a consequence of the large amounts of ionic and hydrogen bond donor species in DESs formulations.^[109] This expanded the applications of DESs in polymer synthesis and further demonstrated the potential of these “greener” solvents for the synthesis of PANI with good electrical properties.

In contrast to previous efforts where ILs and DESs have been used for PANI synthesis, in this work, DESs simultaneously played the role of monomer and solvent for the chemical synthesis of PANI. By this novel synthetic method, porous 3D-interconnected structures were readily formed in its doped state. Furthermore,

since the point of view of toxicity, AHCl-based DESs definitely represents a greener alternative for PANI synthesis as the use of aniline and harsh reactions conditions are avoided.

4.4 Conclusions

PANI in its conductive form was successfully prepared by oxidative polymerization of AHCl-based DESs with APS in the absence of water. The dual role of DES — as monomer and reaction medium — allowed, after addition of the oxidant, the facile synthesis of doped PANI in one-pot without further addition of solvent and in the absence of water. It is noteworthy that in contrast to the typical PANI synthesis, where specific acidic conditions are needed in order to ensure formation of conductive PANI chains, DESs formed by anilinium cations provide a unique environment where acid-base equilibrium is different in nature than in water, and hence pH control becomes superfluous. The problems associated with the low solubility of the monomer in organic solvents are circumvented given the liquid nature of DESs. Furthermore, incorporation AHCl salt at high concentrations was possible through DES formation, allowing the synthesis in one-step of crosslinked porous 3D-interconnected polymer networks with electrical conductivities up to $1.17 \text{ S}\cdot\text{cm}^{-1}$ with potential applications in electrocatalysis and energy storage. It should also be noted that from the point of view of toxicity and storage stability, preparation of PANI from AHCl instead of aniline is advantageous. Definitely, this novel synthetic method represents a step towards eco-friendly alternatives since harsh reaction conditions and complex synthetic routes are avoided.

Bibliography

- [1] H. Shirakawa, E. J. Louis, A. G. MacDiarmid, C. K. Chiang, A. J. Heeger, *J. Chem. Soc. Chem. Commun.* **1977**, 578–580.
- [2] C. K. Chiang, C. R. Fincher, Y. W. Park, A. J. Heeger, H. Shirakawa, E. J. Louis, S. C. Gau, A. G. MacDiarmid, *Phys. Rev. Lett.* **Oct. 1977**, *39*, 1098–1101.
- [3] C. K. Chiang, M. A. Druy, S. C. Gau, A. J. Heeger, E. J. Louis, A. G. MacDiarmid, Y. W. Park, H. Shirakawa, *J. Am. Chem. Soc.* **1978**, *100*, 1013–1015.
- [4] J. Bredas, R. Silbey, D. Boudreaux, R. Chance, *J. Am. Chem. Soc.* **1983**, *105*, 6555–6559.
- [5] R. J. Waltman, J. Bargon, A. Diaz, *J. Phys. Chem.* **1983**, *87*, 1459–1463.
- [6] Y. Furukawa, M. Akimoto, I. Harada, *Synth. Met.* **1987**, *18*, 151–156.
- [7] K. K. Kanazawa, A. F. Diaz, R. H. Geiss, W. D. Gill, J. F. Kwak, J. A. Logan, J. F. Rabolt, G. B. Street, *J. Chem. Soc. Chem. Commun.* **1979**, 854–855.
- [8] K. K. Kanazawa, A. Diaz, W. Gill, P. Grant, G. Street, G. P. Gardini, J. Kwak, *Synth. Met.* **1980**, *1*, 329–336.
- [9] A. Diaz, J. Logan, *J. Electroanal. Chem. Interfacial Electrochem.* **1980**, *111*, 111–114.
- [10] J.-C. Chiang, A. G. MacDiarmid, *Synth. Met.* **1986**, *13*, 193–205.
- [11] W.-S. Huang, B. D. Humphrey, A. G. MacDiarmid, *J. Chem. Soc. Faraday Trans. 1* **1986**, *82*, 2385–2400.
- [12] A. Macdiarmid, J. Chiang, A. Richter, A. Epstein, *Synth. Met.* **1987**, *18*, 285–290.
- [13] A. J. Heeger, *Angew. Chem. Int. Ed.* **2001**, *40*, 2591–2611.
- [14] S. Bhadra, D. Khastgir, N. K. Singha, J. H. Lee, *Prog. Polym. Sci.* **2009**, *34*, 783–810.

- [15] G. Ćirić-Marjanović, *Synth. Met.* **2013**, *177*, 1–47.
- [16] I. Y. Sapurina, M. A. Shishov in *New Polymers for special applications*, (Ed.: A. D. S. Gomes), INTECH Open Access Publisher, **2012**, Chapter 9, pp. 251–312.
- [17] Y. Cao, P. Smith, *Polymer* **1993**, *34*, 3139–3143.
- [18] Y. Cao, P. Smith, A. J. Heeger, *Synth. Met.* **1993**, *57*, 3514–3519.
- [19] T. Kobayashi, H. Yoneyama, H. Tamura, *J. Electroanal. Chem. Interfacial Electrochem.* **1984**, *161*, 419–423.
- [20] E. Genies, M. Lapkowski, C. Santier, E. Vieil, *Synth. Met.* **1987**, *18*, 631–636.
- [21] R. J. Mortimer, A. L. Dyer, J. R. Reynolds, *Displays* **2006**, *27*, 2–18.
- [22] H. Sangodkar, S. Sukeerthi, R. S. Srinivasa, R. Lal, A. Q. Contractor, *Anal. Chem.* **1996**, *68*, 779–783.
- [23] J. Huang, S. Virji, B. H. Weiller, R. B. Kaner, *Chem. - Eur. J.* **2004**, *10*, 1314–1319.
- [24] Z. M. Tahir, E. C. Alocilja, D. L. Grooms, *Biosens. Bioelectron.* **2005**, *20*, 1690–1695.
- [25] C. Dhand, M. Das, M. Datta, B. Malhotra, *Biosens. Bioelectron.* **2011**, *26*, 2811–2821.
- [26] D. Zhai, B. Liu, Y. Shi, L. Pan, Y. Wang, W. Li, R. Zhang, G. Yu, *ACS Nano* **2013**, *7*, 3540–3546.
- [27] G. Gustafsson, Y. Cao, G. M. Treacy, F. Klavetter, N. Colaneri, A. J. Heeger, *Nature* **1992**, *357*, 477–479.
- [28] Y. Yang, A. J. Heeger, *Appl. Phys. Lett.* **1994**, *64*, 1245–1247.
- [29] H. Wang, A. MacDiarmid, Y. Wang, D. Gebier, A. Epstein, *Synth. Met.* **1996**, *78*, 33–37.
- [30] L.-Z. Fan, Y.-S. Hu, J. Maier, P. Adelhelm, B. Smarsly, M. Antonietti, *Adv. Funct. Mat.* **2007**, *17*, 3083–3087.
- [31] J. Xu, K. Wang, S.-Z. Zu, B.-H. Han, Z. Wei, *ACS Nano* **2010**, *4*, 5019–5026.

- [32] H.-P. Cong, X.-C. Ren, P. Wang, S.-H. Yu, *Energy Environ. Sci.* **2013**, *6*, 1185–1191.
- [33] D. C. Trivedi, S. K. Dhawan, *Polym. Adv. Technol.* **1993**, *4*, 335–340.
- [34] S. Dhawan, N. Singh, D. Rodrigues, *Sci. Technol. Adv. Mat.* **2003**, *4*, 105–113.
- [35] M. A. Soto-Oviedo, O. A. Araújo, R. Faez, M. C. Rezende, M.-A. D. Paoli, *Synth. Met.* **2006**, *156*, 1249–1255.
- [36] B. Wessling, *Adv. Mat.* **1994**, *6*, 226–228.
- [37] W.-K. Lu, R. L. Elsenbaumer, B. Wessling, *Synth. Met.* **1995**, *71*, 2163–2166.
- [38] M. Kraljić, Z. Mandić, L. Duić, *Corros. Sci.* **2003**, *45*, 181–198.
- [39] M. R. Anderson, B. R. Mattes, H. Reiss, R. B. Kaner, *Science* **1991**, *252*, 1412–1415.
- [40] G. Wu, K. L. More, C. M. Johnston, P. Zelenay, *Science* **2011**, *332*, 443–447.
- [41] W. Gao, S. Sattayasamitsathit, J. Orozco, J. Wang, *J. Am. Chem. Soc.* **2011**, *133*, 11862–11864.
- [42] J. Zhang, Z. Zhao, Z. Xia, L. Dai, *Nat Nano May* **2015**, *10*, 444–452.
- [43] M. Li, Y. Guo, Y. Wei, A. G. MacDiarmid, P. I. Lelkes, *Biomaterials* **2006**, *27*, 2705–2715.
- [44] A. Subramanian, U. M. Krishnan, S. Sethuraman, *J. Biom. Sci.* **2009**, *16*, 108.
- [45] T. H. Qazi, R. Rai, A. R. Boccaccini, *Biomaterials* **2014**, *35*, 9068–9086.
- [46] J. Stejskal, R. Gilbert, *Pure Appl. Chem.* **2002**, *74*, 857–867.
- [47] G. D'Aprano, M. Leclerc, G. Zotti, *J. Electroanal. Chem.* **1993**, *351*, 145–158.
- [48] H. S. O. Chan, S.-C. Ng, P. M. L. Wong, H. S. O. Chan, A. J. Neuendorf, D. J. Young, *Chem. Commun.* **1998**, 1327–1338.
- [49] H. J. Salavagione, D. F. Acevedo, M. C. Miras, A. J. Motheo, C. A. Barbero, *J. Polym. Sci. Part A: Polym. Chem.* **2004**, *42*, 5587–5599.
- [50] J. Yue, A. J. Epstein, A. G. Macdiarmid, *Mol. Cryst. Liq. Cryst. Incorporating Nonlinear Opt.* **1990**, *189*, 255–261.

- [51] J. Yue, G. Gordon, A. J. Epstein, *Polymer* **1992**, *33*, 4410–4418.
- [52] T. A. Skotheim, *Handbook of conducting polymers*, CRC press, **1997**.
- [53] J. Stejskal, P. Kratochvíl, M. Helmstedt, *Langmuir* **1996**, *12*, 3389–3392.
- [54] J. Stejskal, *J. Polym. Mat.* **2001**, *18*, 225–258.
- [55] P. Ghosh, S. K. Siddhanta, S. Haque, A. Chakrabarti, *Synth. Met.* **2001**, *123*, 83–89.
- [56] M. Can, S. Uzun, N. Ö. Pekmez, *Synth. Met.* **2009**, *159*, 1486–1490.
- [57] E. N. Konyushenko, S. Reynaud, V. Pellerin, M. Trchová, J. Stejskal, I. Sapurina, *Polymer* **2011**, *52*, 1900–1907.
- [58] E. N. Konyushenko, J. Stejskal, M. Trchová, J. Prokeš, *Polym. Int.* **2011**, *60*, 794–797.
- [59] A. A. Rakić, M. Vukomanović, S. Trifunović, J. Travas-Sejdic, O. J. Chaudhary, J. Horský, G. Ćirić-Marjanović, *Synth. Met.* **2015**, *209*, 279–296.
- [60] Y. Huang, C. Lin, *Polymer* **2009**, *50*, 775–782.
- [61] J. Huang, R. B. Kaner, *Angew. Chem. Int. Ed.* **2004**, *43*, 5817–5821.
- [62] Y.-F. Huang, C.-W. Lin, *Polym. Int.* **2010**, *59*, 1226–1232.
- [63] Y. Huang, C. Lin, *Synth. Met.* **2010**, *160*, 384–389.
- [64] J. Huang, R. B. Kaner, *J. Am. Chem. Soc.* **2004**, *126*, 851–855.
- [65] J. Huang, S. Virji, B. H. Weiller, R. B. Kaner, *J. Am. Chem. Soc.* **2003**, *125*, 314–315.
- [66] L. Pan, H. Qiu, C. Dou, Y. Li, L. Pu, J. Xu, Y. Shi, *Int. J. Mol. Sci.* **July 2, 2010**, *11*, 2636–2657.
- [67] C.-G. Wu, T. Bein, *Science* **1994**, *264*, 1757–1759.
- [68] C. Wang, Z. Wang, M. Li, H. Li, *Chem. Phys. Lett.* **2001**, *341*, 431–434.
- [69] C. Schönenberger, B. Van der Zande, L. Fokkink, M. Henny, C. Schmid, M. Krüger, A. Bachtold, R. Huber, H. Birk, U. Staufer, *J. Phys. Chem. B* **1997**, *101*, 5497–5505.
- [70] J. A. Syed, S. Tang, H. Lu, X. Meng, *Ind. Eng. Chem. Res.* **2015**, *54*, 2950–2959.

- [71] M. S. Cho, Y. H. Cho, H. J. Choi, M. S. Jhon, *Langmuir* **2003**, *19*, 5875–5881.
- [72] E. Ruckenstein, S. Yang, *Synth. Met.* **1993**, *53*, 283–292.
- [73] Y. Meng, K. Wang, Y. Zhang, Z. Wei, *Adv. Mat.* **2013**, *25*, 6985–6990.
- [74] Y. Sun, D. Shao, C. Chen, S. Yang, X. Wang, *Environ. Sci. Technol.* **2013**, *47*, 9904–9910.
- [75] J. Anand, S. Palaniappan, D. Sathyaranayana, *Prog. Polym. Sci.* **1998**, *23*, 993–1018.
- [76] H. Guo, W. He, Y. Lu, X. Zhang, *Carbon* **2015**, *92*, 133–141.
- [77] L. Pan, G. Yu, D. Zhai, H. R. Lee, W. Zhao, N. Liu, H. Wang, B. C.-K. Tee, Y. Shi, Y. Cui, Z. Bao, *Proc. Natl. Acad. Sci. U. S. A.* **2012**, *109*, 9287–9292.
- [78] Y. Gawli, A. Banerjee, D. Dhakras, M. Deo, D. Bulani, P. Wadgaonkar, M. Shelke, S. Ogale, *Sci. Rep.* **Feb.** **2016**, *6*, 21002.
- [79] Y. Zhao, B. Liu, L. Pan, G. Yu, *Energy Environ. Sci.* **2013**, *6*, 2856–2870.
- [80] S. Kivelson, A. Heeger, *Synth. Met.* **1988**, *22*, 371–384.
- [81] A. Uhlir, *Bell Syst. Tech. J.* **1955**, *34*, 105–128.
- [82] F. Smits, *Bell Syst. Tech. J.* **1958**, *37*, 711–718.
- [83] Y. Yang, S. Chen, L. Xu, *Macromolecular Rapid Communications* **2011**, *32*, 593–597.
- [84] A. G. MacDiarmid, A. J. Epstein, *Faraday Discuss. Chem. Soc.* **1989**, *88*, 317–332.
- [85] C. Dhand, N. Dwivedi, S. Mishra, P. Solanki, V. Mayandi, R. Beuerman, S. Ramarishna, R. Lakshminarayanan, B. Malhotra, *Nanobiosensors in Disease Diagnosis* **2015**, *4*, 25–46.
- [86] A. G. MacDiarmid, *Angew. Chem. Int. Ed.* **2001**, *40*, 2581–2590.
- [87] S. N. Kumar, F. Gaillard, G. Bouyssoux, A. Sartre, *Synth. Met.* **1990**, *36*, 111–127.
- [88] S. Golczak, A. Kanciurzewska, M. Fahlman, K. Langer, J. J. Langer, *Solid State Ionics* **2008**, *179*, 2234–2239.
- [89] M. M. Mahat, D. Mawad, G. W. Nelson, S. Fearn, R. G. Palgrave, D. J. Payne, M. M. Stevens, *J. Mater. Chem. C* **2015**, *3*, 7180–7186.

- [90] J.-C. Chiang, A. G. MacDiarmid, *Synthetic Metals* **1986**, *13*, 193–205.
- [91] A. Ray, G. Asturias, D. Kershner, A. Richter, A. MacDiarmid, A. Epstein, *Synth. Met.* **1989**, *29*, 141–150.
- [92] H. Tang, A. Kitani, S. Maitani, H. Munemura, M. Shiotani, *Electrochim. Acta* **1995**, *40*, 849–857.
- [93] R. Borah, S. Banerjee, A. Kumar, *Synth. Met.* **2014**, *197*, 225–232.
- [94] R. Borah, A. Kumar, M. K. Das, A. Ramteke, *RSC Adv.* **2015**, *5*, 48971–48982.
- [95] Z. Ping, *J. Chem. Soc. Faraday Trans.* **1996**, *92*, 3063–3067.
- [96] S.-J. Tang, A.-T. Wang, S.-Y. Lin, K.-Y. Huang, C.-C. Yang, J.-M. Yeh, K.-C. Chiu, *Polym. J. Aug.* **2011**, *43*, 667–675.
- [97] C. Samba-Fouala, J.-C. Mossoyan, M. Mossoyan-Deneux, D. Benlian, C. Chaneac, F. Babonneau, *J. Mater. Chem.* **2000**, *10*, 387–393.
- [98] G. Jiang, J. Qiao, F. Hong, *Int. J. Hydrogen Energy* **2012**, *37*, 9182–9192.
- [99] J. Stejskal, P. Kratochvíl, N. Radhakrishnan, *Synth. Met.* **1993**, *61*, 225–231.
- [100] J. de Albuquerque, L. Mattoso, R. Faria, J. Masters, A. MacDiarmid, *Synth. Met.* **2004**, *146*, 1–10.
- [101] S. Stafström, J. L. Brédas, A. J. Epstein, H. S. Woo, D. B. Tanner, W. S. Huang, A. G. MacDiarmid, *Phys. Rev. Lett.* **1987**, *59*, 1464–1467.
- [102] H.-W. Park, T. Kim, J. Huh, M. Kang, J. E. Lee, H. Yoon, *ACS Nano* **2012**, *6*, 7624–7633.
- [103] W. Lu, A. G. Fadeev, B. Qi, E. Smela, B. R. Mattes, J. Ding, G. M. Spinks, J. Mazurkiewicz, D. Zhou, G. G. Wallace, D. R. MacFarlane, S. A. Forsyth, M. Forsyth, *Science* **2002**, *297*, 983–987.
- [104] P. Innis, J. Mazurkiewicz, T. Nguyen, G. Wallace, D. MacFarlane, *Current Appl. Phys.* **2004**, *4*, 389–393.
- [105] H. Gao, T. Jiang, B. Han, Y. Wang, J. Du, Z. Liu, J. Zhang, *Polymer* **2004**, *45*, 3017–3019.
- [106] W. Yang, J. Liu, R. Zheng, Z. Liu, Y. Dai, G. Chen, S. Ringer, F. Braet, *Nanoscale Res. Lett.* **2008**, *3*, 468.

- [107] F. F. C. Bazito, L. T. Silveira, R. M. Torresi, S. I. Cordoba de Torresi, *Phys. Chem. Chem. Phys.* **2008**, *10*, 1457–1462.
- [108] X. Zhou, T. Wu, B. Hu, G. Yang, B. Han, *Chem. Commun.* **2010**, *46*, 3663–3665.
- [109] P. M. Fernandes, J. M. Campiña, C. M. Pereira, F. Silva, *J. Electrochem. Soc.* **2012**, *159*, G97–G105.
- [110] P. M. V. Fernandes, J. M. Campiña, N. M. Pereira, C. M. Pereira, F. Silva, *J. Appl. Electrochem.* **2012**, *42*, 997–1003.

Fall in love with some activity, and do it! Nobody ever figures out what life is all about, and it doesn't matter. Explore the world. Nearly everything is really interesting if you go into it deeply enough. Work as hard and as much as you want to on the things you like to do the best. Don't think about what you want to be, but what you want to do. Keep up some kind of a minimum with other things so that society doesn't stop you from doing anything at all.

— Richard Feynman

5

Concluding remarks and future perspectives

DESs have increasingly shown promise as solvents in a plethora of applications in the fields of electrochemistry, organic synthesis, separation processes, biomass processing, catalysis and material synthesis. The “non-volatility”, i.e., negligible vapor pressure, and recyclability of these solvents, as well as the fact that can be easily prepared from biodegradable or low toxic compounds, have made DESs a “green” alternative to replace typical organic solvents and ILs in materials synthesis, especially in cases where solvent evaporation is not essential or where the characteristic high viscosity of DESs does not represent a drawback.

Particularly, throughout this research work, the versatility and potential of DESs as multifunctional solvents for the sustainable synthesis of polymers have been demonstrated. The case studies presented here include polymer-drug delivery systems, biocatalysis in nearly non-aqueous media and novel 3D-interconnected conductive polymer networks. The feasibility to design DESs by suitably combining different quaternary ammonium salts and HBDs allowed preparation of task-specific DESs with tailored properties for the all-in-one synthesis of polymers, where DESs simultaneously played the role of monomer, solvent and compound with specific

functionality. It is noteworthy that the multifunctionality of DESs offers an appealing gain from the environmental point of view, as greater use of chemical compounds and generation of waste products are avoided.

Beyond all the already mentioned outstanding features of these solvents, herein DESs also served as a propitious chemical environment to perform each of the proposed synthetic procedures. For instance, DESs composed of lidocaine hydrochloride with either acrylic acid and methacrylic acid, provided a polymerization medium with sufficiently high viscosity to suppress buoyancy-driven convection during the reaction without the need of additional fillers. The control of the exothermicity in this case allowed to accomplish the free-radical polymerization of the acrylates at relatively low temperature. Additionally, the tailored composition of DESs allowed designing of pH responsive polymer– and copolymer–drug complexes for potential applications as drug delivery systems. It should be noticed that only materials with monolithic form were obtained. Hence, preparation and study of these systems as films, as well as the use of less toxic catalysts would be highly desirable for practical biomedical applications (*e.g.*, transdermal drug delivery).

Albeit DESs only played the role of solvents for the enzyme-mediated polymerization of acrylamide, they turned out advantageous for the enzyme performance, allowing to obtain high conversions and polymers with high molecular weight. The thermal stability of horseradish peroxidase was enhanced in choline chloride /urea aqueous mixtures in comparison to that in water probably due to formation of a “rigid” structure resulting from hydrogen bonding interactions between urea, choline and choline ions with the surface residues of the enzyme. Furthermore, DESs being liquid over a wide temperature range, enabled the exploration of the biocatalytic process at 4 °C and, while no polymer was formed at the same temperature in aqueous solution, acrylamide was successfully polymerized in choline chloride/glycerol DES. Undoubtedly, this behaviour deserves a deeper study and changes on the enzyme conformation in DESs at different temperatures must be additionally studied by a more accurate characterization technique such as circular dichroism. Moreover, the extrapolation of these biocatalytic systems to more complex synthetic routes, *e.g.*, preparation of functionalized polymers, would be of great interest.

The non-aqueous synthesis of conductive polyaniline monoliths was accomplished by polymerizing non-Previously reported aniline hydrochloride-based DESs. The incorporation of high aniline hydrochloride concentrations through DESs formation, allowed the facile synthesis of self-crosslinked porous 3D-interconnected polymer networks. It is important to highlight that by this novel synthetic approach, polyaniline was readily obtained in its doped form and the electrical conductivity values achieved are, to the best of our knowledge, the highest reported for pristine polyaniline 3D-interconnected architectures. Unfortunately, the monoliths were stiff and further work must be done to improve the elastic behaviour of polyaniline structures, which is highly desirable for the development of flexible electronic devices. The potential applicability of conductive polymers is not limited to electronics, but also includes energy storage, electrocatalysis and gas absorption, among others. In order to evaluate the material performance for any of these applications, a more complete characterization, including mechanical properties, porosity and surface area, and electrochemical characterization (cyclic voltammetry, chronopotentiometry, electrochemical impedance spectroscopy) is needed.

Compared to conventional ILs, the research into DESs is comparatively in its infancy, with the first paper on the subject only published in 2003. Given the scope of applications, further physicochemical characterization of these solvents is of paramount importance. To date only a few works describe the use of DESs in polymerization processes despite the attractive scenarios offered by these solvents for materials synthesis. The research work developed here greatly contribute to this field and definitely represent a step towards eco-friendly alternatives for polymer synthesis.

Appendices

Appendix A

Supplementary information of Chapter 2



Fig. A.1 Experimental setup for the frontal polymerization of LidHCl-based DESs. The reactor was covered for thermal isolation and the bottom part of the tube was heated with an electrical resistance for thermal initiation, whereas the upper end of the reactor remained open to atmospheric pressure.

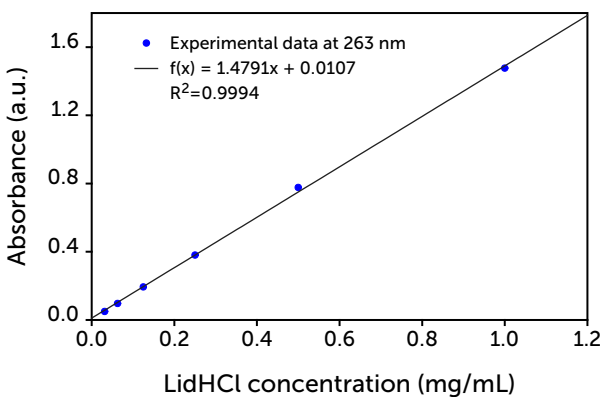


Fig. A.2 Calibration curve for LidHCl quantification by UV-Vis spectroscopy at 263 nm.

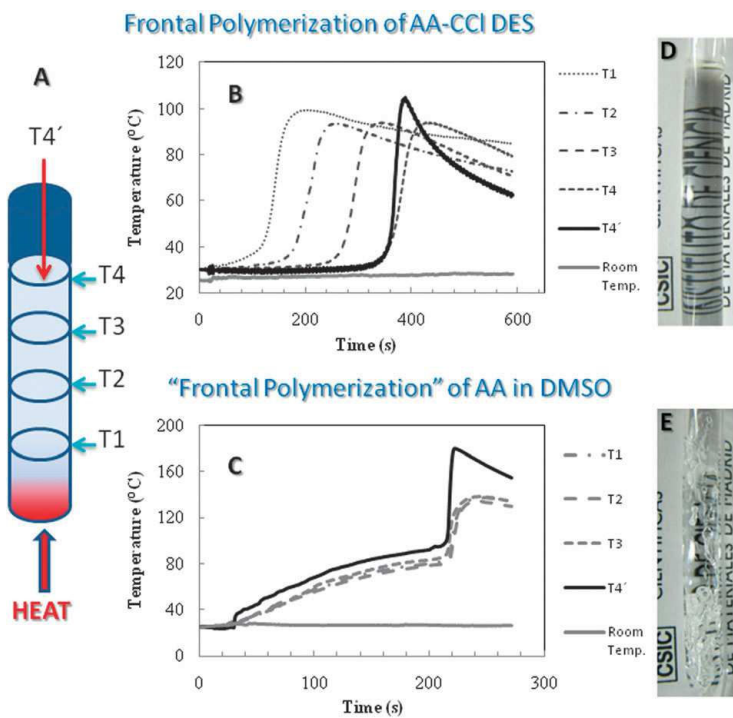


Fig. A.3 Scheme representing the allocation of the thermocouples (T1–T4) along the reactor for frontal polymerization (A). Plot of temperature profile of the front at positions T1–T4 versus time of propagation for polymerizations carried out in acrylic acid/choline chloride DES (B) and dissolved acrylic acid in DMSO (C). Picture of the gels obtained by frontal polymerization from acrylic acid/choline chloride DES (D) and acrylic acid in DMSO (E). Reproduced from Ref. [26] (Chapter 2) with permission from the Royal Society of Chemistry.

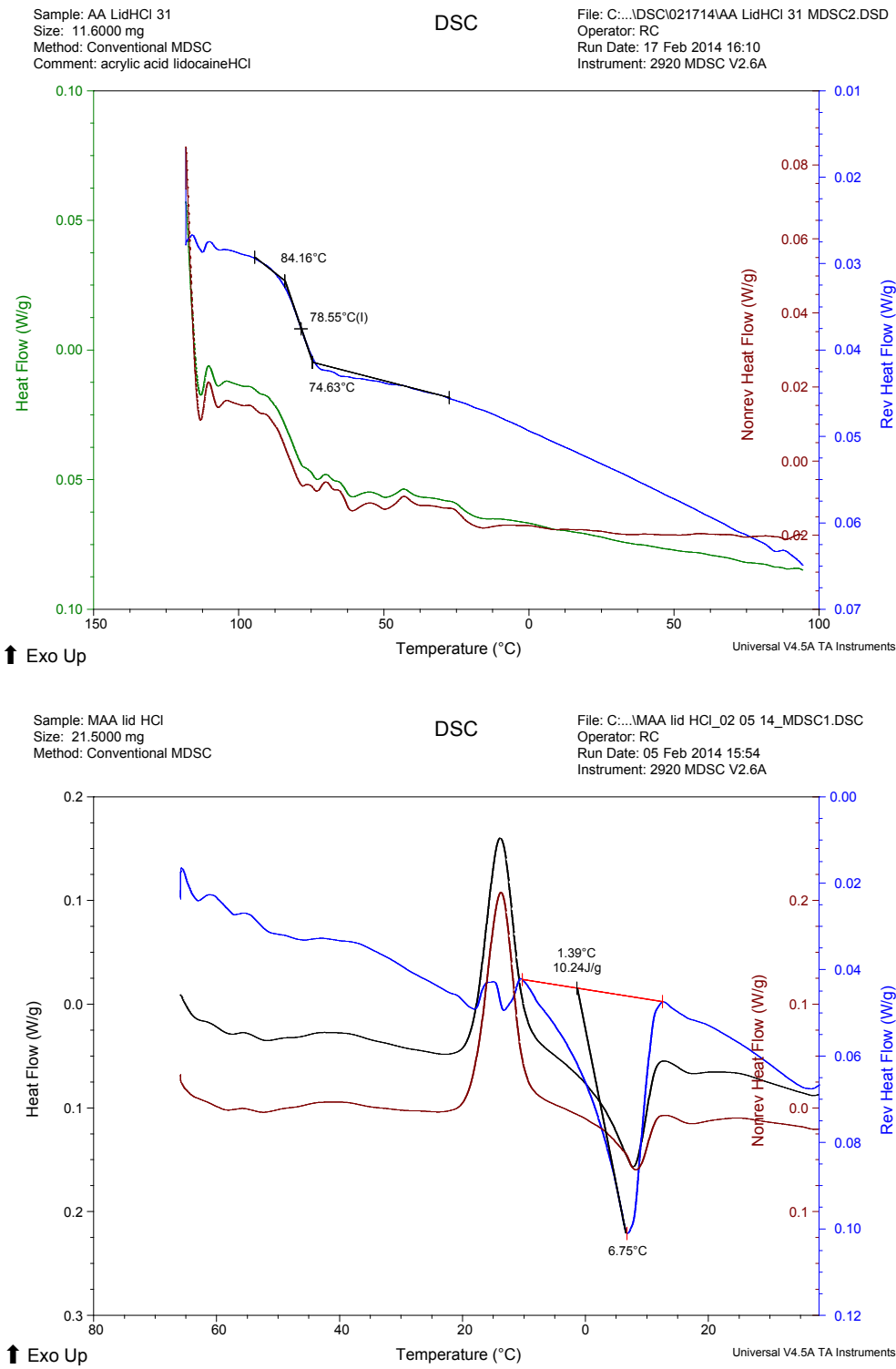


Fig. A.4 DSC scans of AA–LidHCl (top) and MAA–LidHCl (bottom) DESSs.

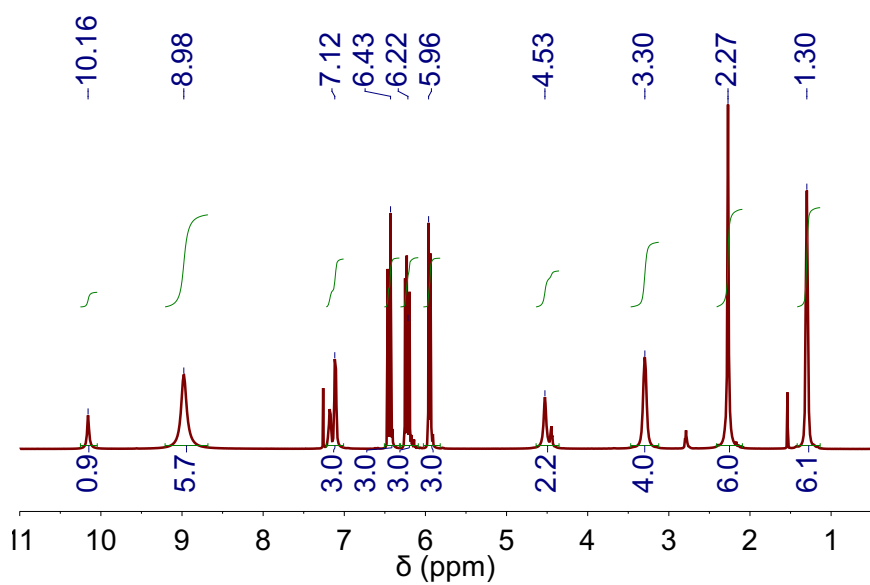


Fig. A.5 ^1H NMR spectrum of AA–LidHCl DES in CDCl_3 . Reproduced with permission of Ref. [27] (Chapter 2), Copyright (2012) Wiley-VCH.

Table A.1 ^1H NMR signal assignment of AA–LidHCl DES.

Sample	δ (ppm)							
	AA				$\text{LidHCl}\cdot\text{H}_2\text{O}$			
	$\text{H}-\text{C}-\text{H}=\text{C}-\text{H}-\text{COOH}$				$(\text{CH}_3)_2-\text{C}_6\text{H}_3-\text{NHCO}-\text{CH}_2-\text{NH}^+- (\text{CH}_2-\text{CH}_3)_2$			
LidHCl**					2.12	7.19	9.15	3.22
AA*	6.52	5.96	6.14	12.0			7.00	3.37
AA–LidHCl	6.43	5.96	6.22		2.27	7.12	10.16	4.53
							8.98	3.30
								1.30

* Data from SDBS Web: <http://riodb01.ibase.aist.go.jp/sdbs/> (National Institute of Advanced Industrial Science and Technology, 08.15.2014).

** Data from ChemDraw™ ^1H NMR estimation.

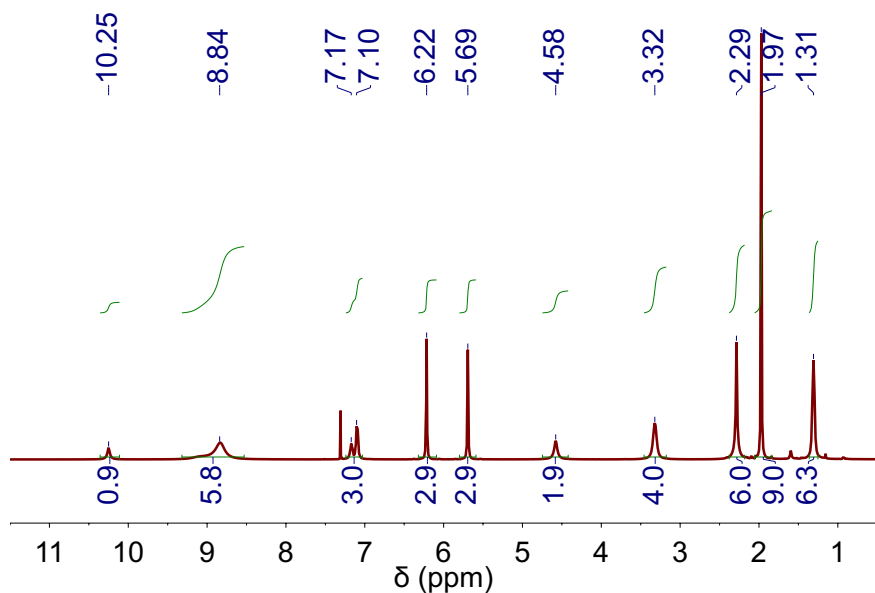


Fig. A.6 ^1H NMR spectrum of MAA–LidHCl DES in CDCl_3

Table A.2 ^1H NMR signal assignment of MAA–LidHCl DES.

Sample	δ (ppm)							
	MAA				$\text{LidHCl}\cdot\text{H}_2\text{O}$			
	$\text{H}-\text{C}-\text{H}=\text{C}-\text{H}_3-\text{COOH}$				$(\text{CH}_3)_2-\text{C}_6\text{H}_3-\text{NHCO}-\text{CH}_2-\text{NH}^+-\text{(CH}_2-\text{CH}_3)_2$			
LidHCl**					2.12	7.19	9.15	3.22
MAA*	6.26	5.68	1.96	11.13			7.00	3.37
MAA–LidHCl	6.22	5.69	1.97		2.29	7.14	10.25	4.58
							8.84	3.32
								1.31

* Data from SDBS Web: <http://riodb01.ibase.aist.go.jp/sdbs/> (National Institute of Advanced Industrial Science and Technology, 08.15.2014).

** Data from *ChemDraw*TM ^1H NMR estimation.

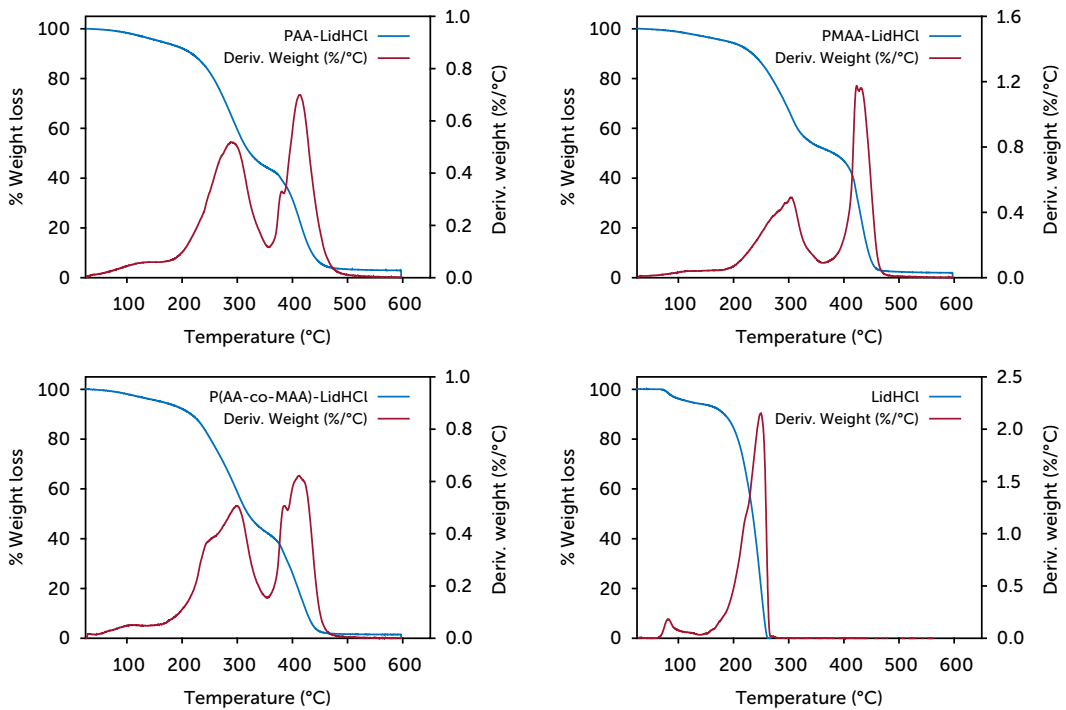


Fig. A.7 Thermogravimetric analysis of the polyacrylates–LidHCl and LidHCl monohydrate.

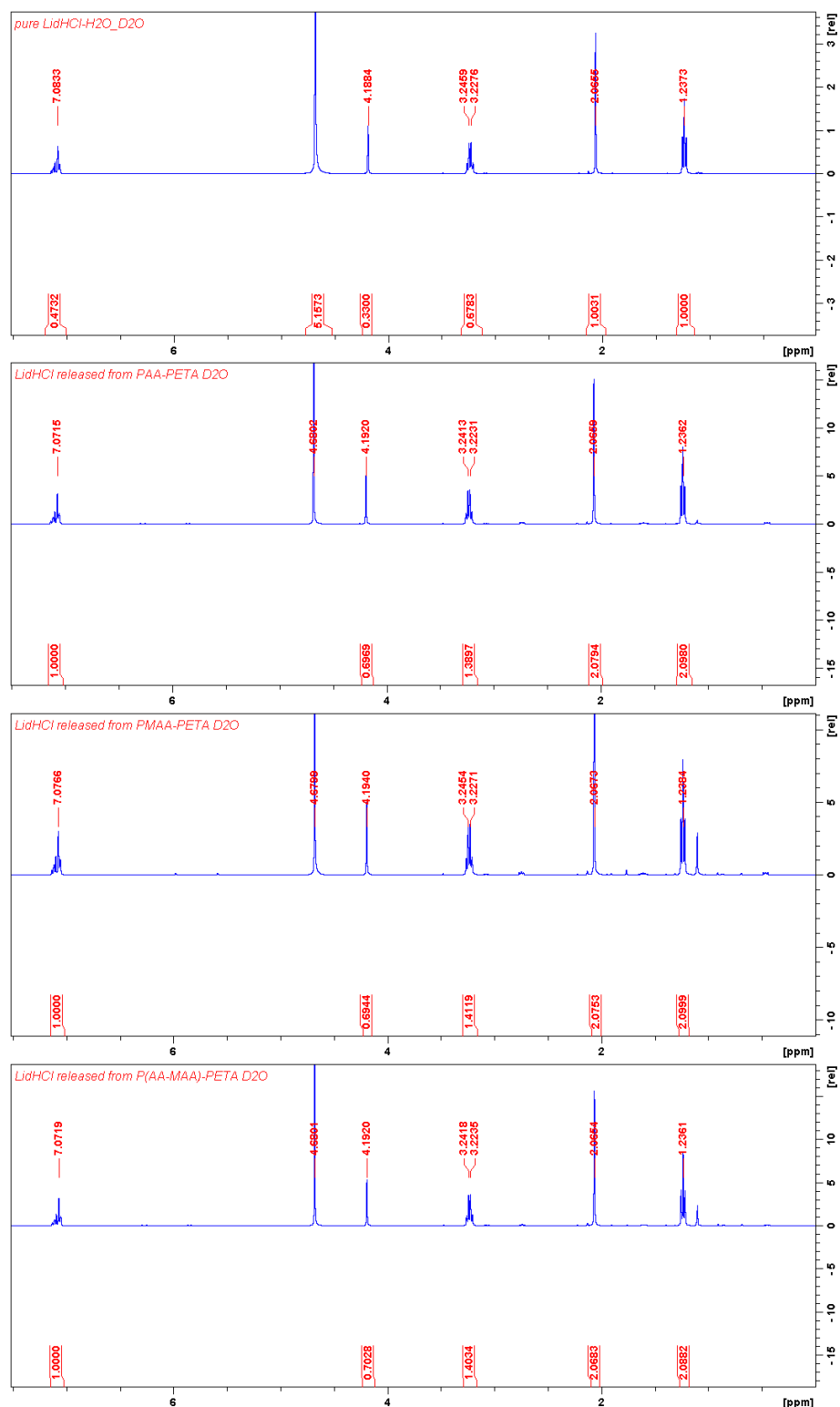


Fig. A.8 ^1H NMR spectra in D₂O of (from top to bottom): pure LidHCl monohydrate, LidHCl from PAA–LidHCl, PMAA–LidHCl and P(AA–co–MAA)–LidHCl with PETA as crosslinker.

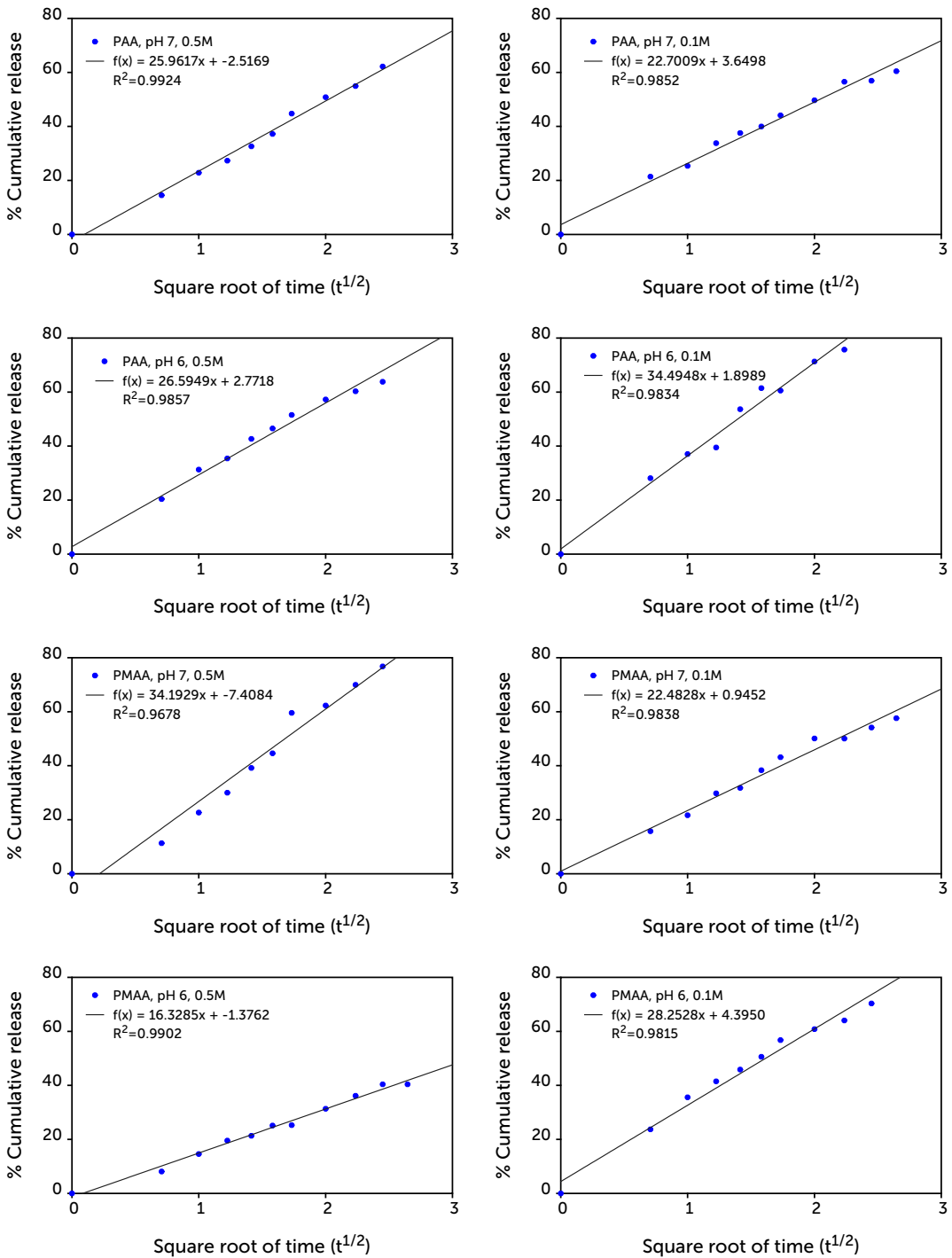


Fig. A.9 Cumulative release of LidHCl vs the square root of time and linear fitting to Fickian model with $n=0.5$

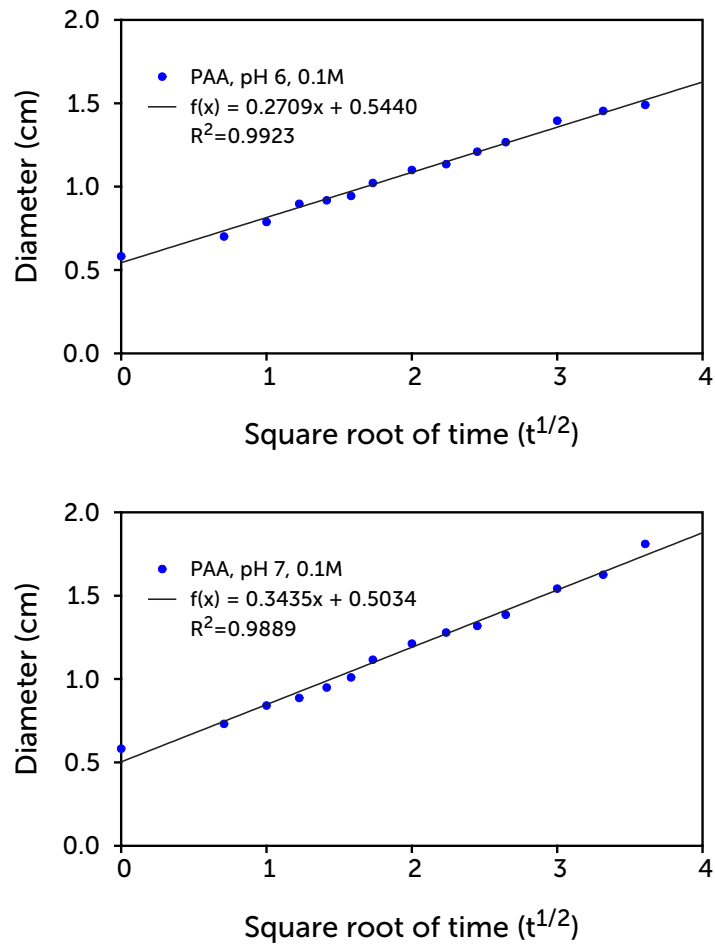


Fig. A.10 Diameter of PAA–LidHCl with EDGMA as crosslinker at pH 6 (top) and pH 7 (bottom) vs the square root of time and linear fitting to Fickian model with $n=0.5$.

Appendix B

Supplementary information of Chapter 3

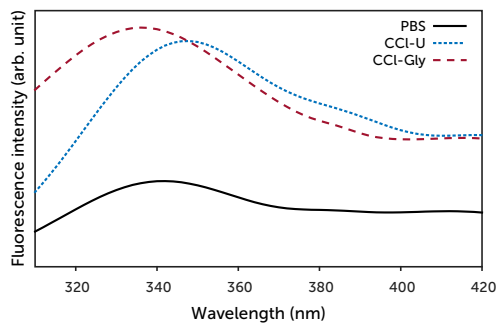


Fig. B.1 Raw tryptophan fluorescence emission spectra of HRP (excitation wavelength 295 nm) in PBS (0.1M, pH 7) and DESs-aqueous mixtures (80 % v/v DES) at RT.

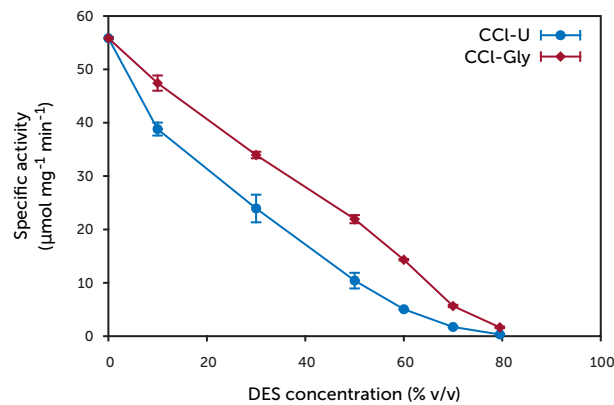


Fig. B.2 Specific activity of HRP in DESs-aqueous mixtures at RT and different DES concentrations. Experiments were at least triplicated and the standard deviation error bars for each point are shown.

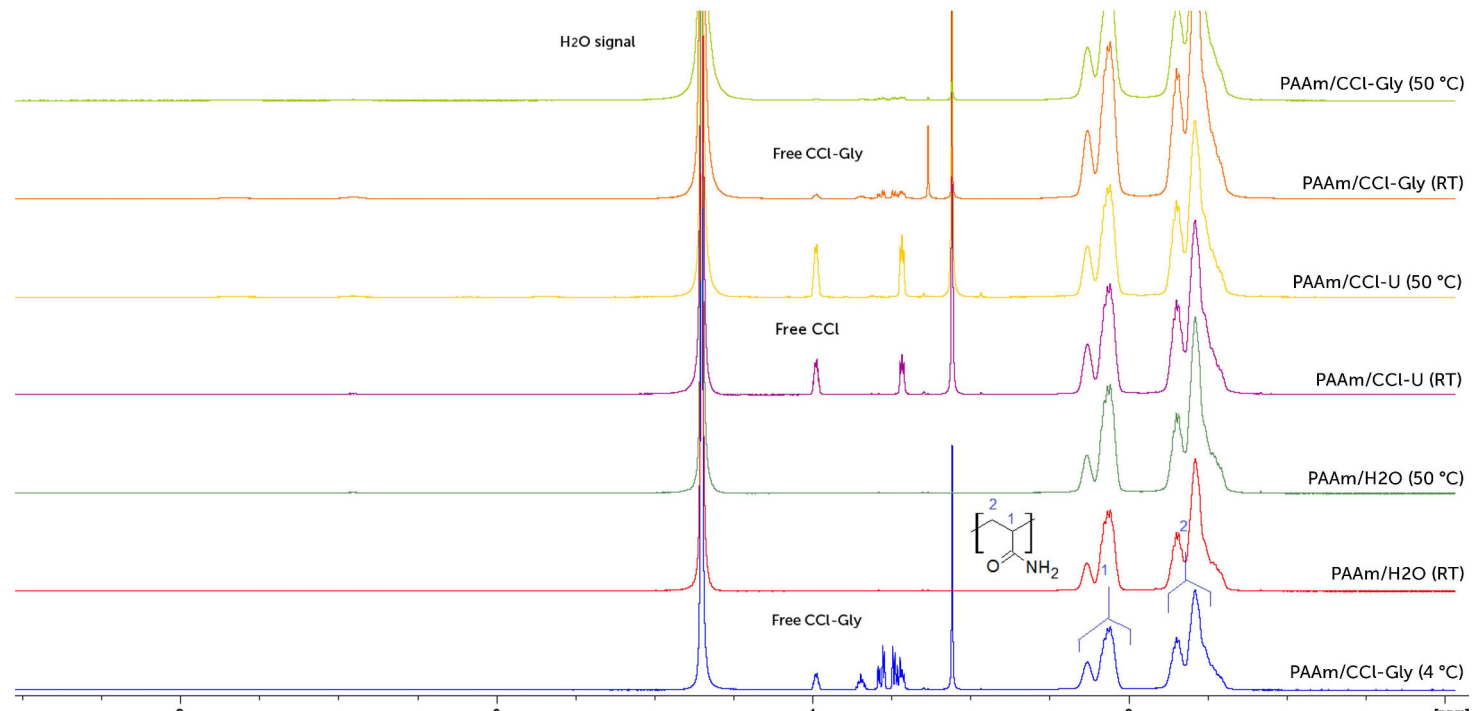


Fig. B.3 ¹H-NMR spectra of PAAm samples synthesized in DESS-aqueous mixtures and H₂O at RT, 50 °C and 4 °C.

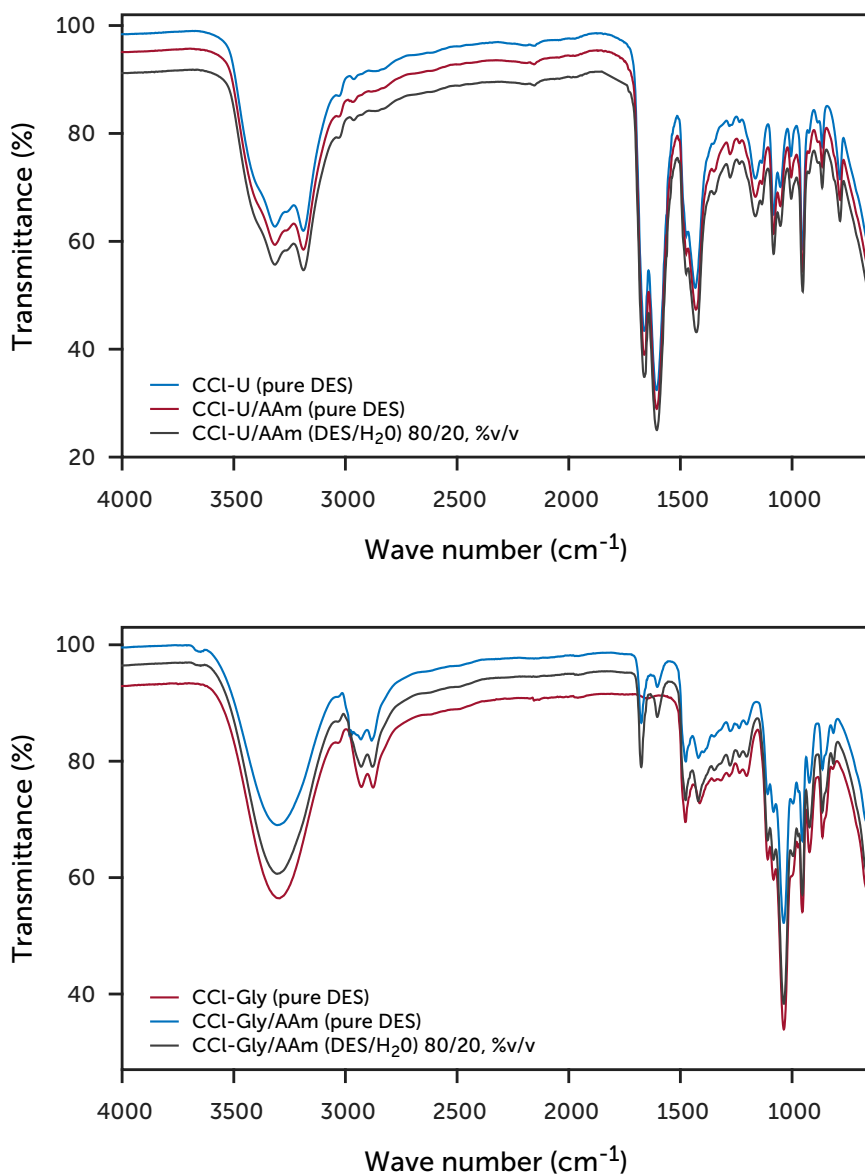


Fig. B.4 ATR-FTIR spectra of CCl-U (top) and CCl-Gly (bottom) DESs in pure state, and DESs-aqueous mixtures (80% v/v DES), 0.64 M AAm (based on DESs volume) in all cases.

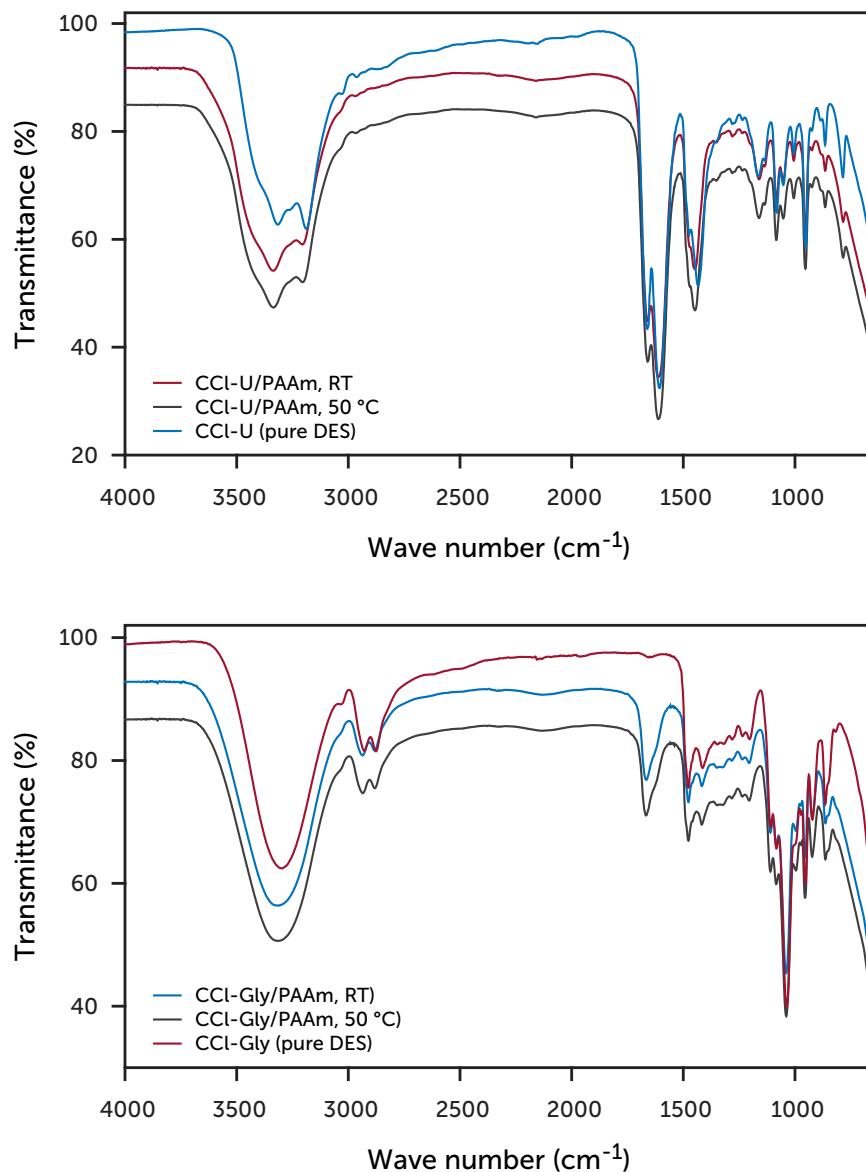


Fig. B.5 ATR-FTIR spectra of CCl-U (top) and CCl-Gly (bottom) DESs in its pure state, and PAAm solutions in DESs-aqueous mixtures (80% v/v DES) synthesized at different temperatures, 0.64 M AAm (based on DESs volume) in all cases.

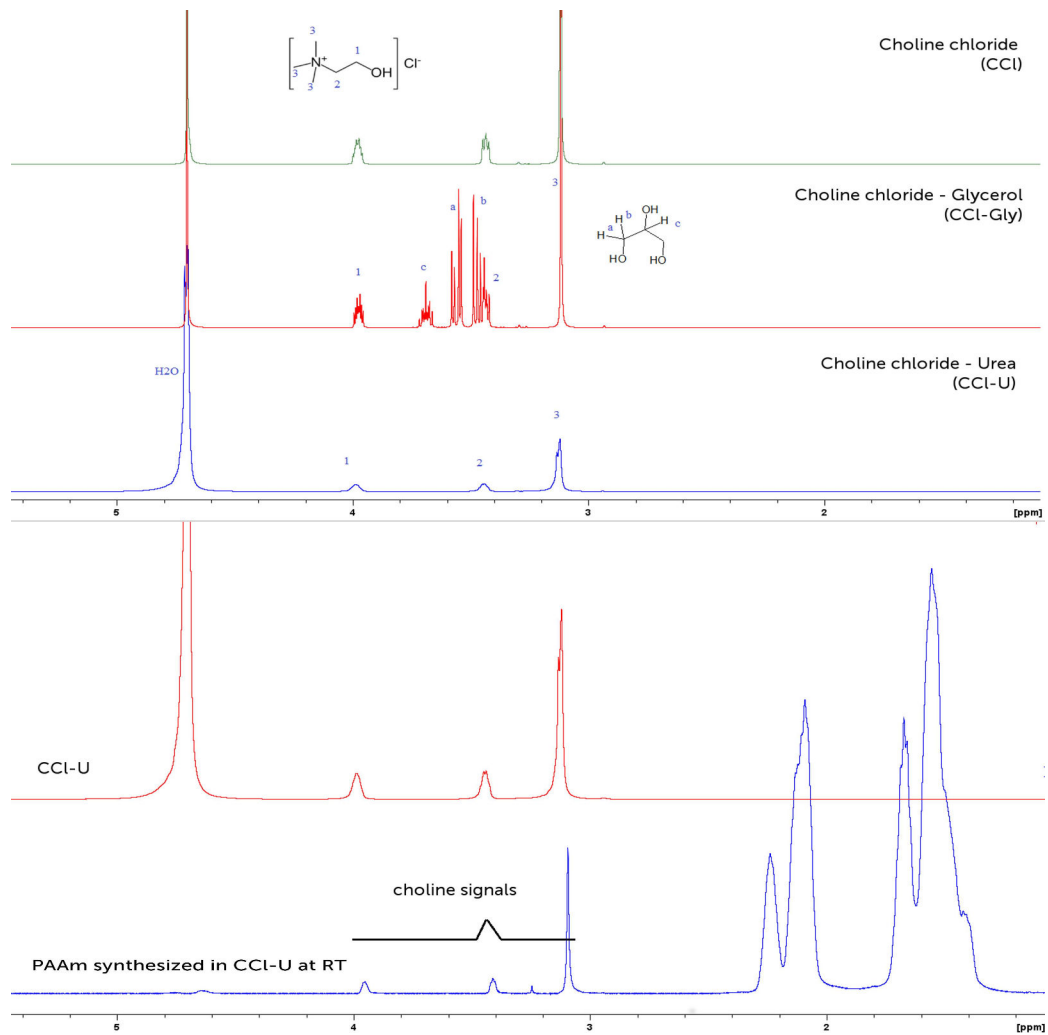


Fig. B.6 ^1H -NMR spectra of CCl , CCl-Gly , CCl-U and PAAm synthesized in CCl-U aqueous mixture at RT.

List of publications

- [1] R. J. Sanchez-Leija, J. A. Pojman, G. Luna-Barcenas, J. D. Mota-Morales, *J. Mater. Chem. B* **2014**, *2*, 7495–7501.
- [2] R. J. Sanchez-Leija, J. R. Torres-Lubian, A. Resendiz-Rubio, G. Luna-Barcenas, J. D. Mota-Morales, *RSC Adv.* **2016**, *6*, 13072–13079.
- [3] D. G. Ramirez-Wong, M. Ramirez-Cardona, R. J. Sanchez-Leija, A. Rugerio, R. A. Mauricio-Sanchez, M. A. Hernandez-Landaverde, A. Carranza, J. A. Pojman, A. M. Garay-Tapia, E. Prokhorov, J. D. Mota-Morales, G. Luna-Barcenas, *Green Chem.* **2016**, *18*, 4303–4311.